An Environment for Advanced Simulation and Control of Lighting Systems

by

Gaspare Boscarino

M.Eng., Polytechnic University of Milan, 1997

A Thesis submitted in partial fulfillment
of the requirements for the degree of

Master of Applied Science

in the
School of Mechatronic Systems Engineering
Faculty of Applied Sciences

SIMON FRASER UNIVERSITY
Spring 2014

APPROVAL

Name:	Gaspare Boscarino
Degree:	Master of Applied Science
Title of Thesis:	An Environment for Advanced Simulation and Control of Lighting Systems
Examining Committee:	Dr. Siamak Arzanpour, Associate Professor, School of Mechatronic Systems Engineering Chair
	Dr. Mehrdad Moallem, Professor, School of Mechatronic Systems Engineering Senior Supervisor
	Dr. Ahmad Rad, Professor, School of Mechatronic Systems Engineering Supervisor
	Dr. Carlo Menon, Associate Professor, School of Engineering Science SFU Examiner
Date Approved:	April 24th, 2014

Partial Copyright Licence

Abstract

Development of smart lighting systems can be considered under different perspectives. While a main business case for smart lighting is energy savings, another important consideration is the level of visual comfort experienced by the occupants. The latter aspect has been documented mainly in the context of the circadian system. A growing body of knowledge is related to the environmental impact of energy consumption related to lighting. The so-called layered lighting design, which aims at an effective combination of artificial and natural light, plays a key role in formal certification procedures for building design. This thesis presents two main contributions to the challenging area of the lighting industry: First, a lighting control scheme is proposed which integrates artificial lighting and daylight harvesting. Secondly, the development of an application programming interface is presented which allows one to integrate a control scheme with a simulated scene. The latter part of the contribution could be particularly beneficial for quasi-real-time validation of a lighting control algorithm against a virtual environment. The simulation environment can be deployed on a cloud environment. The case study discussed in this thesis is a scaled down version of an open-plan office lit through a set of individually addressable LED luminaries. It is further assumed that a second source of luminous flux is available in the form of natural light. The control problem consists of maintaining a level of illuminance which meets the users' requirements while minimizing the energy consumption. The proposed intelligent lighting system is based on an adaptive multivariable control scheme where the parameters of the model are determined through a simple identification procedure. The behaviour of the control system was validated through simulation studies and tested on a small scale room. Test results clearly show that a smart lighting system designed around the layered lighting design paradigm is indeed a compelling business case.

To my wife Nadereh and my children Nima and Soheila

"The good life is one inspired by love and guided by knowledge."

Bertrand Russell, *1872-1970*

Acknowledgments

There are many people who have contributed in many ways to the development of this work. Professor Mehrdad Moallem, I owe you a great deal of thanks for having given me the opportunity to expand my knowledge in the Mechatronic System Engineering field. Your immense patience and tireless support has had a tremendous impact on both my personal and professional life. Many thanks also to Dr. Edward Park, Jennifer Leone, and David Maris for their support during the final phases of the development of this thesis. Special thanks to Anthony Blake, Tom Duggan, Sarb Sarkaria, and Chirag Pathak from Nokia for their constant support and encouragement. I would also like to thank Randolph Fritz from the University of California Lawrence Berkeley National Laboratory for his advices on the use of Radiance. Many thanks to Dr. Siavash Vojdani, Mark Godsy, and Robert Ziola from Inteluma Energy Systems for giving me the opportunity to enter the fascinating world of the lighting engineering industry. Thanks also to Michael Fisher, Younes Rashidi from Inteluma Energy Systems, for their advice and constant support during the development of this project. Special thanks to Sepehr Attarchi for his invaluable insights and support during the testing phase at the SFU laboratory. And finally, I would like to express my gratitude to my wife Nadereh and my children Nima and Soheila for their patience and support while I was working on this project.

Contents

List of Tables

List of Figures

Chapter 1

Introduction

1.1 Motivation

A possible definition of *intelligent lighting system* is the combination of light sources, sensors, communication networks and information systems whose purpose is the satisfaction of the users' visual and non-visual experiences while minimizing the environmental footprint. This definition, albeit simple, should already provide a starting point to reflect on the possible impacts that intelligent lighting systems will have on both the technology landscape and the environment. Advances in the web services and cloud computing areas are fostering the development of products which integrate multiple services, technologies, and methods in the form of new services which ultimately will be the enablers of new forms of businesses.

Hence, intelligent lighting systems are increasingly becoming more service-oriented by borrowing ideas, perhaps unintentionally, mostly from the principles of *service oriented architecture* (SOA), which is a well established method of structuring complex software systems. Examples of possible web services could be services which provide weather data to support daylight harvesting algorithms, energy pricing for defining peak shaving policies, or even simply firmware upgrade over the air.

One of the biggest challenges that the designers of intelligent lighting systems will face is how to design economically viable systems which embody the principles of quality lighting and environmental sustainability. Particular attention has already been placed by the research community on the quality lighting factor, which includes both the visual and non-visual systems. While design techniques aimed at satisfying the human visual system are fairly mature, many questions with regard to the non-visual system are still unanswered.

Two of the major areas of research are focused on the effects of artificial light on the human *circadian rhythm* and human health. It is the writer's opinion that the non-visual system will play a major role in shaping the future of intelligent lighting systems.

Perhaps the most remarkable part of the evolution of the intelligent lighting system is the confluence and fusion of disparate technologies which not long ago where used only in specific sectors. Business intelligence, data warehousing, data mining, and computational intelligence techniques, are nowadays extensively used in electric utilities and other industrial systems for analysis, monitoring, and control. Heat, ventilation, and air conditioning (HVAC) systems are another example of a domain where a multidisciplinary approach will dominate the development of future products and services. It is definitely appropriate to state that the variegated nature of intelligent lighting systems is perfectly aligned with the vision of the mechatronic systems engineering discipline.

This thesis is meant to provide two main contributions to the lighting industry. Firstly, an adaptive control scheme which incorporates the daylight harvesting paradigm is proposed as a viable control system to be applied in open-plan office applications. The second part presents a service-oriented simulation environment based on the Radiance software which allows a given lighting system controller, simulated or real, to interact with a virtual scene in a quasi-real-time fashion. The latter is perhaps the major contribution from this work since, as emphasized before, one of the pillars of intelligent lighting systems will be openness based on the service-orientation paradigm.

In many respects we are at the dawn of a new era of the lighting industry which is witnessing a revolution triggered by two powerful forces: environment and information. Light sources are increasingly evolving from simple units dedicated to the production of light to devices capable of considerable computational power. The ability to individually address each light fixture is already a fact and it will further evolve in the near future alongside the internet of things (IoT) paradigm. Predicting the impacts of this wave of innovation is not a simple endeavour since new unthinkable scenarios could appear in the near future. However, exciting and encouraging beginning suggests that intelligent lighting systems will bring large benefits to the humankind and the earth.

1.2 Document Outline

The first chapter presents a background of the lighting engineering discipline by providing fundamental concepts from physics and light sources. The second chapter discusses some of the key topics which define the objectives of the intelligent lighting systems including the so-called sustainable design. Chapters four covers one of the contributions of this thesis: a proposed daylight harvesting system based on a self-tuning multi-input multi-output (MIMO) lighting control scheme. Chapter five is focused on the second contribution of this work: the development of a scene simulator based on the Radiance software accessible through a REST API for quasi-real time simulations. The scene simulator is then used to validate the effectiveness of the control scheme defined in chapter four. Chapter six is dedicated to a further validation of the control system through a test bed implemented with real LED light fixtures and a small scale room. Chapter seven summarizes the finding and presents possible areas for future research. Three appendices present materials that support the main topics.

Chapter 2

Fundamentals of Lighting Engineering

This chapter provides basic concepts from physics which are part of the foundations of lighting engineering. The chapter also introduces some of the characteristics of the most common light sources with particular emphasis on the solid state lighting and natural light.

2.1 Fundamentals of Lighting

Light is essential not only because it is necessary for the visual system but also for its influence on the health, behaviour, and psychological well-being of humans as largely documented in the growing body of research on the human circadian system [46]. The study of the light is considered one of the most difficult topics in physics. Currently the most comprehensive theory of the light can be found within the quantum electrodynamics (QED) domain which allows to explain well known phenomena including interaction with matter, diffraction, blackbody radiation, the laser, and the photoelectric effect which is at the core of the light emitting diode (LED) technology [25]. However, in the context of the applications related to interior and outdoor lighting systems, the tools provided by the QED are by far too complex. In order to design these type of systems, lighting designers have traditionally adopted techniques derived from two other classical branches of physics: geometrical optics and physical optics. Geometrical optics is concerned with the development of models which rely on the assumption that the propagation of the light can be described through rays

which represent the paths connecting the light sources to the target objects. Geometrical optics provides the theoretical foundations to the lighting engineering discipline. Therefore, the core of the material described in this work is based on the building blocks developed in the context of the geometrical optics. Physical optics is based on the electromagnetic wave theory which has at its core the well known Maxwell equations. From the physical optics perspective, the light is considered as a radiation composed of electromagnetic waves which stimulate the human vision system. Experiments have demonstrated that the range of the frequencies associated to the light goes from 4.05×10^{14} Hz (740 nm) to 7.89×10^{14} Hz (380 nm) as shown in Figure 2.1. One aspect which is traditionally not well explained in neither the geometrical optics nor in the physical optics is the energy carried by the light. Although a thorough theoretical analysis of this topic is well beyond the scope of this work, it is important to mention that the light carries energy in discrete amounts modelled through the concept of photons. The energy associated to a photon is $E = h\nu$ where $h = 6.6256 \times 10^{-34} J \cdot s$ is the Plank's constant and ν is the temporal frequency of the radiation (Hz). The concept of photon constitutes a bridge between the wave theory and the QED. It also important to note that the phenomena related to the coherence and the polarization are not discussed in this work since most natural light sources, including the sun, are incoherent and unpolarized. Moreover, the human eye is not sensitive to polarization [25].

2.1.1 Radiometry and Photometry

From the physics perspective, the foundations upon which lighting engineering is based, rely on three disciplines: radiometry, photometry, and colorimetry. This section provides a simple summary of the main radiometric and photometric quantities. This thesis does not address any topics related to color control. Therefore, colorimetric quantities will not be discussed.

Radiometry is the branch of physics which studies the energy flow associated with light. The core of the theory is based on geometrical optics. Photometry, on the other hand, involves quantities which quantify how the human vision system perceives light. Each radiometric quantity has a correspondent photometric quantity. For example, the photometric quantity luminous flux corresponds to the radiometric quantity radiant energy. Luminous flux Φ_v and radiant flux Φ_e are related through the luminous efficacy of the human eye as shown in 2.1.

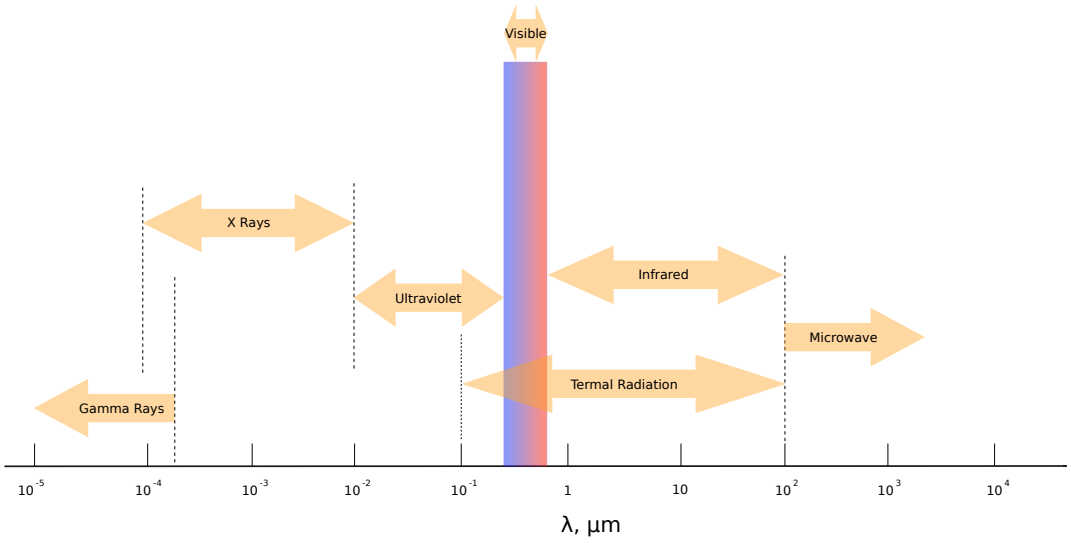

Figure 2.1: Spectrum of electromagnetic radiation.

$$\Phi_v = K\Phi_e. \tag{2.1}$$

Radiometric and photometric quantities which are used in the lighting industry are listed in Table 2.1 and Table 2.2 respectively.

The candela is the SI base unit for the luminous intensity; the symbol for the candela is cd. The operational definition is the following [40]: The candela is the luminous intensity, in a given direction, of a source that emits monochromatic radiation of frequency 540×10^{12} Hz and that has a radiant intensity in that direction of $1/683$ W/sr. A regular candle emits roughly 1 cd of luminous intensity.

Table 2.1: Radiometric Quantities

Quantity	Definition	Unit
radiant energy	Q_e	J
radiant flux	$\Phi_e = dQ_e/dt$	$W(J/s)$
radiant intensity	$I_e = d\Phi_e/d\omega$	W/sr
irradiance	$E_e = d\Phi_e/dS$	W/m^2
radiant existance	$M_e = d\Phi_e/dS$	W/m^2
radiance	$L_e = d\Phi_e/(dS \cdot cos\theta \cdot d\omega)$	$W/(sr \cdot m^2)$

Table 2.2: Photometric Quantities

Quantity	Definition	Unit
quantity of light	Q_v	$lm \cdot s$
luminous flux	$\Phi_v = dQ_v/dt$	lm
luminous intensity	$I_v = d\Phi_v/d\omega$	$lm/sr(cd)$
illuminance	$E_v = d\Phi_v/dS$	$lm/m^2(lx)$
luminous existance	$M_v = d\Phi_v/dS$	lm/m^2
luminance	$L_v = d\Phi_v/(dS \cdot cos\theta \cdot d\omega)$	$lm/(sr \cdot m^2)$

2.2 Light Sources

A key factor in sustainable design is the ability to integrate natural and artificial light sources. A solid understanding of the characteristics of the light sources is an essential part of the background of a lighting professionals. The following parts provide a background for both natural and artificial lights.

2.2.1 Natural Sources

The source for natural light is the sun whose spectral radiance distribution can be approximated through a blackbody at 5750 K. The solar radiation which reaches the earth can be split in two components: sunlight and daylight.

The sunlight is the solar radiation attenuated by the atmosphere. In lighting design, the effects associated with this component of the natural light are usually considered problematic due to glare and heat [46].

The daylight, which is also called skylight, is the solar radiation scattered by particles which are present in the atmosphere. This is the component of the solar radiation that lighting designers include in the so-called daylight harvesting design.

The average irradiance received on a clear day at sea level is around $1,200\,\mathrm{W/m^2}$ but only 40% is part of the visible range.

Modeling

In order to asses the quality of a given solution, interior designers can rely on tools which simulate an environment under several light conditions. Simulation systems like Radiance, allow to model artificial light sources by importing photometric data via IES files, where IES is the acronym of the Illuminating Engineering Society. Similar mechanism are available for modeling both sunlight and daylight. The light associated with the sunlight and the daylight is influenced by several factors including the geometry of the sun, that is its position during the day and during the year, and the weather. Those factors are somewhat difficult to consider in a very general model especially due to the unpredictability of the weather conditions. The complexity of the model becomes even larger is one includes factors like air pollution. In order to provide a solid background for daylighting design, the CIE has formalized a set of fifteen sky models which covers a large range of scenarios including clear sky and overcast sky. The CIE sky type standard has been adopted by the ISO (ISO 15469:2004/CIE S 011/E:2003 Standard: Spatial Distribution of Daylight - CIE Standard General Sky). Simulation systems like Radiance can include those models in order to offer a large array of option to the interior designer for complex daylighting design [16]. The challenge is in selecting the most accurate sky model based on the local conditions. In some cases, sky data are obtained through measurements performed by means of sky scanners, which measure the spatial distribution of the radiance and the luminance. Those devices are installed in ground stations which are fairly expensive to maintain. By using the data acquired through the ground station it is then possible to select the proper CIE sky model. However, in most places measurements through ground stations are not possible. Therefore, in those cases selecting a sky model is a very challenging task. Recently, researchers have proposed procedures which rely on satellite-based methods to predict sky data conditions [17]. The European Database of Daylight and Solar Radiation (Satel-Light) was the first large scale application to rely on satellite-based images [17]. He and Ng have proposed an interesting method to predict sky types and hourly zenith luminance from the so-called *cloud index* which is a paremeter calculated from data collected from geostationary satellite [17]. Researchers have also shown that meteorological data could also be used to estimate the sky types of a given location although in most cases some parameters cannot be fully

identified [16].

2.2.2 Electrical Light Sources

Since invention of the incandescent lamp by Joseph Swan and Thomas Edison in the late 1800s, the main source of energy for artificial light has been the electric energy. Discoveries in techniques related to the use of vapours of mercury and sodium in combination with electricity led to the development of fluorescent lamps and hight pressure sodium lamps. Although light emitting diode (LED) devices are drawing a substantial attention in large applications, they were already fairly popular in the 1960s mostly as indicators. The following parts present an overview of the main characteristics of electric light sources which are used in the lighting industry for evaluating the quality of a given product. A brief summary of the technologies, from incandescent lamp to LED devices is also provided.

Light Quality: Color Temperature, Correlated Color Temperature and Color Rendering Index

The quality of an artificial light source can be defined through several measures each of which considers specific aspects. One perspective particularly important is the chromaticity of the light source. One way to quantify the amount of colors in the light supplied by the light source is to consider as a reference a blackbody radiator. It can be shown that the colors associated with the radiation emitted by the blackbody radiator can be specified by only one measure, the absolute temperature expressed in Kelvin (K). Therefore, for all the light sources which have a spectral power distribution of a blackbody, the chromaticity can be expressed by only one number, that is the temperature of the blackbody; this number is called color temperature. The chromaticity expressed through this method is called color temperature. However, in most cases the light source does not have the spectral distribution of a blackbody. In those cases, one considers the temperature of the blackbody which is has the closest chromaticity to that of the radiation of the light source. The corresponding temperature of the blackbody is called correlated color temperature (CCT)[33][40]. It is important to note that the color temperature of the radiation of a given light source is not the temperature of the light source. Let T_{ct} the color temperature of a radiation emitted by a given light source. T_{CT} (K) represents the chromaticity of the radiation and corresponds to temperature of a blackbody having the same chromaticity of the radiation. The same

consideration is valid for the CCT. That is, if T_{CCT} is the CCT of a lamp, then T_{CCT} indicates that the color of the lamp is similar to the color of the radiation generated by a blackbody heated at T_{CCT} K [33].

The color rendering index (CRI) is a number ranging from 0 to 100 that describes how well a given light source reveals the colors of an object [46][26]. in applications where the rendering of colors is important, one should choose lamps with CRI of 80 or higher.

Efficacy

The *efficacy* is a measures of the efficiency of a given luminaire and it is defined as the ratio between the amount of luminous flux generated by the light source and the amount of power received as input. The efficacy is measured in lm/W and is also referred in technical data sheets as *lumens per watt* (LPW). As shown in Table 2.4, incandescent bulbs are at the bottom of the list since they are essentially large resistors.

Incandescent and Halogen Lamps

Incandescent lamps are the oldest and still the most used electric light sources. An incandescent bulb emits light by heating a piece of metal, called filament, until it glows. The filament is usually made from tungsten because it has a very high melting point ($3,422\,^{\circ}$C) and emits radiation around $2,850$ K. The amount of power injected in the filament determines the color of the light. In order to prevent the filament for failing due to oxidation caused by the contact with the air, the filament is included within a glass shell which maintains a partial vacuum, since the temperature of the filament can reach over $2,000\,^{\circ}$C. The temperature of the glass shell in a 40 W can reach $140\,^{\circ}$C

Halogen lamps are essentially incandescent lamps with the difference that glass shell contains a halogen, typically iodine or bromine gas. The use of a halogen allows the filament to reach higher temperature allowing an increase in the efficacy. Halogen lamps have also a longer life time compared to simple incandescent light bulbs.

Fluorescent Lamps

Fluorescent lamps are part of the family of the so-called electric-discharge lamps. They consists of a glass tube containing vapours of mercury. There are two filaments at each end of the tube which emit electrons when they are heated. The emission of electrons ionize the

mercury causing the generation of ultraviolet (UV) radiations. The phosphor, which covers the internal part of the tube, absorbs the high energy radiation and emits radiations in the visible range. In order to control the emission mechanism, the lamp needs a device called ballast. The temperature of the glass shell for fluorescent lamps is around 40 °C which is considerably lower than the temperature of the incandescent lamps.

Induction Lamps

Induction lighting devices are essentially fluorescent lamps without filaments. The energy used to create the plasma arc is generated through transformers instead of filaments. Induction light fixtures have an extremely long life time, in the order of 100,000 hours. It is not entirely clear why these lamps have not been widely adopted in the lighting industry; possible reasons could be related to the emission of 13.6 MHz radiation [26].

High Intensity Discharge (HID) Lamps

High intensity discharge (HID) lamps are based on the same principle used in the fluorescent lamps with the difference that instead of emitting UV radiation, the lamp emits radiation already in the visible range eliminating in this case the need for conversion through phosphors. The lack of the conversion leads to an higher efficacy compared to fluorescent lamps. Examples of HID lamps are the sodium vapour light fixtures which emit yellow light and are widely used in parking lot applications. Other examples of HID lamps include metal halide lamps extensively used in parking garages.

Solid State Lighting

Light emitting diodes (LEDs) are semiconductor diodes which are designed explicitly for emitting light by using the electroluminescence effect. The popularity of the LEDs started in the 1970s mostly as indicators due to the then very limited luminous output flux. Small red LEDs are characterized by a forward voltage of around 2.2 V and a current of 20 mA. For both general and task lighting applications, light fixture manufacturers use arrays of power LEDs which are characterized by a drive current of 350 mA and an input power from 1 W to 3 W.

Generation of White Light: LED devices generate monochromatic light, typically as red, green, blue, and yellow radiation. In order to produce white light there are two main

approaches:

- Use of phosphors which absorb blue light generated by the LED and emit radiations on a larger spectrum which approximate the white light. The reason why the color of the radiation which is absorbed by the phosphor is blue can be explained by observing that the spectrum of the radiations which is usually perceived as white from the human visual system starts from around 450 nm. Considering that the energy of a radiation is proportional to the inverse of the wavelength, from the balance of the energy applied to the phosphors one has that the input radiation has to have a level of energy higher than the energy associated to the output radiations. Hence, an input radiation with a wavelength smaller than 450 nm is needed and this constraint is certainly satisfied by the blue radiation which has a wavelength of around 435 nm. Therefore, using a blue LED is a very efficient way to generate white light [26]. It is important to mention that phosphors degrade at high temperatures. This degradation is one of the leading causes for the reduction of luminous flux in the LEDs at high temperature [26] which is tightly related to the input power as shown in the following section regarding the photo-electro-thermal model of LED systems.
- Combination of multiple LED devices which generate red, green, and blue radiations.

A Photo-Electro-Thermal Model for LED Devices: Recent research in photo-electro-thermal theory for light emitting diode (LED) systems have provided models which link the photometric, electrical, and thermal properties of an LED system [18][41][35]. Let φ_v be the total luminous flux generated by a set of N LED devices having a luminous efficacy E (lm/W). Let P_d the real power of one LED. Then φ_v can be expressed as in 2.2:

$$\varphi_v = N \times E \times P_d. \tag{2.2}$$

It can be proved that 2.2 can be expanded as in 2.3

$$\varphi_v = NE_o \left\{ [1 + k_e(T_a - T_o)]P_d + k_e k_h (R_{jc} + NR_{hs})P_d^2 \right\}. \tag{2.3}$$

where the descriptions of the symbols in 2.3 are listed in Table 2.3.

Therefore, 2.3 can be rewritten as

$$\varphi_v = \alpha_1 P_d - \alpha_2 P_d^2 \tag{2.4}$$

Table 2.3: Photo-Electro-Thermal Model Symbols

Symbol	Description
E_o	Rated efficacy at the rated temperature T_o (typically 10°C).
k_e	Relative rate of reduction of efficacy with increasing temperature.
T_a	Ambient temperature.
T_o	Rated temperature.
k_h	Constant less than one which represents the portion of the power converted to heat.
R_{hs}	Thermal resistance of the heat sink.
R_{jc}	Junction to case thermal resistance.

where α_1 and α_2 are two positive coefficients. From 2.4 one can see that φ_v is linearly dependent on P_d for small values of P_d since the term dependent on α_2 can be ignored for small values of P_d. The quasi-linear dependency between φ_v and P_d is a very important observation since allows a considerable simplification during the system modeling phase of a lighting control system design, as discussed in the system modeling section of this thesis. However, as P_d grows, the term in α_2 will cause a decrease in φ_v because of the effect of the square of P_d. Therefore there is a value of P_d beyond which φ_v decreases. The maximum value of φ_v can be calculated from $d\varphi_v/dP_d = 0$. By introducing simplification to the model, it can be shown that the maximum point for φ_v is reached for

$$P_d^* = -\frac{[1 + k_e(T_a - T_0)]}{2k_e k_h(R_{jc} + NR_{hs})}. \tag{2.5}$$

Haitz's laws: Dr. Roland Haitz, a former scientist at Agilent Technologies, developed a model to forecast the improvements in the LED devices. The model, which is the counterpart of Moore's law, states that every decade the lumen per package increases by a factor of 30 while the cost per lumen falls by a factor of 10 [26]. The model also predicts that the efficacy of LED devices could reach 200 lm/W by 2020. As a side note, the luminare CR24 from Cree which has been used in the lighting simulator presented in this thesis, is rated at a maximum of 130 lm/W. It is important to note that by considering the definition of the luminous flux, the maximum efficacy that any device can reach is 683 lm/W. It should also be noted that phosphor-based white LED devices have a limit of around 238 lm/W. Therefore, higher efficacy will have to obtained through red-green-blue (RGB) methods [26].

Comparison of Electrical Light Sources

Given the fairly large variety of electrical light sources, it is useful to compare the characteristics offered by each technology in order to asses which type of light source is suitable for a given applications. Table 2.4 lists the main characteristics of the most used electrical light sources [46]. From Table 2.4 it is clear that the incandescent lamps are at the bottom of the list as far as the efficacy is concerned. This is the reason why the incandescent bulbs are in the process of being phased out in many countries.

Table 2.4: Main Characteristics of Electrical Light Sources.

Characteristics of Electrical Light Sources					
Type	**Efficacy**	**CRI**	**CCT (K)**	**Rated Hours**	**Mercury**
Incandescent	5-22	100	2,800	750-2,000	No
Halogen	12-36	100	3,000	2,000-6,000	No
Linear Fluorescent	75-100	T12:58-62 T8: 75-98 T5: 80	2,700 3,000 3,500 4,100 5,000 6,500	5,000-36,000	Yes
Compact Fluorescent	27-80	80-85	2,700 3,000 3,500 4,100 5,000 6,500	9,000-20,000	Yes
Metal Halide	80-115	65-95	2,900 3,100 4,100 5,000	10,000-20,000	No
High Pressure Sodium	90-140	22-85	1,900 2,100 2,200 2,700	10,000-40,000	No
LED	45-107	50-90	2,700 3,000 warm white 4,000 cool white 6,500 daylight	50,000	No

Photometric Data

Light fixture manufactures usually provide photometric data for their light fixtures in several formats. Two of the most common ways are: IES files and photometric diagrams.

IES files are the standard mechanism defined by the Illuminating Engineering Society

of North America (IES) and are widely adopted in the lighting industry to transmit photometric data in an electronic format. They are used mostly in lighting analysis and design programs in order to asses the light distribution in a given environment. Radiance, the software which has been used in this thesis, allows to import the data from a given IES file through the tool ies2rad. IES files are text files and are recognized by the file extension .ies.

Photometric diagrams provide a visual representation of the luminous intensity. There are several representations based on the type of coordinate system. Perhaps one of the most common diagram is the so-called C-γ diagram which is a polar coordinate system similar to that used on terrestrial globes [40][36]. This representation was defined by the Commission internationale de l'eclairage (CIE) in the standard CIE 121-1996. The C-γ shows the luminous intensity expressed in cd on two perpendicular planes which intersect in the polar axis. Each plane is then divided in two half planes. The half plane are named as follows; C0, C90, C180, and C270, where the number after the letter C is the angle from the C0 half plane on a counter-clockwise direction with respect to the polar axis. γ is the angle between the polar axis of the luminaire and the direction on a specific half plane along which the luminous flux has been measured. Figure 2.2 shows an example of a C-γ diagram for a luminaire whose luminous intensity is symmetrical in the C90-C270 plane and asymmetrical with respect to the C0-C180 plane. Figure 2.3 shows a three-dimensional view of the diagram in Figure 2.2.

The C-γ system is considered oriented rigidly in the space; therefore, it does not follow any tilt of the light fixture [40]. Sometimes the values of the luminous intensity are expressed in candelas per 1000 lumens (cd/lm). In those cases, the actual luminous intensity is calculated by multiplying the value read from the diagram times the actual amount of luminous flux (lm). For example, let us suppose that from the diagram one reads 1000 cd/klm. If the luminous flux is 500 lm then the actual luminous intensity would be 500 cd.

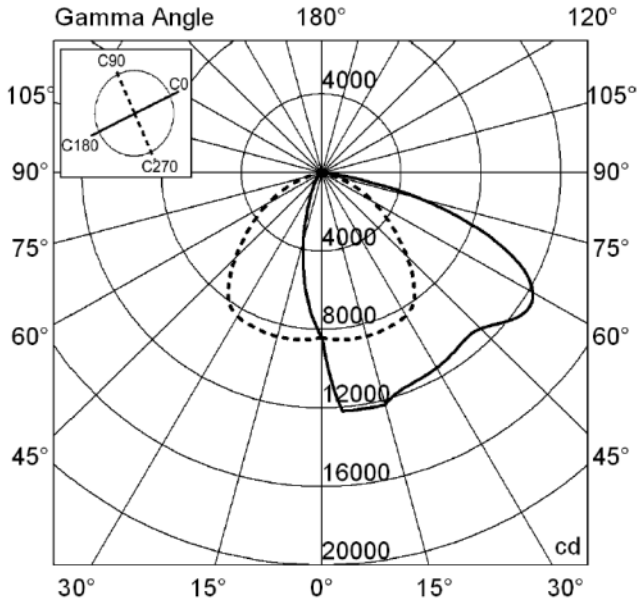

Figure 2.2: Example of a C-γ diagram (with permission from Ransen Software).

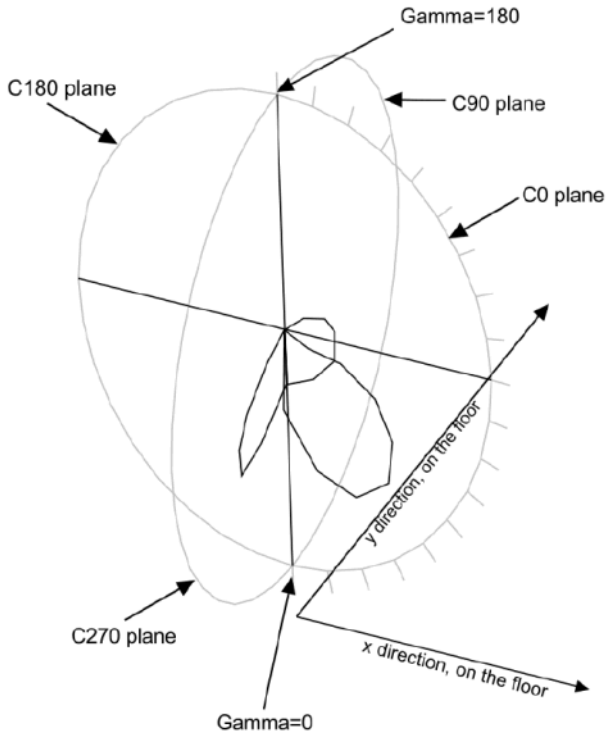

Figure 2.3: Example of a C-γ diagram (with permission from Ransen Software).

Chapter 3

Literature Review on Intelligent Lighting Systems

This chapter presents some of the main topics which are driving a new wave of innovation in the lighting industry. While the first part covers the relatively new concept of sustainable design, the other parts are more specific and address some case studies and standard communication protocols which forms the backbone of the intelligent lighting systems.

3.1 Sustainable Design

The term sustainable design refers to design practices that minimize the negative impact on the environment by balancing the interaction of the earth, society, and the economy [46]. Several agencies around the world have been created to formalize the approach to sustainable design practices. Although most of those agencies are governmental institutions, several voluntary programs are actively used in many industries in order to identify sustainable products which include buildings [46]. The environmental life-cycle assessment (LCA) is a processes used to asses the impact of a given product on the environment. The LCA covers the whole life cycle of a product from raw material to waste disposal. One of the parameters measured during the assessment is the so-called *embodied energy* which is the total energy used during the entire life time of a given product.

There are several programs specific for assessing the sustainability of buildings and lighting systems in particular. The *Leadership in Energy and Environment Design* (LEED)

program, developed by the U.S. Green Building Council (USGBC), is an international green building certification system which focus on estimating metrics related to energy savings, water efficiency, CO_2 emissions reduction, improved indoor environmental quality, and stewardship of resources and sensitivity to their impacts [46]. There are several levels of LEED certification ranging from silver to platinum. Other international green building certification programs include the *Building Research Establishment's Environmental Assessment Method* (BREEAM) in the United Kingdom, the *Comprehensive Assessment System for Built Environment Efficiency* (CASBEE) in Japan, and the *Green Star* in Australia.

Overall, the objectives of sustainable design principle in the case of lighting systems can be summarized as follows: maximization of daylighting, reduction of non-renewable resources, minimization of air and water, protection of natural habitats, elimination of toxic products, recycling lamps, reduction of light pollution and light trespassing [46].

Electric lighting accounts for 19% of the total electrical energy worldwide while the electrical energy consumed for lighting in offices accounts for 19% of the total lighting energy used by all types of commercial buildings [1]. The U.S. Environmental Protection Agency (EPA) has estimated that the portion of the electrical energy due to lighting is around 35% in commercial buildings and 20% for residential buildings. Daylighting is definitely part of the tools used by interior designers who embrace sustainable design as part of their best practices. It has been estimated that with a proper adoption of daylighting solutions, the electrical energy saved in commercial building is in the order of 40% [2]. However, a daylighting system has to be designed so that a proper balance among several requirements is reached. In order to asses the daylighting quality of a given interior space, a set of daylight metrics have been proposed by Cantin and Dubois as an alternative to the traditional *daylight factor* [6].

An interesting study conducted by Jeff Tsao and Paul Waide shows that during the last three centuries, the cost for lighting compared to the GDP is in the order of 0.72% [26][42]. Considering that the lighting devices are constantly improving in terms of efficiency, the model then predicts that the overall amount of light will increase. Therefore, the model predicts a reduction energy consumption due to lighting only if either the GDP or the cost of electricity are reduced.

The aforementioned numbers clearly show that the adoption of energy efficient lighting systems in commercial buildings can play a substantial role in the effort of reducing electrical energy consumption.

3.1.1 Quality Lighting

Interior designers have recently embraced design strategies which include factors that go beyond the quantity of light. Aspects related to the visual comforts now play a paramount role since the early stages of the design of a lighting system. The concept of *quality lighting* incorporates the psychological elements associated with the visual comfort. Organizations like IES which are specialized in setting standards in the lighting industry, have emphasized the importance of quality lighting best practices. Layered lighting, which is part of the quality lighting design, consists in layering natural light and artificial light in order to achieve both a pleasant visual experience and also a significant reduction in electric energy consumption [46]. The lighting control scheme proposed in this thesis is indeed based on the layered lighting paradigm.

Interior Lighting

Interior designers classifies interior lighting systems in four categories: *ambient lighting*, *task lighting*, *accent lighting*, and *decorative lighting*. Ambient lighting, also known as general lighting, is meant to provide an overall general illumination in spaces shared by several people, like common areas and hallways. Task lighting is the type of lighting required for performing specific tasks like reading, writing, or manufacturing tasks. The values of the illuminance associated to task lighting are significantly higher compared with the illuminance values expected in ambient lighting. Accent lighting is used for emphasize architectural elements of a given environment. Decorative lighting is purely ornamental and covers applications where light sources are essentially artistic artifacts. Table 3.1 shows a list of the range of illuminance values for specific applications [36].

Human Circadian System

Humans have an internal clock which coordinates functions related to waking and sleeping. This clock is known as *circadian system* and is strongly dependent from the level of illumination. In particular, high level of illumination are needed to start the circadian process while low level of illumination are required to start the generation of melatonin, the hormone necessary for sleeping. Studies have proved that the circadian rhythm is particularly

Table 3.1: Ranges of the illuminance values for several applications.

Application	Mininum (lx)	Maximum (lx)
Retail lighting	400	500
Office lighting	450	500
Video terminal work	100	200
Classroom	300	750
Hospital public areas	100	200
Hospital operating theatre	1,500	2000
Hospital operating table	50,000	60,000
Sewing room	1,000	2,000
Electronic test room	800	1,200
Factory assembly area	200	500

sensitive to the blue light. This aspect is important to consider during the design phase of a lighting system especially when blue-rich LED luminaires will be employed. On the other hand, blue-rich LED devices could be used in applications related to the photomedicine which studies the applications of light to address problems related to depression, sleep quality, alertness, and other health problems [37][46]. A growing body of research is focus on the effects of artificial lighting on the circadian system. It has been largely confirmed that the response of the circadian system to the light is very different from the visual system. Rea, from the Lighting Research Center, has proposed an approach for modeling the spectral sensitivity of the human circadian system [38]. One of the missing pieces for understanding the relationship between light and health is the ability to measure the circadian light exposure [13]. The growing research in the human circadian rhythm will certainly force the development of intelligent lighting systems which will embed components dedicated to the monitoring and control of the interaction between light sources and circadian system.

3.2 Intelligent Lighting Systems

Advanced Control Schemes

The effectiveness of employing intelligent lighting system from the energy conservancy perspective has been thoroughly documented by Chioma et al. in [8]. In that work, experimental results demonstrate that the use of intelligent systems allow to reach levels of energy savings between 40% and 60%. The definition of the control problem which focuses only

on the visual experience of the occupants and energy conservation is usually fairly simple since the objectives essentially consists in satisfying the level of illuminance values in a given working plane while minimizing the consumption of energy. The requirements could be expanded by including factors related to the glare due to daylighting and occupancy. The main problem consists in determining a viable control scheme which satisfies the users' requirements. The overall design has to consider sensors, communication systems, controllers, blinders, and luminaires. A simple but effective approach was proposed by Agogino and Wen in order to control the lighting level in an open-plan office exposed to daylight through wireless photosensors and luminaires which are interconnected in the so-called *wireless sensor and actuator network* (WSAN) [1]. In this approach, the system under control is modelled as a linear static multi-input multi-output (MIMO) system while the control problem is formulated as a linear programming problem. Some of the topics presented in [1][45] have been used as the building blocks for the adaptive control scheme presented in this thesis. Villa and Labayrade have proposed *multi-objective optimisation method* (MOM) based on the Pareto-optimality concept in order to incorporate both user's visual preferences and energy savings [43]. In [9], Kurian et al. have proposed a real-time implementation of control scheme which integrates an ANFIS control of the luminaries with a *fuzzy* control of window shades so that the desired level of illuminance is maintained. A key component in the proposed scheme is a daylight illuminance predictor. Daylight guidance systems are an interesting area of research with a large potential for real applications. Passive tabular daylight guidance systems (TDGS) have been successfully employed in commercial applications. Mayhoub and Carter have presented a study on the performances of hybrid lighting system (HLS) which combine natural light delivered through daylight guidance and electric light in the same device [28]. This study concludes that although a potential energy savings is a key factory, the technology has not reached the level of maturity sufficient for large commercial deployments.

3.3 Industrial Standard Protocols

DALI

At the core of any solid intelligent lighting system there is the communication system which acts as a nervous system. Nowadays is still common among lighting system designers to propose proprietary communication protocol especially in the wireless domain. Although

there are many benefits in customized solutions, the adoption of industrial standards largely simplifies the design and deployment of very complex systems. The Digital Addressable Lighting Interface (DALI) is an industry standard protocol specifically developed for intelligent lighting systems. DALI is an open standard for digital communication developed in Europe and formalized in IEC 60929 and is becoming a global lighting communication standard. DALI is a Machester encoded half-duplex digital communication protocol composed of forward and backward frames. Each DALI loop can control up to 64 devices each of which is fully addressable. Moreover, DALI has been designed since the inception as a protocol to be easily interfaced with several *Building Management Systems* (BMS). DALI can also be integrated with wireless network through commercial wireless gateways.

Chapter 4

Daylight Harvesting Control System

This chapter provides the description of a daylight harvesting control scheme which is one of the contributions of this work. The formulation of the control problem is based on two fundamental aspects which are somewhat related: conservation of the energy and visual comfort. As underlined in the previous chapters, the consumption of electric energy due to lighting accounts for roughly 19% of the total energy worldwide [1]. The amount of energy which could be saved by adopting an intelligent lighting system, that is a system which combines the use of daylight, artificial light, and occupancy data, has been estimated in the range between 40% and 50% [1]. While the energy conservation is certainly a dominant factor in designing a lighting system, another extremely important aspect is related to the level of visual comfort of the occupants. Researchers have shown that the human body is strongly affected by the quality of the light which is mostly determined by the spectral composition and the intensity of the illuminance at the work plane level. Therefore, there is a compelling business case in developing a lighting control system which satisfies both the energy efficiency and the visual comfort requirements. The control of the composition of the spectrum is a topic related to the color control and it is outside the scope of this work. Therefore, assuming that the color of the light produced by the light fixtures is white, the only component related to the visual comfort which will considered in the design of the lighting control system is the distribution of the illuminance in specific points of interest.

4.1 Lighting Control System: Problem Domain

Let us consider an open plan office consisting of a certain number of cubicles. There are two main sources for ambient lighting: a set of n addressable light fixtures located in the ceiling and a large window which allows a considerable intake of daylight. Let us assume that each occupant can define her own preferred level of illuminance at the desk level. The objective of the lighting control system is to determine the amount of luminous flux which the light fixtures have to generate so that the combination of the natural and artificial light produce a profile of illuminance at the work plane level which is as close as possible to the users' preferred values. Furthermore, the light fixtures are assumed to be LED luminaries.

Daylight Harvesting

Considering that the intake of the daylight plays an active role in meeting the user's expectations, one can state that the aforementioned control problem is part of a larger body of research known as daylight harvesting. The perspective taken in the design of the control system presented in this work is that the contribution of the daylight is a positive element which shall be used for at least two reasons: the reduction of the energy required to feed the luminaries and the quality of the light associated to the daylight. Some of the main challenges posed to a daylight harvesting control strategy are due to the variability of the daylight caused by the changes in the weather conditions and also because of possible changes in the use of the work space. For example, an occupant could decide to close completely or partially the curtains which cover the window. While a good estimation of the changes of the intake of daylight related to the weather conditions could be achieved by combining historical data with weather forecast, the unpredictability of the occupants' behaviour is much more difficult to model. The difficulties associated with the variations of the daylight lead to consider this large and important source of luminous flux as a form of disturbance. Notwithstanding the foregoing issues, the active use of the daylight is an extremely powerful tool which allows not only to satisfy the users' preferences by providing a high quality light but also to meet the ever increasing demands in the energy conservation area. For these reasons, the approach adopted in modelling the lighting control system considers the contribution of the natural light as a disturbance albeit a good disturbance. The details related to the effects of the daylight as a disturbance are covered in the system modelling section. Figure 4.1 shows a lateral view of the room which is the subject of the

control problem.

Figure 4.1: The case study.

4.2 Lighting Control System: Introduction to the Solution Domain

The formulation of the control problem covered in the previous section provided the context necessary to understand the problem to be addressed. Like in many other cases, the control problem under consideration could be solved by adopting various strategies ranging from traditional PID control techniques to artificial neural networks and fuzzy inference systems (ANFIS). Therefore, the set of possible solutions is fairly large. The main criteria behind the choice of the control scheme presented in this work have been based on the idea that the control algorithm should be implemented on a microcontroller suitable for typical building automation applications. On the other hand, other major factors which have been considered are related to fundamental structural requirements like stability and robustness. From a pure systems engineering perspective the development cycle of the control scheme can be seen as a sequence of requirement and modelling activities [19]. Therefore, system modelling plays a critical role in the control system design and it will covered in great details in the

following section.

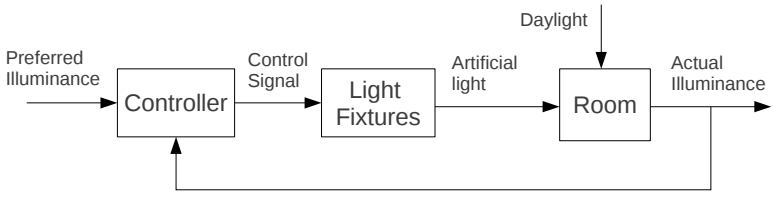

Figure 4.2: High level block diagram of the control problem.

A very high level representation of a closed-loop control system which will be described in the following sections is depicted in Figure 4.2. The main elements of the block diagram are:

- The room, which is the system under control.
- The light fixtures which generate the artificial light based on the control signal generated by the controller. From a control system perspective, the light fixtures act the actuators of the control system. In this diagram it is assumed that the light fixtures block includes also the drivers of the luminaires, that is the electronic circuit responsible for changing the level of current or voltage needed to reach a desired level of luminous flux.
- The users' preferred levels of the illuminance (reference or set point).
- The actual level of the illuminance in the points of interests of the work plan.
- The luminous flux due to the daylight.
- The controller, which is the system to be designed so that actual level of the illuminace is as close as possible to the preferred value considering that the room is subject to a large disturbance represented by the daylight. The controller has also to compensate the inherent imperfect knowledge of the dynamics of the system under control.
- The control signal generated by the controller in order to drive the light fixtures through a proper driver. Depending on the characteristics of the luminaires and the

control strategy, the control signal could be the duty cycle of a pulse-width modulation (PWM) signal or a 0-10 V control signalling system.

4.3 System Modeling

As often happens in the engineering field, the first step to perform before proceeding with designing a system is the definition of the representation of the portion of the world that includes the system to be designed. The result of this effort is a model which is a simplified description of the reality. The design of a control system can be accomplished by following two main approaches: model-based design and non-model-based design. The model-based approach is the traditional method which consists in calculating the control law by using the information extracted from the model of the system. On the other hand, the non-model-based method relies on techniques which tend to mimic the behaviour of human beings who are able to control systems without any mathematical descriptions of the systems under consideration. While the former method has been traditionally accepted by the engineering community as a solid starting point for designing complex control systems, the latter approach has the potential to overcome the difficulties of designing systems whose complexity cannot be represented with a manageable mathematical model of the system under control. For example, Mandami fuzzy control systems are part of the non-model-based approaches [27]. However, it has been widely documented in the control literature that even a limited knowledge of the system could be beneficial in the process to define a set of candidate solutions to the control problem. The portions of the system which are extremely difficult to describe or are unknown, can be accounted for by adopting several techniques including computation intelligence methods like neuro-fuzzy or reinforcement learning algorithms. Based on the level of knowledge of the system to be controlled, the model-based approaches are traditionally grouped in the following families [31]:

- White-box modeling: a very thorough understanding of the dynamics of the process is available so that a first-principle model can be determined.
- Gray-box modeling: a partial knowledge of the system is known. In this case if some experiments can be performed, then a reasonable model of the process can be determined through the so-called *identification* techniques.
- Black-box modeling: no knowledge or extremely limited knowledge about the physics

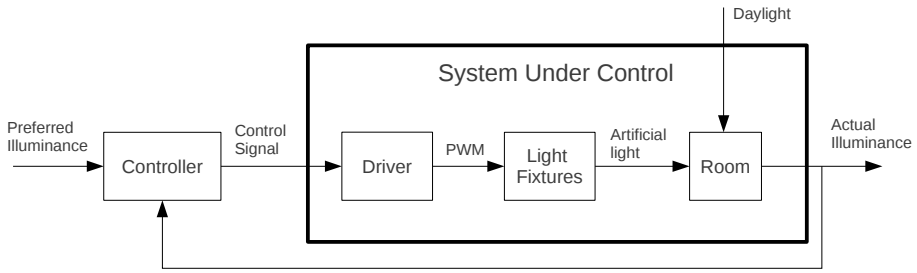

Figure 4.3: The system under control.

of the system.

The System Under Control

Before proceeding with a detailed discussion regarding the structure of the control system, it is important to define the boundaries of the system under control which, in the control literature, is also named the process to be controlled. By following a typical approach of the control literature [3], one assumes that the actuators are considered part of the system and the sensors are ideal [3]. Therefore, with respect to the case study described in the problem domain chapter, the process to be controlled includes the room, the fixtures, the drivers, and the sensors as shown in Figure 4.3.

Although the lighting engineering discipline is firmly based on a large body of knowledge which includes radiometry and photometry, the formulation of a first-principle model which includes the room, the light fixtures, and the driver poses serious challenges. If one considers only the room, the main problem is due to the impact of the geometry and the structure of a given room to the relationship between luminous flux and illuminance. On the other hand, an accurate description of the LED luminaries has to consider a non trivial relationship between electrical, photometric, and thermal aspects. Therefore there is a need to determine a simplified view of the system under control. The strategy adopted in this work is based on the idea that in general is useful to use the knowledge embedded in the mathematical models of the subsystems that compose the whole system under consideration. On the other hand, unknown dynamics due to simplifications which are sometimes inevitable, might lead to a model where some of the parameters need to be determined. Notwithstanding the inherent

complexity of each subsystem, it is possible to formulate a model which is simple enough to allow the development of a control scheme that can be easily implemented on a regular microcontroller; the proposed model for the whole process to be controlled is a linear, static, time invariant system. The following sections provide the theoretical background to support the validity of the aforementioned model with regard to a reasonable set of temporal and geometrical constraints. Therefore, the system modelling process which has been chosen for designing the proposed control system is part of the gray-box modelling strategies and can be summarized as a two-step procedure:

- Determination of a simple mathematical model which describes the relationship between the input and the output variables for the system under control. As will be shown later, the model is a linear, static, time invariant system represented through a matrix having unknown entries.
- Estimation of the entries of the matrix through a simple identification procedure.

Let us refer to the block diagram in Figure 4.4. The objective is to identify possible linear models for each of the subsystems composing the system under control. Let us emphasize that from the controller perspective, the input and the output of the system under control are the following:

- The input u is the vector having as components the low level power input signals for the LED driver representing the percentage of the power level to be set for the LED luminaires. If one used a PWM control driving strategy, u would be a vector of duty cycles.
- The output y is the vector of the actual illuminance values in the point of interest of the work plane.

LED Driver Modelling

For industrial grade LED drivers, one can certainly assume that there is a linear relationship between u and p. This assumption might not be valid under extreme operating conditions, like very high or very low temperatures. However, in normal circumstances the LED driver operates in conditions where its temperature is kept within a safe range of values.

LED Luminaire Modeling

From a pure system point of view, the set of LED light fixtures can be considered as a subsystem which receives as input the electrical power provided by the driver unit and generates as output the luminous flux which is the artificial component of the overall luminous flux which illuminates the room, being the other component the daylight.

As described in the section regarding the photo-electro-thermal model of LED systems, for each LED device the relationship between the luminous flux φ and the input power P is given by 4.1 [18].

$$\varphi = \alpha_1 P - \alpha_2 P^2. \tag{4.1}$$

From 4.1 one can state that it is reasonable to assume that φ is linearly dependent on P for $P < P^*$, where P^* is the point of maximum for φ as calculated in 2.5. With reference to Figure 4.4, considering that the total luminous flux Φ_A emitted by all the luminaries is given by the sum of all the luminous fluxes generated by all the LED devices, one can conclude that there is an approximate linear relationship between the luminous flux vector Φ_A and the power vector p.

Room Modeling

Let us determine the relationship between the luminous flux vector Φ_A generated by the light fixture and the illuminance vector y. Unless otherwise stated, the term room includes the walls, ceiling, floor, furniture, and occupants. While the artificial light sources will be considered as one of the subsystems composing the system under control, the luminous flux due to the daylight will be considered as a disturbance, albeit a good disturbance, since this project does not consider any active control of the intake of daylight, for example through automatic shades. Therefore, in this section we will consider only the part of y which is related to the artificial light. As will be shown later in the complete model, y will also include the effects of the daylight.

In general, the illuminance in a given point of the work plane has two components: direct illuminance, which derives from the direct light coming from the luminaires, and indirect illuminance, which is due to the interreflected light. Let us analyse both components.

Direct Illuminance: Illuminance can be considered as a vector [40]. Let S be a point source of luminous flux and P a point of a given surface which is receiving the luminous

radiation emitted by S. Let I be the luminous intensity of the radiation. The illuminance at the point P is given by the inverse square law as shown in 4.2

$$E_P = \frac{I \cos\theta}{d^2} \tag{4.2}$$

where d is the distance between S and P, while θ is the angle between the normal to the surface and the luminous ray from S to P.

The result from 4.2 cannot be applied directly to a real light fixture since a luminare cannot be considered a point source of light, except in cases where the distance between the luminaire and the point of the work plane is much bigger than the maximum size of the luminare. However, if one considered a given luminare as composed of an array of point sources, then the inverse-square law 4.2 could be applied to each component of the array. Hence, the resulting illuminance in a given point of the work plane is the sum of the illuminance due to each component of the array.

Let us note that 4.2 expresses a linear relationship between E, the illuminance, and I, the luminous intensity. However, from the modeling perspective, we are interested in the relationship between E and the luminous flux Φ. On the other hand, from the definition of luminous intensity, which is the portion of the luminous flux $d\Phi$ within a solid angle $d\omega$, one has that the luminous intensity is proportional to the overall luminous flux Φ. This linear dependency is explicitly documented by the luminaire manufactures through the so-called C-γ diagrams where the values of the luminous intensity are reported in cd/klm. For example, $1,000\,\mathrm{cd/klm}$ corresponds to $400\,\mathrm{cd}$ for a luminous flux of $400\,\mathrm{lm}$ and to $1000\,\mathrm{cd}$ for a luminous flux of $1000\,\mathrm{lm}$.

Interreflection: In general, part of the light generated by a set of luminaires is reflected by the surfaces that are present in a room. Therefore, the actual luminous flux received by a given surface, hence the illuminance, has two components: the direct flux and the flux received by reflection from the other surfaces. Assuming that the direct luminous flux has been calculated, the interreflected luminous flux can be calculated through the *radiosity* method which is based on the conservation of energy principle [40]. Although a thorough description of the radiosity method is beyond the scope of this document, the main result of this method can be summarized by stating that the total luminous flux received by a given surface is proportional to the total flux generated by the luminaires. From the definition of illuminance, one can infer that the total illuminance is also linearly dependent from the

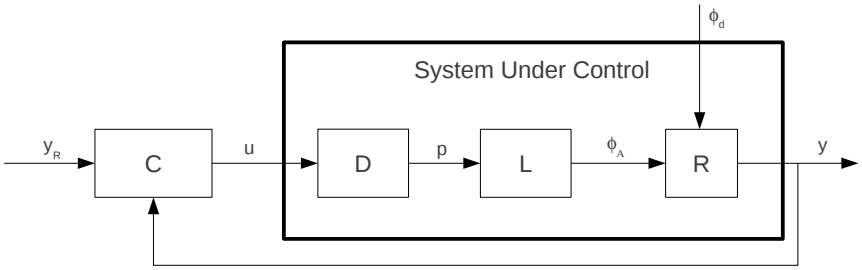

Figure 4.4: The block diagram of the control system.

total flux emitted by the light fixtures.

The Complete Model

The previous sections have shown that it is reasonable to assume that each subsystem can be modelled as a linear static system. Therefore, by combining the models of the subsystems one can assume that the whole system under control can be modelled as a linear, static, time invariant system. Let us modify the block diagram in Figure 4.3 in order to introduce the variable to be included in the complete mathematical model. Figure 4.4 introduces the control variable u generated by the controller C, the set point y_R, and the output y.

Let us further modify the block diagram in order to explicitly show the distinction between control variables and disturbances. If one denotes with R_L the representation of the room considering only the light fixtures and with R_D the model of the room which includes only the intake of the daylight, then the control system can be represented as shown in Figure 4.5.

Table 4.1 lists the symbols used Figure 4.5. One element to note is the variable d; this is the illuminance due to only the daylight, that is the solar radiation through the window. In this work d is considered as a partially measurable disturbance whose estimate can be used to improve the performance of the control system through a dedicated feedforward rejection path. Therefore, as far as the control system is concerned, the only portion of the system under control that will be modelled is the subsystem T, which includes only the artificial light, and the disturbance d as shown in Figure 4.6. Note that the disturbance d is added to the output y_L of the system T. Assuming a linear, static relationship between u and y_L,

Table 4.1: Enhanced Block Diagram (List of the Symbols)

Symbol	Description
R_L	Room with only the light fixtures
R_D	Room with only the daylight
L	System of Luminaires
C	Controller
D	Luminaire Driver
u	Control variable
y_R	Preferred illuminance values
y	Actual values of the illuminance
y_L	Illuminance due to only the light fixtures
d	Illuminance due to only the daylight
p	Input power for the light fixtures
ϕ_D	Luminous flux due to the daylight
ϕ_A	Luminous flux due to the luminaires

one has that:

$$y_L(t) = Tu(t) \tag{4.3}$$

The entries of the T matrix can be estimated by using the algorithm described in the System Identification section.

In conclusion, the block diagram of the control system has been simplified up the the point where the system under control is represented by the linear, static, time invariant system T as shown in Figure 4.7.

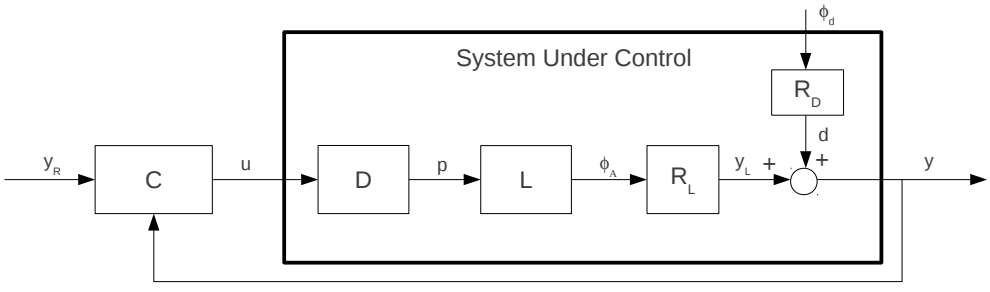

Figure 4.5: The enhanced block diagram of the control system.

System Identification

Let us consider a system with n light fixtures and m ambient light sensors placed in the points of interested of the work plane. Let us assume that the room is lit by only the luminous flux generated by the luminaires. In this case $y = y_L$, that is the measured illuminance is equal to the illuminance generated by only the light fixtures. Therefore one has that $y = Tu$ where y is a $n \times 1$ vector, u is a $m \times 1$ vector, and T is a $m \times n$ matrix:

$$\begin{bmatrix} y_1 \\ y_2 \\ \cdots \\ y_m \end{bmatrix} = \begin{bmatrix} t_{1,1} & t_{1,2} & \cdots & t_{1,n} \\ t_{2,1} & t_{2,2} & \cdots & t_{2,n} \\ \vdots & \vdots & \ddots & \vdots \\ t_{m,1} & t_{m,2} & \cdots & t_{m,n} \end{bmatrix} \begin{bmatrix} u_1 \\ u_2 \\ \cdots \\ u_n \end{bmatrix} \tag{4.4}$$

The following part of this section describes a simple identification method to estimate the entries of the T matrix. Let us assume that all the luminaries and all the sensors are uniquely identifiable. Therefore, u_i is the control variable for the luminaire number i while y_j is the illuminance value from the sensor number j. The parameter estimation algorithm is described in the pseudo-code 1. Note that in general the term δ is not null; in those cases δ can be considered as part of the imperfect knowledge of the model of the system. It is one of the tasks of an effective closed-loop control to counteract modelling errors.

Table 4.2 shows the list of the vectors produced during the sampling and measurement procedure in the case of the input u_i.

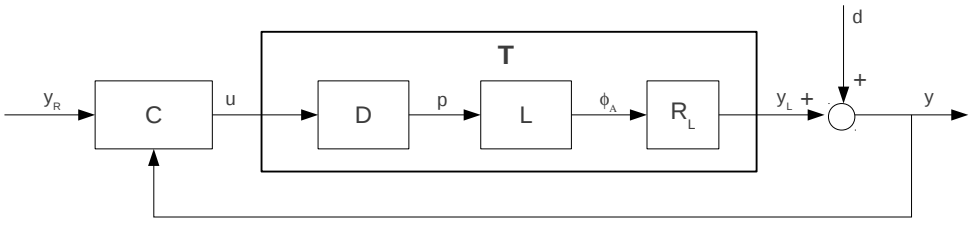

Figure 4.6: The subsystem to consider in the control scheme.

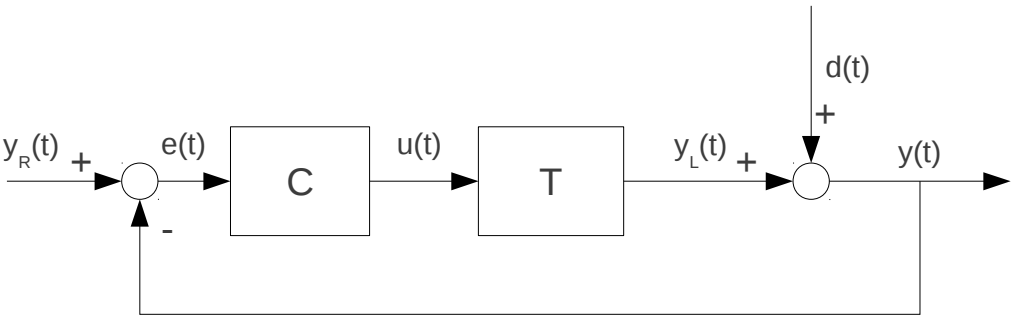

Figure 4.7: The base block diagram for the control scheme.

Table 4.2: Sampling data for parameter estimation.

u_i	y_1^i	y_2^i	...	y_m^i
$u_{i,1}$	$y_{1,1}^i$	$y_{2,1}^i$	...	$y_{m,1}^i$
$u_{i,2}$	$y_{1,2}^i$	$y_{2,2}^i$	...	$y_{m,2}^i$
...	...	...	...	...
$u_{i,k}$	$y_{1,k}^i$	$y_{2,k}^i$	...	$y_{m,k}^i$

4.4 Basic Considerations Regarding the Control Problem

The characteristics of the control problem defined in the system modelling section can be summarized in the following main aspects which are critical in the designing phase of the control system:

- The system under control is a linear static system. In a closed-loop control scheme, the lack of dynamics from u to y would cause instability in the presence of a hidden dynamics[29].
- With respect to the system to be controlled, there are n input and m outputs, where n is the number of luminaires and m is the number of the illuminance sensors; therefore, one has a multi-input multi-output (MIMO) control system.
- The daylight is considered as the primary large disturbance whose effect can be partially measured.

Algorithm 1 The parameter estimation algorithm.

1: **for** $i = 1 \rightarrow n$ **do**
2: Turn off all the light fixtures except the fixture i;
3: Generate K values for u_i; ▷ The result is the vector $u_i = \begin{bmatrix} u_{i,1} \\ u_{i,2} \\ \cdots \\ u_{i,K} \end{bmatrix}$
4: **for** $j \leq m$ **do**
5: **for** $h \leq K$ **do**
6: Measure $y^i_{j,h}$ ▷ Value of y_j for $u_{i,h}$. The result is the vector $y^i_j = \begin{bmatrix} y^i_{j,1} \\ y^i_{j,2} \\ \cdots \\ y^i_{j,K} \end{bmatrix}$
7: **end for**
8: Determine $y = t_{j,i}u + \delta$ from u_i and y^i_j ▷ Example least square fitting algorithm.
9: Use $t_{j,i}$ as the entry (j, i) of the T matrix.
10: **end for**
11: **end for**

- y_R, the desired output of the system under control, is a vector which contains the user's preferred levels of the illuminance in a specific set of points of interest. Considering that y_R will remain essentially constant, the control problem can be considered as a *regulation* problem [30].

4.5 Self-Tuning Optimisation-Based Control System

The type of control problem outlined in the previous section can be addressed by using several well known techniques suitable for MIMO systems. For example, a solution based on the linear quadratic control (LQC) theory with a well defined performance index could be a reasonable approach. Another possible solution to the control problem could be based on the formulation of a linear programming problem as proposed by Agogino and Wen [1][45]. Other approaches based on computational intelligent techniques like artificial neural networks and fuzzy inference systems (ANFIS), have the potential to provide solutions to complex problems involving usage patterns and other elements not easily modelled through traditional methods [23]. However, considering that one of the main objectives of this work is to provide a control scheme which can be easily implemented on a typical microcontroller while satisfying structural requirements related to stability and robustness, the design of

the control system presented in the following sections has been largely based on the self-tuning optimisation-based control scheme proposed in Moallem's work on the electron-beam position monitoring and feedback control at the Duke free-electron laser facility [29]. As will be shown later, the proposed control system makes explicit use of the model of the process and guarantees closed-loop stability. It is important to note that very often in the lighting control system literature the stability analysis is a property which is usually overlooked.

So far one has assumed that the structure of the control scheme is based on only a closed-loop architecture. However, as widely documented in the control literature, a proper use of even a partial knowledge of the disturbance could provide a valuable aid to the overall control system. For this reason, under the assumption that the control system is equipped with an estimator of the illuminance due to the daylight, a combination of feedforward and feedback control, also known as two-degree of freedom control structure [3], can be adopted to enhance the performances of the control system. The control scheme assumes that the component of the illuminance due to the intake of daylight is considered as a disturbance. This assumption is plausible since in most cases the variations associated to the daylight are difficult to predict. For example, in a cloudy and windy day, the solar irradiation could vary fairly quickly. Also, considering that in general the level of the illuminance y_R is due to both the daylight and the artificial light, then one can state that even the desired level of the illuminace has in general two components. By subtracting d_R, which is an estimate of the illuminance generated by the daylight, from y_R, $y_R - d_R$, one obtains the portion of the desired illuminance which is due to only the artificial light. Since d_R is an estimate of the illuminance caused by the daylight, that is the measurable part of the disturbance, then d_R could be used in the feedforward (anticipatory) portion of the control scheme which could help the overall control system to take some actions before an error is detected. By combining both the feedback and the feedforward structures one obtains the so-called two degree of freedom (2-DoF) control scheme [3]. The closed loop part of the control system addresses the uncertainties of the model and the components of the disturbance which are not measurable.

4.5.1 Fundamentals of the General Self-Tuning Optimisation-Based Control Scheme

The objective of this section is to provide the mathematical foundations of the self-tuning control scheme [29] which is at the core of the proposed control system. The general solution

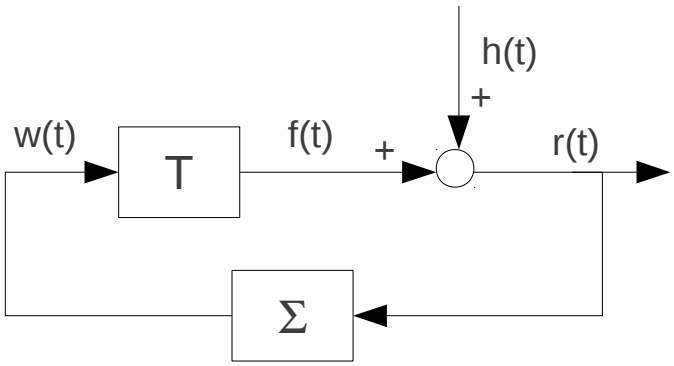

Figure 4.8: General control scheme.

of the control problem will be then adapted through proper transformations to the case represented in 4.7.

General Control Problem Definition

Let us consider the control system represented in 4.8.

Let T be a linear static system represented through a full row rank $m \times n$ rectangular matrix with $m < n$ where m is the number of outputs and n is the number of the inputs represented by the vector $w(t)$. Let $h(t)$ be an external variable representing a bounded disturbance acting on T. Let $r(t)$ the total output of the system, that is $r(t) = f(t) + h(t)$, that is

$$r(t) = Tw(t) + h(t). \tag{4.5}$$

Let us consider the performance index P_I defined in 4.6:

$$P_I = 0.5 \int_0^t r^T r \, \mathrm{d}\tau. \tag{4.6}$$

With reference to the closed-loop control system 4.8, the control problem consists in determining the controller Σ that minimizes the performance index P_I.

One aspect to note is the absence of a set point or reference signal. As a consequence, by enforcing the minimization of the performance index we are implicitly requiring that $r(t)$ shall be as close as possible to zero.

The Performance Index: While the majority of the control systems are usually designed in order to satisfy requirements related to the stability of the overall system, aspects associated with other performances are also extremely important. The formalization of the definition of the quality of a control system started in the 1950s in the context of the optimal control theory. The main concept is based on the idea of representing the overall quality through a performance index also called cost function or objective function. The list of the most popular performance indices includes [12]: the integral of the absolute magnitude of the error (IAE), integral of the time multiplied by the absolute magnitude of the error (ITAE), and the integral of the square error (ISE) [11] [12].

Control Problem Solution

In practical applications, models of processes are only approximations and parameters usually tend to vary with time. Those considerations are definitely valid for the case study covered in this work since a change in the geometry of the room could have an impact on the parameters of the model. Therefore, there are aspects related to the *robustness* of the overall control system that should be taken into account during the design phase of the controller. In this work the term robustness means that the control system provides almost the same performances in the presence of exogenous or endogenous perturbations [30]. One area of the control theory that provides useful and effective tools to deal with the aforementioned problems is the adaptive control system theory; it is in this area of the control literature that the solution of the control problem outlined in the previous section will be determined [29]. Another aspect to consider is that the lack of dynamics in $r(t) = Tw(t) + h(t)$ can cause instability in the closed-loop system [29].

Let us consider the closed-loop control scheme represented in 4.9. Let G a multi-input multi-output (MIMO) linear time-invariant dynamical system represented in the state-space as in 4.7

$$\begin{aligned} \dot{x}(t) &= Ax(t) + Br(t) \\ g(t) &= Cx(t) \end{aligned} \tag{4.7}$$

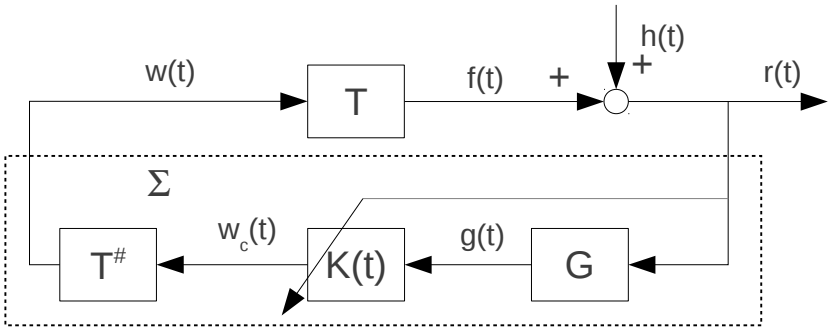

Figure 4.9: Self-tuning controller for the general control problem.

where A is a $m \times m$ Hurwitz matrix, B is a $m \times m$ matrix, and C is a $m \times m$ matrix. Let $K(t)$ a $m \times m$ time variant matrix whose dynamics is defined as follows:

$$\dot{k}(t) = -\mu r(t) g^T(t), \tag{4.8}$$

where $\mu \geq 0$. The rate of change for the matrix k expressed in 4.8 derives from the well known sensitivity method [30]. Therefore, one has the following time-varying output feedback:

$$w_c(t) = K(t) g(t). \tag{4.9}$$

Let $T^{\#}$ be the damped pseudoinverse matrix of T [44][29]

$$T^{\#} = (T^T T + \alpha^2 I)^{-1} T^T \tag{4.10}$$

where $T^{\#}$ is the unique minimizer of the sum expressed in 4.11 which is known as damped least squares [44][29].

$$\|Tw - w_c\|^2 + \alpha^2 \|w\|^2. \tag{4.11}$$

It can be proved [29] that a control law that minimizes the performance index P_I is provided by

$$w(t) = T^{\#} w_c(t) \tag{4.12}$$

It can also be shown [29] that the control law 4.12 guarantees the closed loop stability in the bounded-input bounded-output (BIBO) sense . It can also shown that the degree of the stability as well as the size of the error are strictly dependent from the values of the parameter μ. In particular, more stable performances can be obtained by using a small value of μ although the error would increase.

Real-Time Implementation of the Control Scheme

This section presents an approach to the implement of the control algorithm discussed above on a digital system [29]. The first step involves the discretization of 4.7 by using a sampling period T_s as shown in 4.13

$$\begin{aligned} x[k+1] &= \Phi x[k] + \Gamma r(k) \\ g[k] &= Cx[k] \end{aligned} \tag{4.13}$$

where

$$\Phi = e^{AT_s} \tag{4.14}$$

and

$$\Gamma = \int_0^{T_s} e^{A\eta} \, \mathrm{d}\eta. \tag{4.15}$$

Let us recall that T is an $m \times n$ matrix, where m is the number of outputs and n is the number of inputs. Let us choose the G system as follows:

$$\begin{aligned} A &= aI_m \\ B &= I_m \\ C &= I_m \end{aligned} \tag{4.16}$$

where a is a number such that A is a Hurwitz matrix. Therefore, the discrete form of the output of the G system is

$$g[k+1] = e^{AT_s} g[k] + \frac{e^{AT_s} - 1}{a} r[k]. \tag{4.17}$$

The discretization of the update rule of matrix $K(t)$, can be obtained by applying the trapezoidal integration of 4.8; the result is the following discrete update rule [29]:

$$K[k+1] = K[k] - 0.5\mu T_s(r[k+1]g^T[k+1] + r[k]g^T[k]). \tag{4.18}$$

4.5.2 Application of the General Control Scheme to the Case Study

Let us apply the solution to the control problem explained in the previous section by transforming the block diagram in 4.7 in order to reach the same structure shown in 4.8. The actual illuminance vector $y(t)$ is given by 4.19

$$y(t) = Tu(t) + d(t). \tag{4.19}$$

Let us change the sign and add $y_R(t)$ to both sides of 4.19

$$y_R(t) - y(t) = -Tu(t) + y_R(t) - d(t). \tag{4.20}$$

Since $e(t) = y_r(t) - y(t)$, from 4.19 follows

$$e(t) = -Tu(t) + y_R(t) - d(t). \tag{4.21}$$

The vector $y_R(t)$ is the user's preferred level of the illuminance in a given set of points of interest. In the presence of daylight, the total illumiance is given by two contributions: the luminaires and the daylight. Let $y_{RD}(t)$ be the contribution to y_R due to the daylight and y_{RL} the contribution associated to the luminaires. Therefore, one can state that

$$y_R(t) = y_{RD}(t) + y_{RL}(t). \tag{4.22}$$

It is important to note that $y_{RD}(t)$ is an estimation of $d(t)$; in the ideal case, $y_{RD}(t) = d(t)$. Considering that the illuminance generated by the artificial light is related to the input of the luminarie through the T matrix, one has that

$$y_R(t) = y_{RD}(t) + Tu_{RL}(t), \tag{4.23}$$

where $u_{RL}(t)$ is the input to the light fixtures to generate y_{RL}. Hence, if we apply 4.23 to 4.21 we obtain

$$e(t) = -Tu(t) + y_{RD}(t) + Tu_{RL}(t) - d(t). \tag{4.24}$$

By combining the terms having T one obtains

$$e(t) = T[u_{RL}(t) - u(t)] + y_{RD}(t) - d(t). \tag{4.25}$$

Let us introduces the following variables: $w(t) \doteq u_{RL}(t) - u(t)$ and $h(t) \doteq y_{RD}(t) - d(t)$. We can then rewrite 4.25 as

$$e(t) = Tw(t) + h(t). \tag{4.26}$$

We have then completed the transformation of the block diagram 4.7 up to the point where we have isolated the algebraic relationship between $e(t)$, $w(t)$, and $h(t)$. Let us consider the control problem where the objective is the determination of a control law $w(t)$ which minimizes the performance index P_I defined as

$$P_I = 0.5 \int_0^t e^T e \, \mathrm{d}\tau. \tag{4.27}$$

By considering that the subject of the control problem is a static, linear system and that $e(t)$ in 4.26 plays the same role as $r(t)$ in 4.5 of the general problem, then the performance index 4.27 is the same as 4.6. We can then conclude that we are in the same context described in the general self-tuning control scheme described in the previous section. The new block diagram of the control system is represented in 4.10.

Two-Degree of Freedom Control Scheme

So far the focus has been on $e(t)$, the error signal. Let us transform the block diagram 4.10 in order to show how the control law is related to the other signals, in particular to the control variable $u(t)$. By using the definitions and equalities presented in the previous sections, the complete control system can be represented as in 4.11.

The block diagram clearly shows the relationship between the feedback controller Σ and the rest of the system. However, there are other important elements to emphasize. First of all, it is important to note that the output of the controller is the signal $w(t) \doteq u_{RL}(t) - u(t)$ which is the variation to be applied to $u(t)$, the actual control variable of the system T.

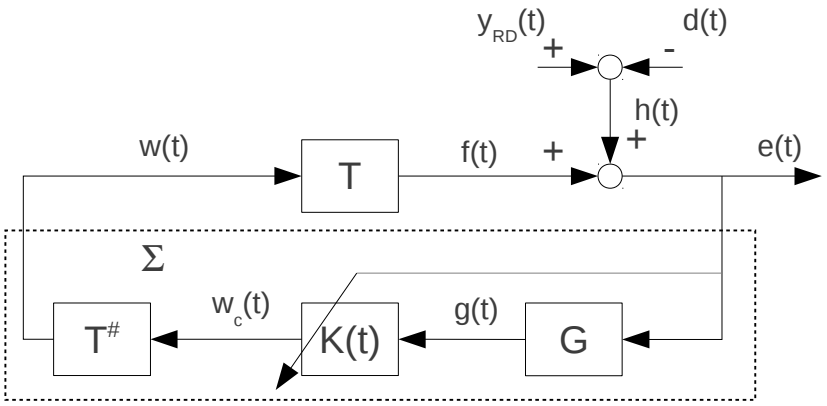

Figure 4.10: Block diagram with the self-tuning controller law for the case study.

Therefore, it is necessary to add $u_{RL}(t)$ to $w(t)$ in order to obtain $u(t)$. The value of $u_{RL}(t)$ is obtained by solving the system of linear equations

$$Tu_{RL} = y_R - y_{RD}, \tag{4.28}$$

which derives from 4.23. Considering that T is a full-row rank $m \times n$ matrix, with $m \leq n$, the system 4.28 is underdetermined; therefore, the purpose of the block U_{RCL} is to solve the system 4.28. For example, in Matlab one could use the operator `mldivide`. The main structural aspect to note is that the blocks U_{RLC} and D_e implement a feedforward controller which uses the information derived from the estimation of the intake of daylight to perform a feedforward rejection of the disturbance with a positive impact on the performances of the control system [3]. Thus, we have a combination of feedforward and feedback control also known as as two-degree of freedom control (2-DoF) in the control literature. The block diagram 4.11 also shows the presence of the saturation block which limits the control signal $u(t)$ within a physically acceptable range. For example, in the case of a PWM control signal, the acceptable range for the input signal $u_s(t)$ would be $[0, 100]$.

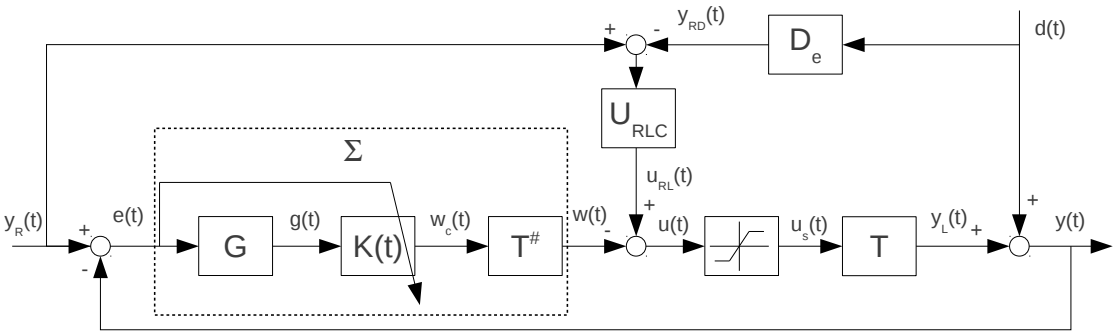

Figure 4.11: Two-degree of freedom self-tuning control system.

Chapter 5

Co-Simulation with MATLAB and Radiance

One of the main contributions of this thesis is the development of a simulation environment which allows a given lighting system controller to interact with a virtual scene in a quasi-real-time fashion. Systems engineers and lighting designers can then assess both the quality of a given control algorithm and the lighting design by comparing expected results with the data obtained almost immediately from the virtual scene. The flexibility of the simulation environment relies also on the ability to change scenarios like variations of sky conditions during a given day. Therefore, the proposed simulation environment allows to use the virtual scene not only for traditional off-line lighting analysis, but most importantly it provides the option to connect a real controller to the simulated scene, which is a model of the real room. The model could then be used not only for the validation of a given control scheme but also as a component to be used in a real environment. For example, some of the calculations could use a combination of virtual and real sensors by using sensor fusion techniques. A possible application could be the estimation of the illuminance due to daylight in parts of the work plane which are not accessible through real sensors.

The control algorithm could be implemented either through a fast prototyping environment like MATLAB or by means of a real microcontroller. Like in a real system, the controller communicates with virtual sensors and virtual luminaires so that commands and data can be used in a feedback loop. The following parts of this chapter describe the details of each component of the simulation system. It should be noted that the term co-simulator

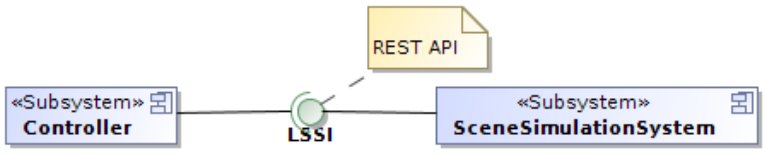

Figure 5.1: High level architectural view of the co-simulator.

derives from the fact that in this thesis the control scheme has been implemented entirely in MATLAB.

5.1 Introduction to Radiance

The centrepiece of the scene simulator is the Radiance software. Radiance is a set of programs for analysis and visualization of lighting systems developed by Greg Ward at the Lawrence Berkeley National Laboratory with the support from the U.S. Department of Energy. Radiance is a powerful *photorealistic rendering* system based on a light-backwards ray-tracing method derived from the computer graphics algorithm introduced in 1980 by Whitted [24]. In this method, light rays are followed from the points of interest up to the light source. Both electric light sources and daylight can be simulated with an extremely high level of accuracy as demonstrated through the comparison between Radiance calculations and real measurements [24][14]. Sky types can be easily defined for a given location, date, and time as well as luminaires can be modelled by importing IES photometric data files. Both features has been used extensively during the development of this thesis project.

5.2 Architecture of the Co-Simulator

The co-simulator is composed of three main components: a controller, a scene simulator, and an application programming interface (API). The controller is the component which calculate the control action, that is the input for the luminaires. The scene simulator represents a complete room including the light fixtures whose power levels are determined by the controller. The third component is the API which allows the communication between the controller and the scene simulator as shown in Figure 5.1.

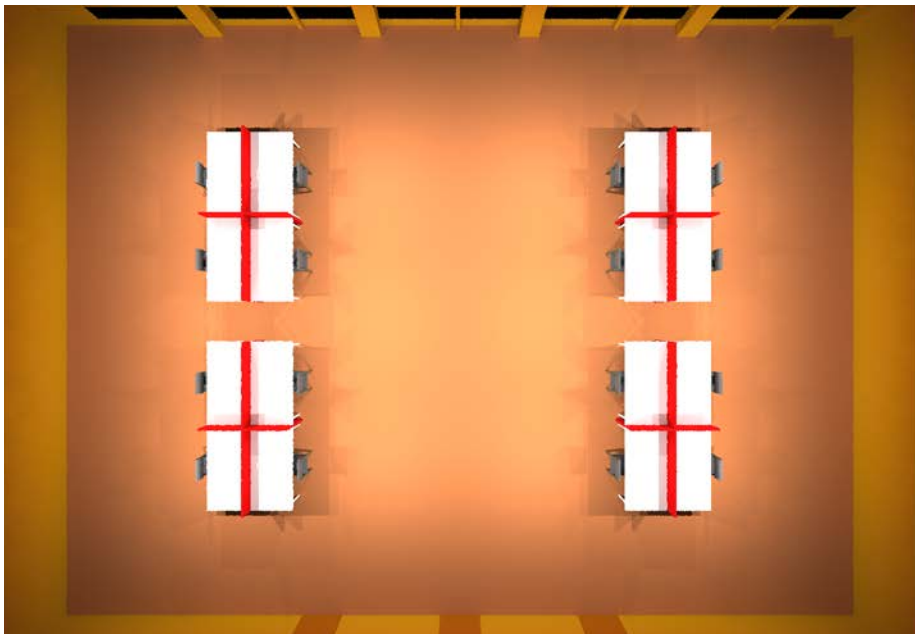

Figure 5.2: Plan view of the scene at night time.

5.2.1 Scene Simulation System

Scene Modelling

The scene simulation has been developed entirely with the Radiance software (version 4.0) in a Linux environment. The scene represents a fictitious office 20 meters long, 15 meters wide, and three meters tall. The room contains four cubicles and it is lit with both natural light through a large window with south exposure, and artificial light by means of twelve LED troffers as shown in Figure 5.2 and Figure 5.3.

An interesting features of Radiance is the ability to generate natural light through a set of sky conditions for any locations, date and time. Some of the sky types are the standard CIE overcast and clear sky with and without sun. The program used to generate sky types is called *gensky* and it has been extensively used in this project.

In Radiance, a scene is implemented through a set of text files structured according to a well defined format. Although any scene could be implemented through a manual configuration, that is by means of a simple text editor, the definition of very complex scenes are usually obtained through the conversion of intermediate artifacts generated through architectural design tools like AutoCAD or Google Sketchup.

Figure 5.3: Lateral view of the scene with daylight.

Luminaire Modeling: Importing Photometric IES Files

One of the most powerful tools provided by Radiance is the ability to model real luminaires. The formal process to create an accurate model of a given luminare is based on the availability of the photometric data of the luminaire. The photometric data are usually available from the manufacturers and are organized according to specific standards. The most widely used standards are: LM-63-2002, from the Illuminating Engineering Society (IES), which is largely used in North America and Europe; the German EULUMDAT, which is the de-facto standard photometric data file in Europe; and the TM14, from the Chartered Institution of Building Services Engineers (CIBSE), which is mostly used in UK [14]. Radiance provides the program `ies2rad` to convert a IES file to a set of Radiance files which can then be used to model and simulate a given light fixture. The scene simulator discussed in this work contains twelve LED luminarires representing the CREE CR24 50L LED architectural troffer. The photometric and mechanical specifications of the CREE CR24 50L luminarire

are included in the appendix B.1. The following is an example of how to convert an IES file to a set of Radiance files:

```
$ ies2rad -dm -t default -m 0.5 -o ./lamp ./file.ies
```

The `-m` option, whose values go from 0 to 1, is used to take into account the reduction of the initial lumen output of the luminarie due to ageing. The `-m` mutiplier can also be used to simulate the dimming of the light fixture. In fact, the LSSI API covered in 5.2.2 uses the `-m` option to set the level of the power of a given set of luminares.

5.2.2 LSSI: An API to Interact with the Scene

In systems engineering, and in software engineering in particular, a best practice consists in designing against standard interfaces so that the interactions among the subsystems is achieved solely through the interfaces. The use of interfaces leads to the design of systems composed of components which are loosely coupled making the overall system robust and resilient to changes because it is possible to replace or modify a component without any impacts on other parts of the system. Therefore, by only using interfaces any subsystem is unaware of the implementation details of any other components. The lighting simulation system interface (LSSI) is an interface that allows the controller to interact with the scene simulation system; therefore, the controller is totally unaware of the implementation details of the scene simulator. LSSI is a *representational state transfer* (REST) *application programming interface* (API) developed in Java and running as a servlet within a servlet container like Apache tomcat. Another major benefit of using LSSI consists in the ability to deploy the controller and the scene simulator in separate environments. The latter aspect is particularly important considering that the computational resources required by Radiance could be very high especially in terms of CPU usage. Considering that Radiance allows to perform parallel computations like illuminance calculations and image rendering, it would be beneficial to deploy the scene simulator on a cloud computing environment like Amazon Web Services (AWS) where multiple servers could be hidden by the LSSI as shown in Figure 5.4.

5.2.3 Controller Implementation with MATLAB

The real-time implementation of the control scheme described in 4.5.1 has been developed entirely with MATLAB (R2011a). The development approach has been based on the object

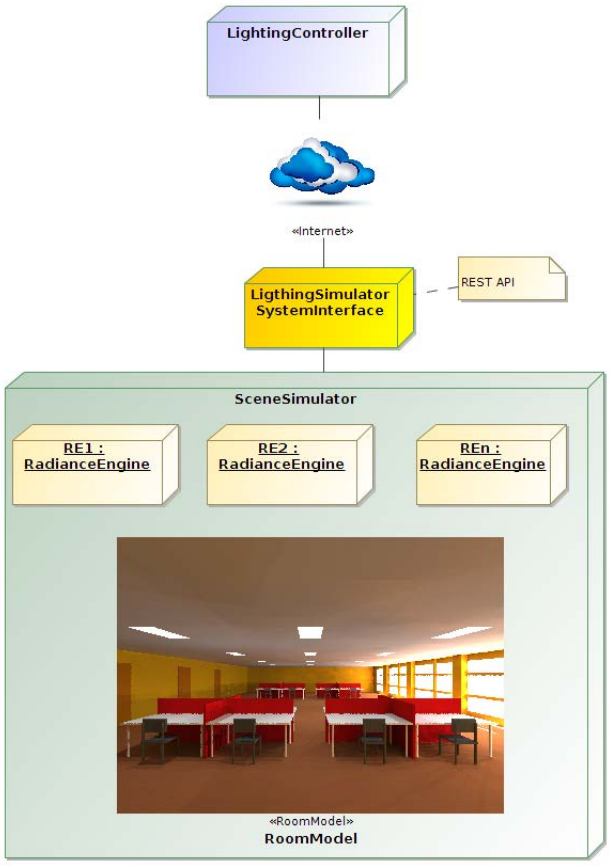

Figure 5.4: The lighting simulator system interface.

oriented capabilities provided by MATLAB. The core of the controller can be depicted through the Unified Modelling Language (UML) class diagram of Figure 5.5. Table 5.1 contains a brief description of each class.

The discrete implementation of the control law implies that the controller will perform its own tasks at specific instants of time. The UML sequence diagram in Figure 5.6 shows a high level view of the behaviour of the controller.

A Simple Anti-Windup Mechanism

One simple way to keep the entries of the K matrix bounded is to stop the integration whenever the saturation occurs due to a large irradiation from natural light. The integration can be partly stopped as follows. Let us assume that a fairly accurate estimation of

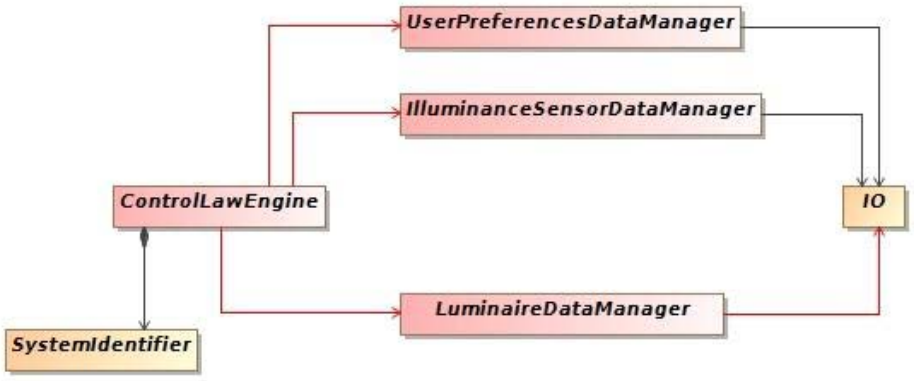

Figure 5.5: Controller: class diagram.

Table 5.1: Controller: Software architecture (Classes)

Class Name	Description
IO	This class provides the interface to communicate with the rest of the lighting network.
UserPreferencesDataManager	This class is responsible for collecting the data related to the user's preferences.
IlluminanceSensorDataManager	This class is responsible for collecting the data coming from the illuminance sensors.
LuminaireDataManager	This class is responsible for interacting with the luminaires.
ControlLawEngine	This class calculates the control output by using the data received by means of the data managers classes.

the illuminance due to the daylight is avaiable. Let us then consider the illuminance measurement at a specific sensor s_i. If the actual illuminance value exceeds the preferred value while the illuminance due to only the daylight already exceeds the set point, then there is no reason for the controller to keep turning off some of the luminaires since at that point those luminaires will be already saturated. One way to inform the controller that one part of the system does not need further control actions consists in simply setting $e_i = 0$. By artificially setting $e_i = 0$, the controller will assume that for that part of the system under control the target has been reached. The error e_i will resume its real value once the effect of the daylight will drop below the set point. This simple solution has proven very effective as shown in the test results.

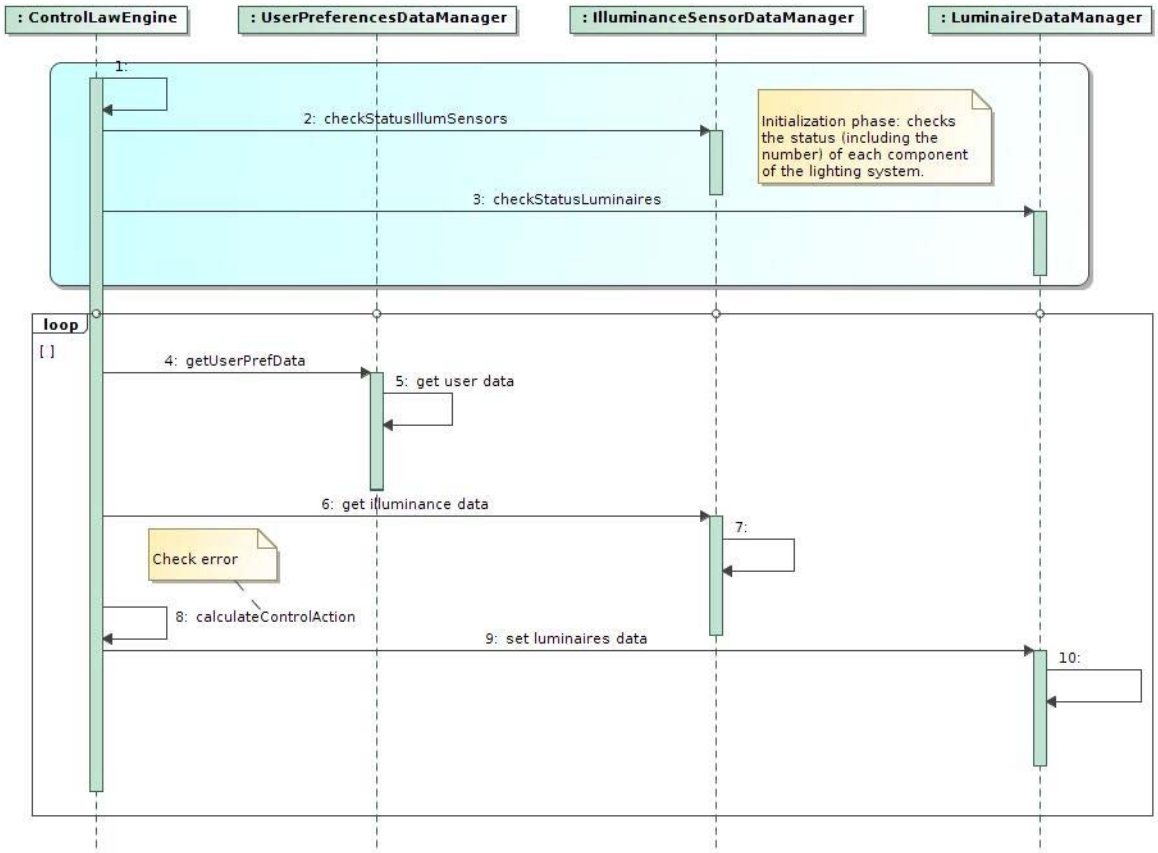

Figure 5.6: Controller: sequence diagram.

5.3 Test Results

This section presents a set of test cases and the corresponding test results by using the Radiance model of the room described before. The test cases are grouped in two sets:

- Control without daylight. This case could happen during night time or when the curtains are completely closed.
- Control with daylight. This case is based on the hypothetical intake of natural light on April 24th in Vancouver, BC, Canada, assuming a clear sky without direct sun. These conditions correspond to a standard CIE clear day.

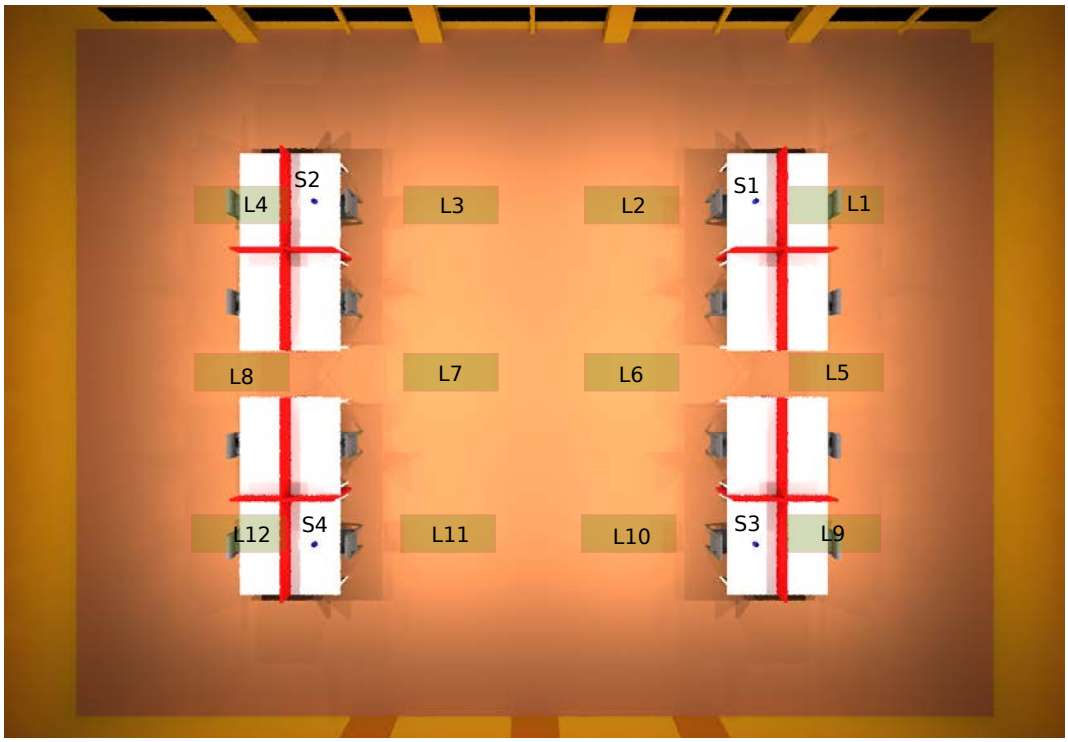

Figure 5.7: Plan view of the simulated room with annotated sensors and luminaires.

5.3.1 System Identification

Before proceeding with any tests, the first step to be addressed is the system identification of the system under control; the result of the identification process is the T matrix described in 4.3. The specific case that will be considered in the following section is a room lit by 12 luminaries. There are four points of interest in the work plane where the illuminance sensors are placed. Figure 5.7 depicts the plan view with the luminaires, identified through the labels L_i where $i = 1, 2, ..., 12$, and the illuminance sensors S_j, $j = 1, 2, 3, 4$.

The identification of the T matrix is obtained by implementing the identification algorithm described in 4.3 in absence of daylight in order to determine an accurate relationship between each luminaire and the illuminance sensors. The entries of the T matrix are shown in 5.1.

$$T = \begin{pmatrix} 2.134 & 0.884 & 0.071 & 0.008 & 0.369 & 0.247 & 0.051 & 0.008 & 0.029 & 0.029 & 0.021 & 0.007 \\ 0.009 & 0.071 & 0.876 & 2.147 & 0.007 & 0.057 & 0.247 & 0.376 & 0.006 & 0.020 & 0.029 & 0.030 \\ 0.028 & 0.028 & 0.020 & 0.006 & 0.369 & 0.247 & 0.051 & 0.011 & 2.142 & 0.890 & 0.074 & 0.010 \\ 0.006 & 0.020 & 0.029 & 0.029 & 0.011 & 0.051 & 0.247 & 0.376 & 0.009 & 0.073 & 0.883 & 2.155 \end{pmatrix}. \tag{5.1}$$

The damped pseudoinverse matrix $T^{\#}$ is described in 5.2 and has been calculated by using

the damping factor $\alpha = 0.03$.

$$T^{\#} = \begin{pmatrix} 0.386 & -0.011 & -0.021 & -0.004 \\ 0.159 & 0.007 & -0.006 & 0.001 \\ 0.007 & 0.157 & 0.001 & -0.006 \\ -0.011 & 0.385 & -0.004 & -0.021 \\ 0.062 & -0.002 & 0.062 & -0.001 \\ 0.041 & 0.006 & 0.041 & 0.006 \\ 0.006 & 0.041 & 0.006 & 0.041 \\ -0.002 & 0.063 & -0.001 & 0.062 \\ -0.021 & -0.004 & 0.385 & -0.012 \\ -0.006 & 0.001 & 0.160 & 0.007 \\ 0.001 & -0.006 & 0.007 & 0.157 \\ -0.004 & -0.021 & -0.012 & 0.384 \end{pmatrix}. \tag{5.2}$$

It should be noted that while T is a 4×12 matrix, $T^{\#}$ is 12×4 matrix.

5.3.2 Control without Daylight

Let us consider the case where the room is lit only through the luminaires. Let us assume that the preferred illuminance values are represented through the vector 5.3

$$y_R = \begin{pmatrix} y_{r1} \\ y_{r2} \\ y_{r3} \\ y_{r4} \end{pmatrix} = \begin{pmatrix} 300 \\ 300 \\ 300 \\ 300 \end{pmatrix}, \tag{5.3}$$

where y_{ri} is the preferred level of the illuminance at the location where the sensor S_i is located with $i = 1, 2, 3, 4$.

Control Action

Let us examine the trend of the control signal $u[k]$ where k represents the discrete time, $k = 0, 1, 2, ...$ The data points are listed in table 5.2.

The values of each component of the control signal are integer from 0 to 100 and represent the power level expressed in percentage. Therefore, a value of 0 means that the luminarie has been turn off while a value of 100 means that the luminarie will receive 100% of the power. One interesting aspect to note is that the controller has chosen to give more weight to the luminaries which are closer to the sensors by setting for them the maximum level of power while using the remaining light fixtures to offset the remaining amount of luminous flux. This solution has an impact of the overall energy savings as shown in the section 5.3.2.

Table 5.2: Control without daylight: control signal values.

k	u_1	u_2	u_3	u_4	u_5	u_6	u_7	u_8	u_9	u_{10}	u_{11}	u_{12}
0	100	0	0	100	0	0	0	0	100	0	0	100
1	100	2	2	100	2	1	1	2	100	2	2	100
2	100	9	9	100	7	5	5	7	100	9	9	100
3	100	18	18	100	14	11	10	13	100	18	17	100
4	100	28	27	100	21	16	16	21	100	28	27	100
5	100	37	36	100	27	22	21	27	100	36	35	100
6	100	43	41	100	32	25	24	31	100	42	40	100
7	100	46	44	100	34	27	26	34	100	45	43	100
8	100	49	47	100	36	29	28	36	100	48	46	100
9	100	49	48	100	37	29	28	37	100	49	47	100
10	100	48	47	100	36	28	28	36	100	48	45	100
11	100	47	46	100	35	28	27	35	100	47	45	100
12	100	47	45	100	35	27	27	35	100	46	45	100
13	100	46	45	100	34	27	27	34	100	45	45	100
14	100	46	45	100	34	27	27	35	100	45	45	100
15	100	47	47	100	35	28	28	36	100	47	46	100
16	100	47	47	100	35	28	28	36	100	47	46	100
17	100	46	46	100	35	27	27	35	100	46	45	100
18	100	45	44	100	34	26	26	34	100	45	44	100

Actual Illuminance Values

Figure 5.8 shows the comparison between the preferred values and the actual illuminance values as measured through the illuminance sensors S_1, S_2, S_3, and S_4. The trends of the error signals obtained during the execution of the control law are reported in the Figure 5.10. Let us recall the the K matrix is a function of the time. The variations of the entries of the K matries with the time are described in Figure 5.9.

Although the reference vector has been chosen arbitrarily, the control system shows that it is able to satisfy the requirement to keep the error as close as possible to zero. Is should be noted that, due to the physical limitations related to the geometry and photometry of the scene, not all the user's preferences can be satisfied. In other words, it might be possible that the user sets levels of the illuminance which are not physically achievable. In those cases, the controller will try to find the control law which minimizes the error. Figure 5.11 shows the plan view with with the isolux contour line illumination analysis.

Energy Savings

One of the requirements for an intelligent lighting system is the ability to save energy while maintaining a certain level of visual comfort. The previous sections have shown that the

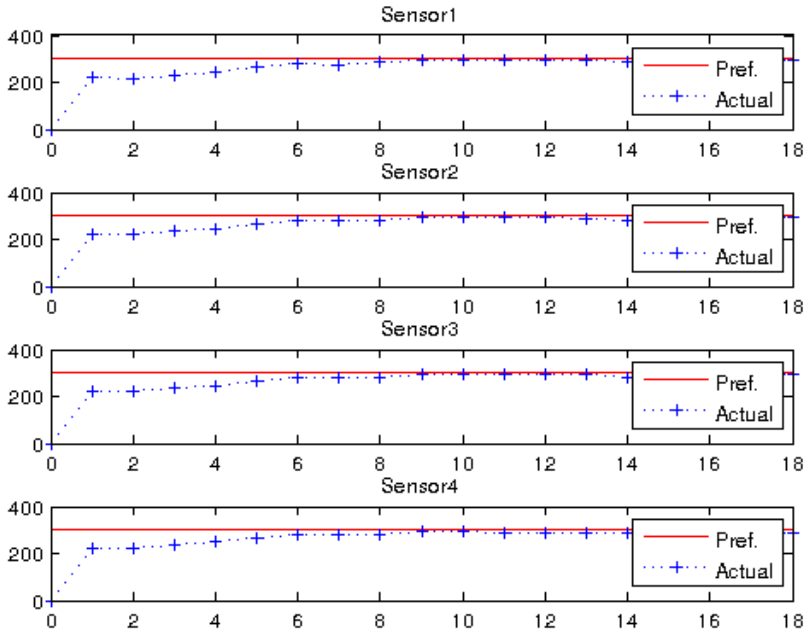

Figure 5.8: Actual illuminance values compared with preferred levels.

user's preferred level of the illuminance at the work plane level can be achieved. Let us then verify that the adaptive control algorithm can indeed bring some level of energy savings. For this purpose, let us compare the power consumption for the following two cases:

1. A traditional lighting system which does not allow to address each single luminaire. The dimming capabilities are limited to change the power level for the whole set of the light fixtures.

2. The lighting system based on the adaptive control scheme described in this work.

In both cases one assumes that all the luminaries are the same and that the product is the Cree CR24 50L which has a rated input power of 50 W.

Power Consumption Estimate for Non-Addressable Luminaires: Tests performed against the Radiance scene model have shown that in order to satisfy the preferred level of illuminace of 300 lx one should set the power level to 76% for all the fixtures. In this case the total power (TP_{NAL}) used by the lighting system would approximately be:

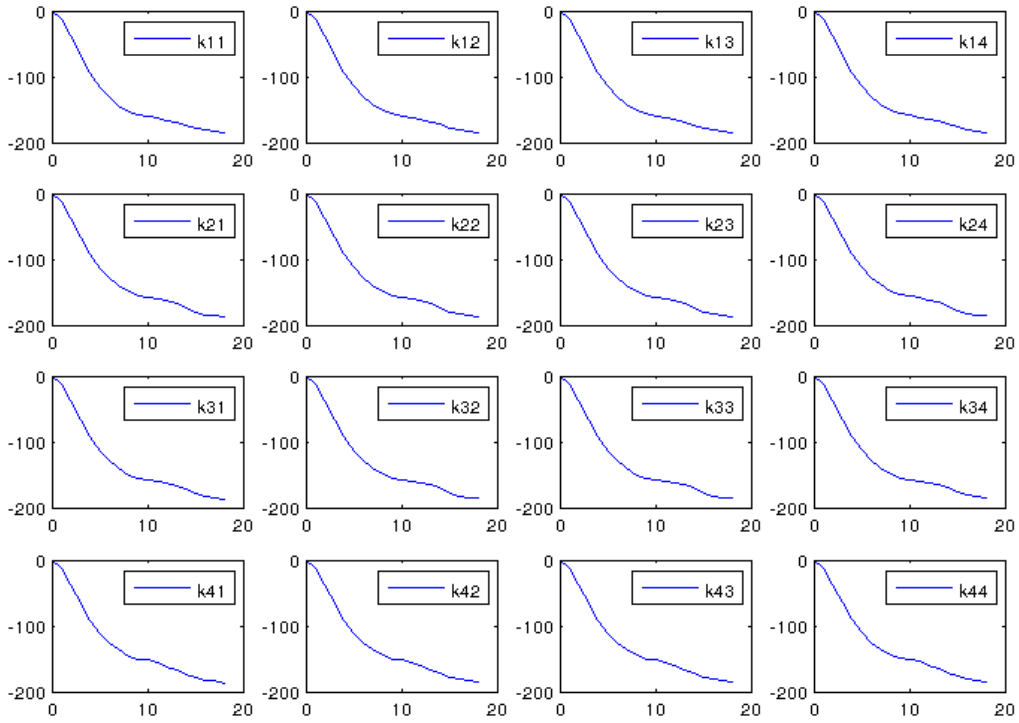

Figure 5.9: Entries of the K matrix.

$$TP_{NAL} = \frac{76}{100} \cdot 50 \cdot 12 = 456\,\mathrm{W}. \tag{5.4}$$

Power Consumption Estimate for Addressable Luminaires (Self-Tuning Control Scheme): Let TP_{AL} be the total power used by the light fixtures controlled through the self-tuning control scheme. TP_{AL} can be estimated by considering the data points listed at the bottom of Table 5.2 which are the power levels for the luminaires when the actual illuminance can be considered equal to the desired level. Therefore, an estimate of TP_{AL} is

$$TP_{AL} = \frac{698}{100} \cdot 50 = 349\,\mathrm{W}. \tag{5.5}$$

By comparing 5.4 with 5.5, the reduction of the power with respect to TP_{NAL} is

$$\Delta Power\% = 23\%. \tag{5.6}$$

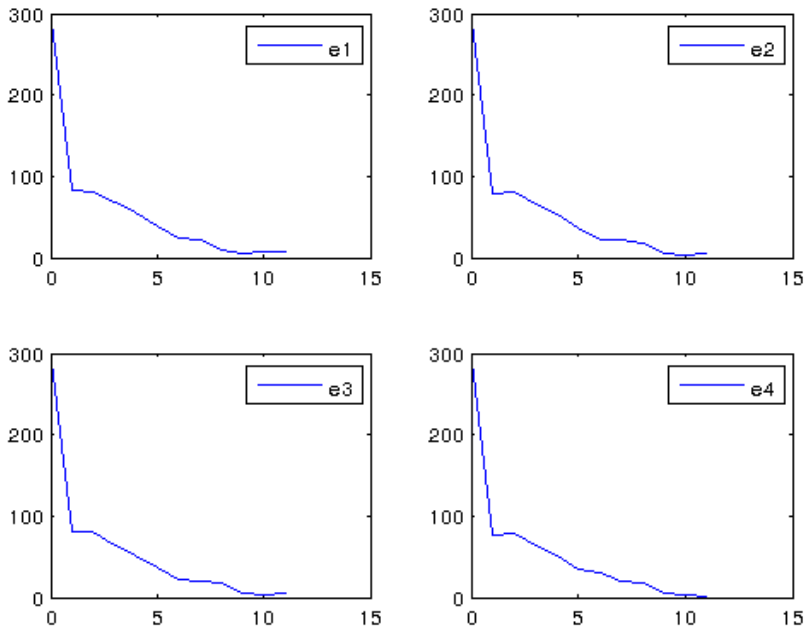

Figure 5.10: Trend of the error signals for the case with preferred illumiance 300 lx without daylight.

Therefore, by controlling the luminaries through the adaptive control scheme the energy savings are in the order of 23%. By adding extra functionalities like daylight harvesting and occupancy detection, the amount of the energy that can be saved can reach significant levels.

5.3.3 Control with Daylight

Let us include the natural light as a second source of the luminous flux. The integration between luminaires and daylighting is part of the *layered lighting* design, a key aspect in quality lighting [46]. Considering that the scope of the project does not include any forms of automatic control for the intake of the daylight through curtains or blinders, the requirement for a fixed level of the illuminance at the work plane level cannot be guaranteed since the irradiation due to the natural light could cause the illuminance to exceed the set point. Therefore, the test results shown in the following sections will have to be interpreted from the perspective that the objective of the control is to guarantee a minimum level of the reference

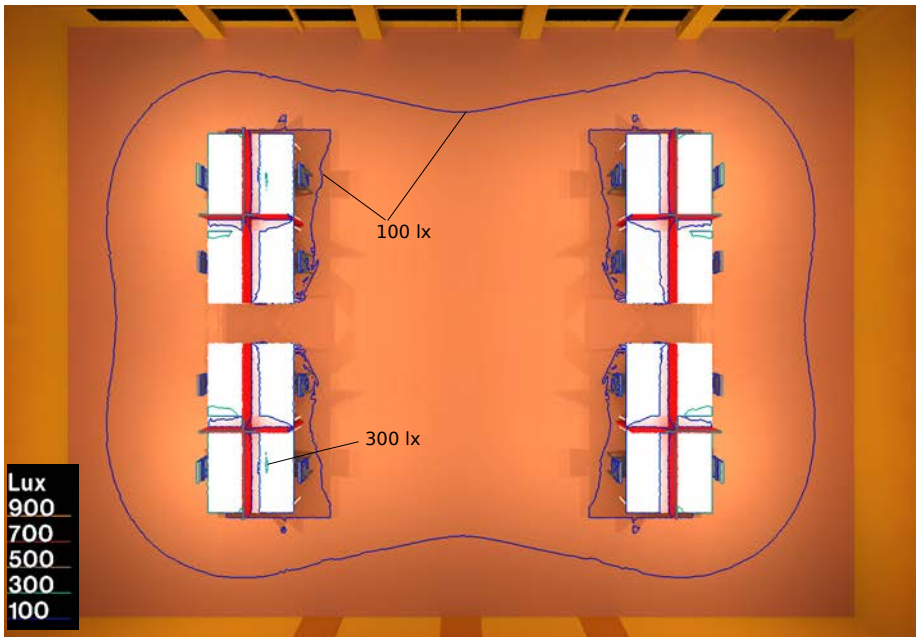

Figure 5.11: Plan view with isolux contour lines.

illuminance vector y_R in each sensor $s_i, i = 1, 2, \ldots, 4$. Tests have shown that the presence of a large contribution of daylight can cause the saturation of most of the luminaires with the consequent generation of a large error. Considering that the K the matrix is obtained through the integration of the error, the entries of the K matrix may assume extremely large values which have a negative impact on the performances of the control system in terms of both accuracy and stability. This is a typical case where the adoption of an anti-windup mechanism could be beneficial. The topic of the anti-windup techniques for MIMO systems is somewhat complex and several approaches have been documented in the control system literature [32]. A simple anti-windup mechanism is presented in section 5.2.3 (A Simple Anti-Windup Mechanism).

Let us then analyse the impact of daylighting on the performance of the control system during time period from 4:00 AM to 8:00 AM on the hypothetical April 24 in Vancouver, BC, Canada. The time line has been used in Radiance to calculate the irradiation through the window assuming a standard CIE clear sky condition. For example, to generate a clear sky conditions without direct sun in Vancouver on April 24 at 9:00 AM PDT, the Radiance program `gensky` can be used as follows [24] :

```
gensky 4 24 09:00PDT -s -a 49 -o 123 > vancouver-april24-0900-nosun.rad
```

The parameter `-a` represents the site latitude in degrees north while the parameter `-o` defines the site longitude in degrees west.

The content of the file `vancouver-april24-0900-nosun.rad` would then be the following:

```
# gensky 4 24 09:00PDT -s -a 49 -o 123
# Local solar time: 7.83
# Solar altitude and azimuth: 27.3 -77.1
# Ground ambient level: 12.3

void brightfunc skyfunc
2 skybr skybright.cal
0
7 1 5.85e+00 1.29e+01 3.78e-01 0.866079 -0.197655 0.459172
```

The file `vancouver-april24-0900-nosun.rad` is then used during the generation of the scene.

Control Action

The presence of a large amount of daylight has a significant impact on the output of the controller. Table 5.4 shows a sample of the data points regarding the control signal u_s the with respect to the discrete time k, starting from $k = 0$. Let us recall that u_s is the output of the controller limited between 0 and 100 as shown in Figure 4.11. The column u_i represents the power level for the luminaire $L_i, i = 1, 2, ..., 12$. It is important to note that the power level for all the luminaries close to the window, that is from L_1 to L_8, are gradually dimmed up to the 0. This is due to the growing intake of the daylight which produces a level of illuminance in the sensors S_1 and S_2 which is well beyond the preferred minimum level of 300 lx. Table 5.3 shows the estimated level of the illuminance produced by only the daylight from 4:00 AM 10:00 PM. The values have been determined through the Radiance software. For example, from Table 5.4 it is clearly visible that after $k = 53$, which in the simulated time line corresponds to approximately at 8:00 AM, the controller

Table 5.3: Measured illuminance values due to only the daylight.

Hour	S_1 (lx)	S_2 (lx)	S_3 (lx)	S_4 (lx)
4:00	0	0	0	0
5:00	31.7	38.8	5.47	5.38
6:00	116.3	134.7	20.22	18.89
7:00	233.7	248.7	40.51	35.90
8:00	467.66	465.68	79.64	68.53
9:00	718.52	691.9	120.28	102.67
10:00	945.3	886.26	151.12	131.75
11:00	1094.2	1065.12	173.69	154.26
12:00	1178.3	1214.2	184.67	170.15
13:00	1179.9	1314.6	188.4	177.95
14:00	1112.5	1332.05	178.57	182.3
15:00	1003.02	1272.51	163.84	171.74
16:00	885.2	1127.15	143.77	155.77
17:00	680.3	895.93	115.31	130.74
18:00	488.03	621.56	83.53	91.67
19:00	276.31	341.75	48.177	49.60
20:00	149.99	173.50	26.33	24.38
21:00	62.9	67.7	10.78	9.43
22:00	0	0	0	0

perceives that there is no need to inject further luminous flux through artificial light and reduces its output u accordingly.

The graphical representation of the the illuminance due to the daylight is shown in Figure 5.12.

Figure 5.13 depicts the trends of the input variables u_{si}, where each variable u_{si} is the input power expressed in percent for the luminaire $L_i, i = 1, 2, \ldots, 12$. Indeed, let us recall from 4.11 that the vector $u_s = [u_{s1}, u_{s2}, ..., u_{sn}]$ is the output of the saturation block which limits the values of each variable u_{si} between 0 and 100. By observing Figure 5.13, it should be noted that the luminaires which are less active are the light fixtures which are closer to the window.

Actual Illuminance Values

An analysis of the actual illuminance values shows that at 8:00 AM the preferred values of the iluminance at the locations S_1 and S_2 cannot satisfied since the illuminance due to only the daylight already exceeds the value of 300 lx. The consequence of the fact that there is no control on the intake of natural light, is shown in Figure 5.16 where is clearly visible that the actual error for both the sensors S_1 and S_2 becomes negative from 8:00 to 19:00.

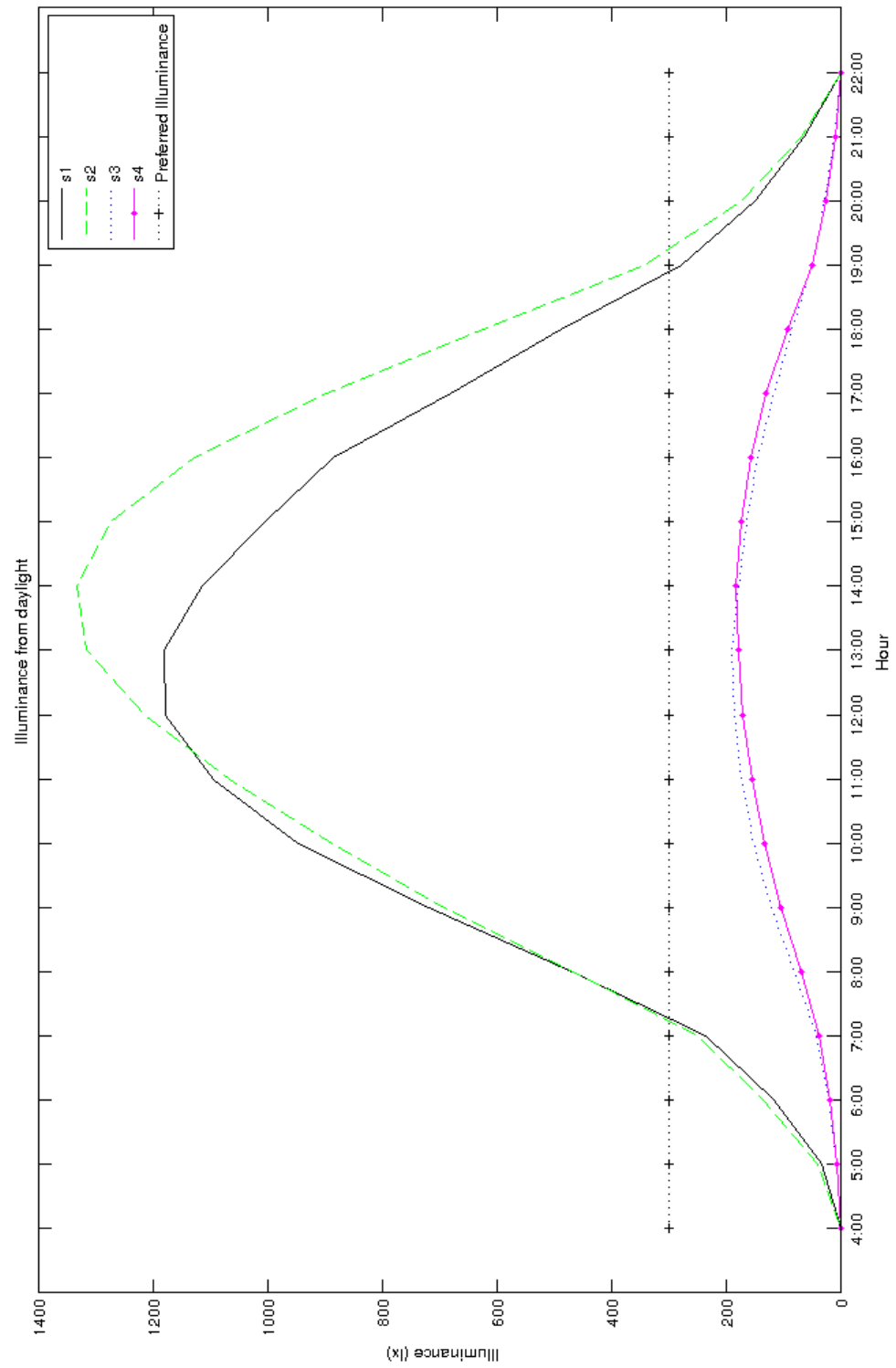

Figure 5.12: Measured illuminance values due to only the daylight.

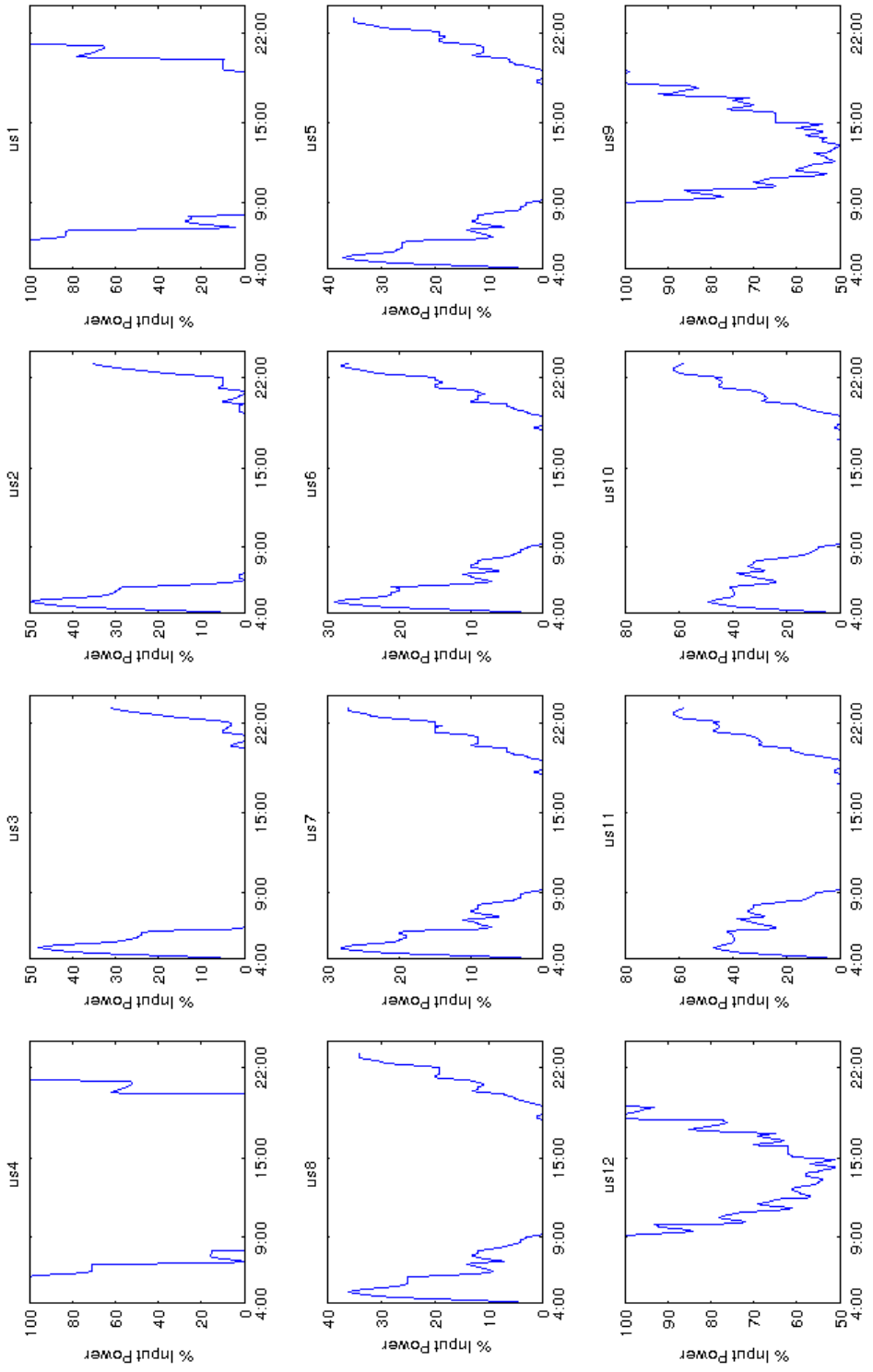

Figure 5.13: Control Input: trends from 4:00 AM to 10:00 PM.

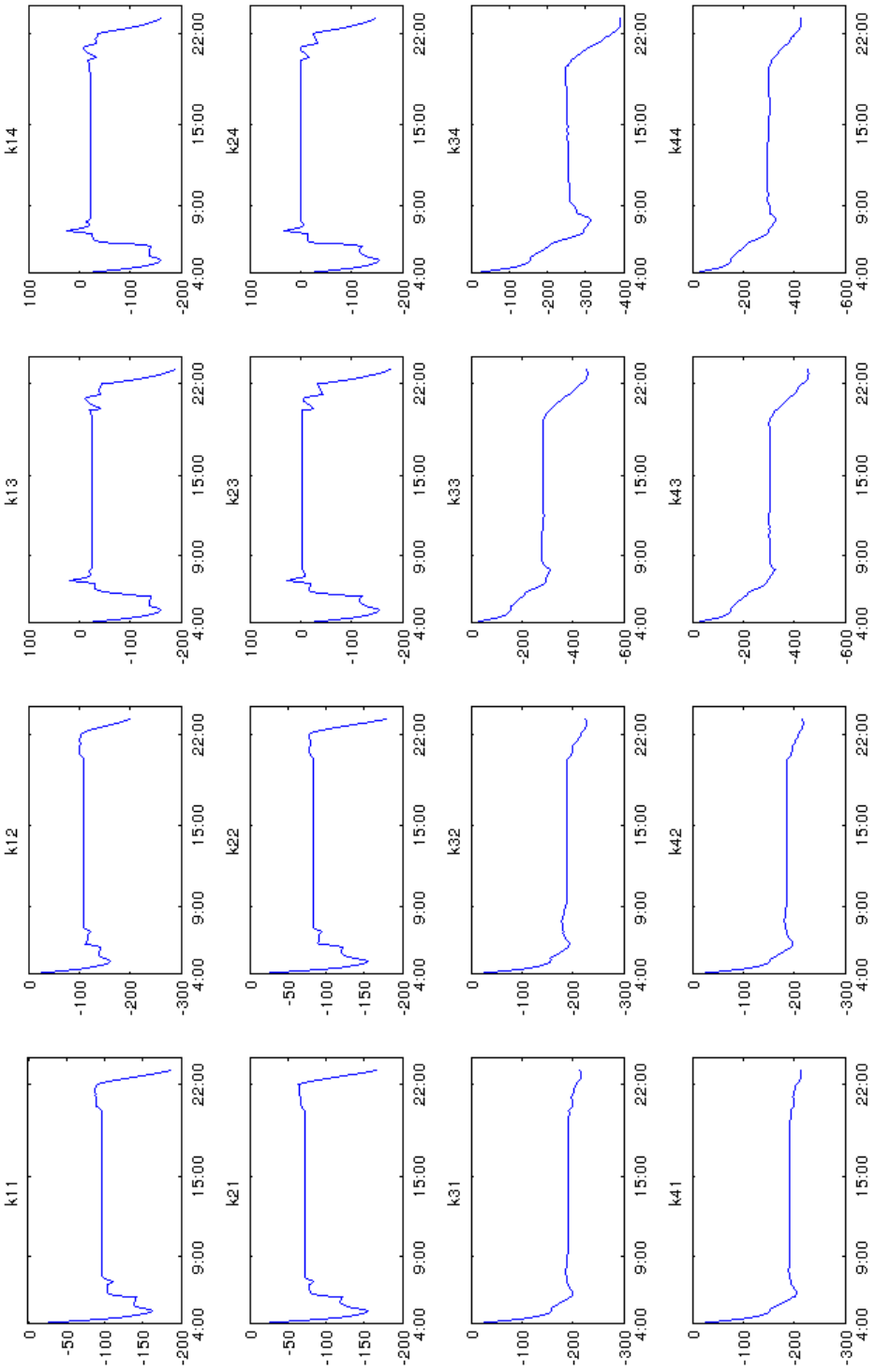

Figure 5.14: Evolution of the k matrix.

On the other hand, the entries of the k matrix are kept bounded as a result of the action of the anti-windup system which turns off the controller whenever the daylight exceeds the minimum levels of the preferred illuminance as show in Figure 5.14.

Energy Savings

One of the main advantages of adopting a layered lighting architecture is the ability to reduce the use of the electric energy, thanks to the intake of natural light. As shown in the previous sections, the control scheme performs an automatic dimming of the light fixtures as a consequence of the daylighting. Let us estimate the energy saved during the time period from 4:00 AM to 22:00 PM due to the automatic adjustment of the power levels by using the data points listed in Table 5.4. Like in the case of control without daylight, let us compare the following cases:

1. A lighting system which does not allow to address each single luminaire. All the luminaires receives the same dimming signal.

2. The lighting system based on the adaptive control scheme described in this work.

All the luminaries are based on the Cree CR24 50L troffer which has a rated input power of 50 W.

Energy Consumption Estimate for Non-Addressable Luminaires During the time period from 4:00 AM to 22:00 PM, assuming a power level of 76% for all the 12 fixtures in order to satisfy the minimum illuminance of 300 lx, the total energy used during that time frame is shown in 5.7:

$$TE_{NAL} = 8.6\,\text{kWh}. \tag{5.7}$$

Energy Consumption Estimate for Addressable Luminaires (Adaptive Control Scheme) An estimate of the energy used by the controlled lighting system can be obtained by considering the last data points after each change in the environment conditions which in the simulation happens at every hour. The data source for calculating the average power is the set of data points from Table 5.4. A simple calculation leads to the total energy for addressable luminaires (TE_{AL}) as shown in 5.8:

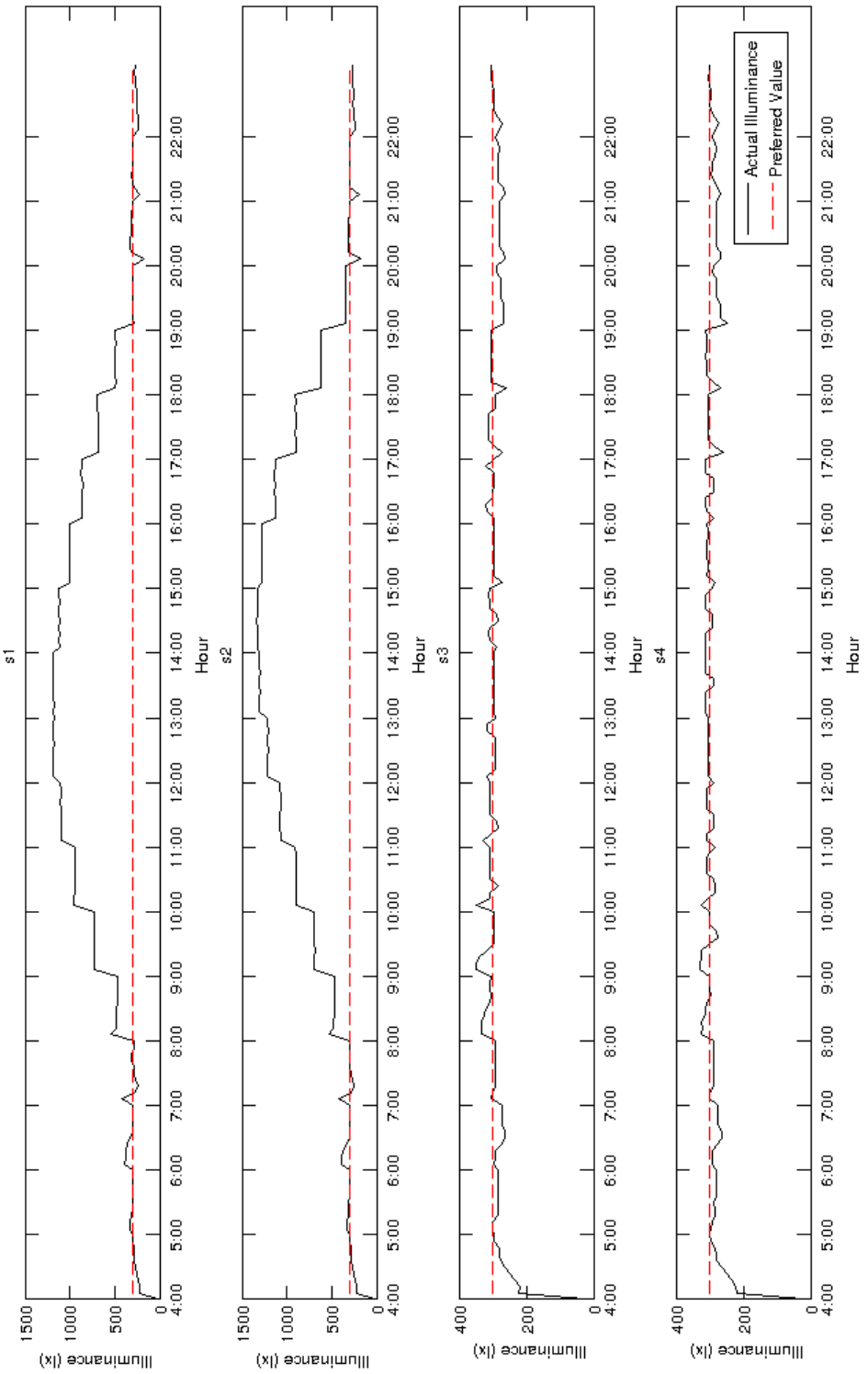

Figure 5.15: Actual vs. preferred illuminance: time line from 4:00 AM to 22:00 PM.

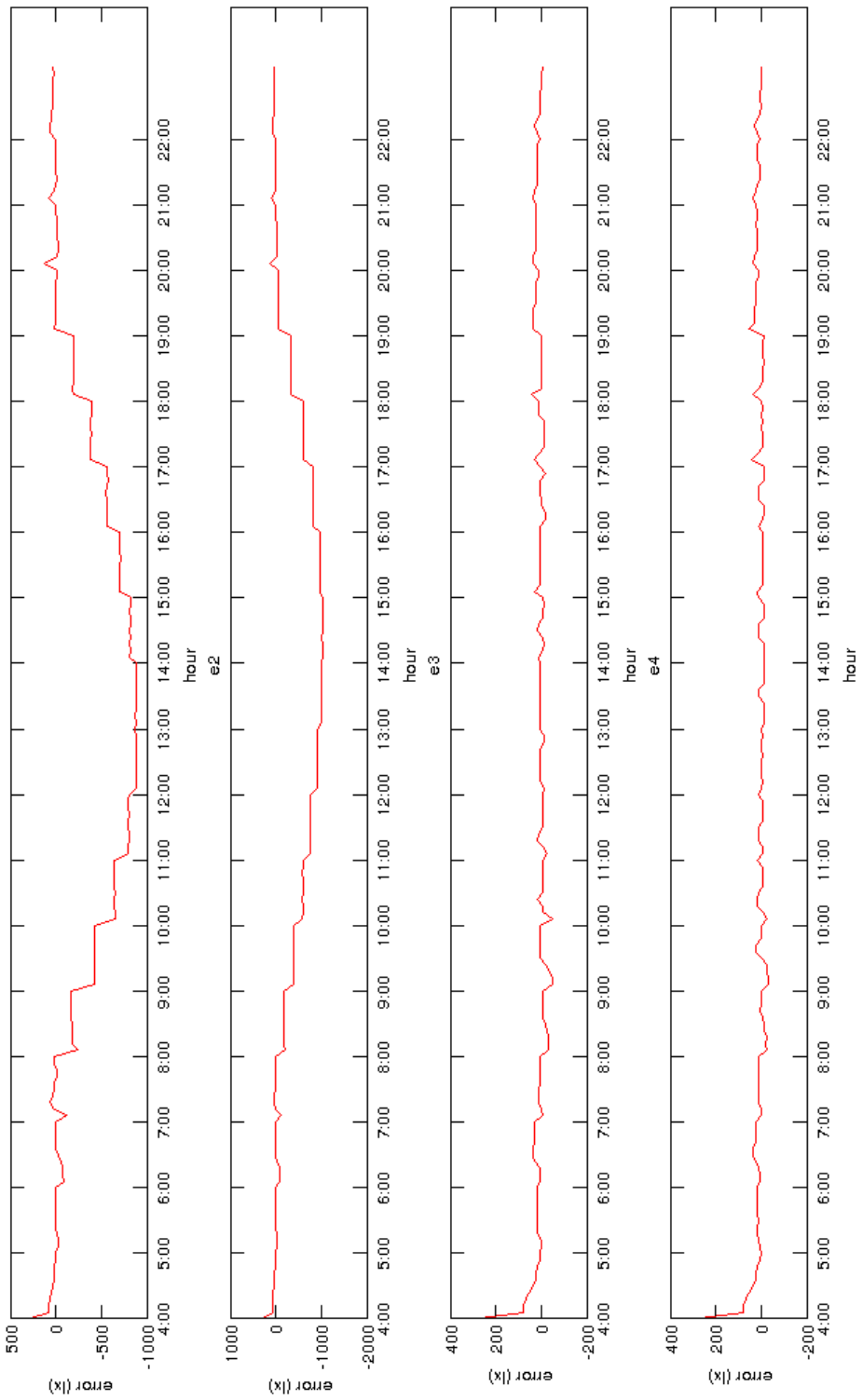

Figure 5.16: Illuminance Error: trend from 4:00 AM to 22:00 PM.

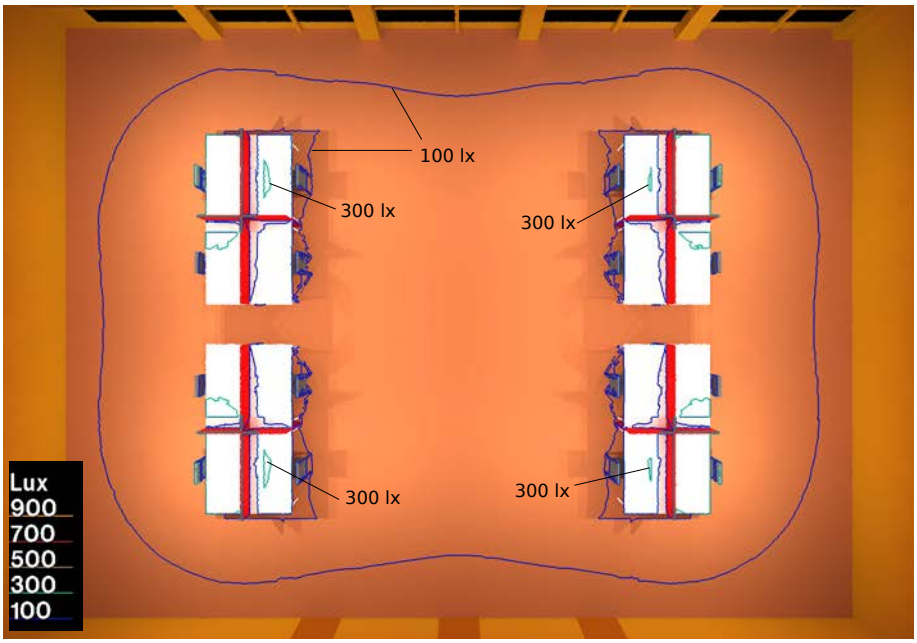

Figure 5.17: Plan view with isolux contour lines at 4:00 AM.

$$TP_{AL} = 2.87\,\text{kWh}. \tag{5.8}$$

By comparing 5.7 with 5.8, the energy saved with respect to TE_{NAL} is $\Delta Energy\% = 66.6\%$. This result clearly shows that an intelligent lighting system which includes a daylighting harvesting strategy is a compelling business case. The hourly breakdown for the energy consumption is show in Figure 5.22.

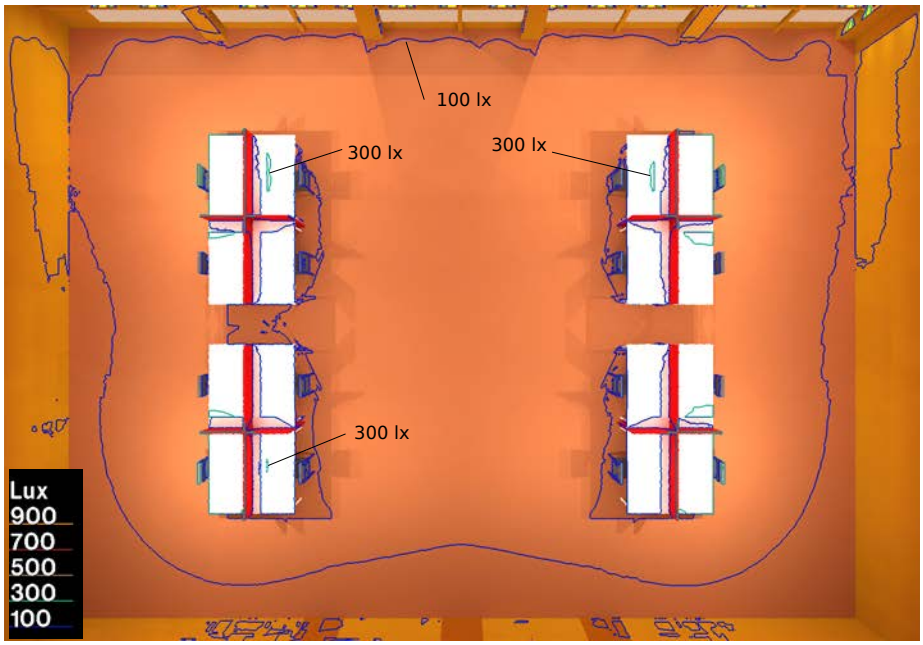

Figure 5.18: Plan view with isolux contour lines at 5:00 AM.

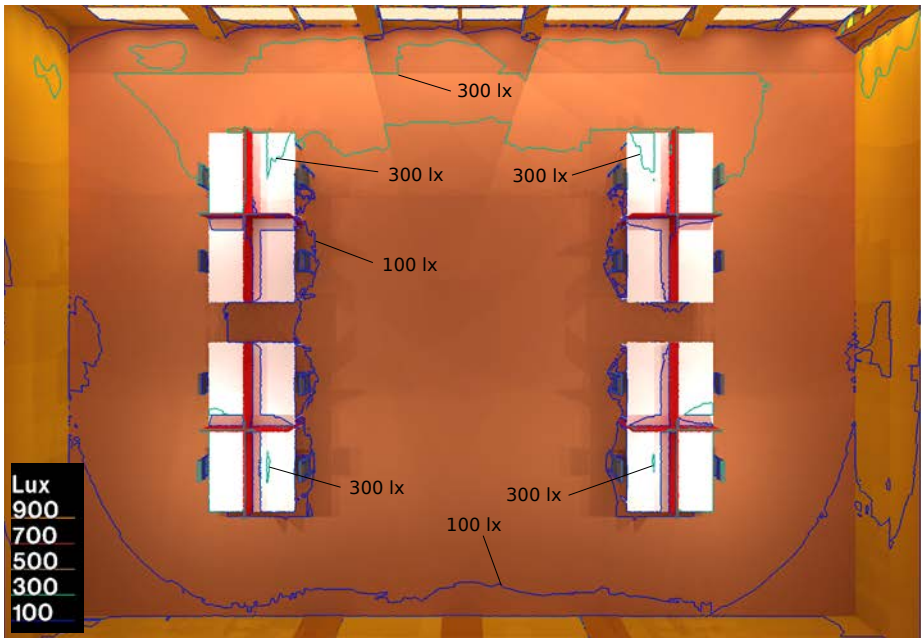

Figure 5.19: Plan view with isolux contour lines at 6:00 AM.

Table 5.4: Control with daylight: control signal values.

k	u_1	u_2	u_3	u_4	u_5	u_6	u_7	u_8	u_9	u_{10}	u_{11}	u_{12}
0	100	0	0	100	0	0	0	0	100	0	0	100
1	100	2	2	100	2	1	1	2	100	2	2	100
2	100	9	9	100	7	5	5	7	100	9	9	10
3	100	18	18	100	14	11	10	13	100	18	17	10
4	100	28	27	100	21	16	16	21	100	28	27	10
5	100	37	35	100	27	22	21	27	100	36	35	10
6	100	42	41	100	32	25	24	31	100	41	40	10
7	100	45	44	100	34	27	26	33	100	45	43	10
8	100	49	47	100	36	28	27	35	100	47	45	10
9	100	50	48	100	37	29	28	37	100	48	47	10
10	100	50	47	100	37	29	28	36	100	47	46	10
...												
16	100	46	45	100	34	27	27	35	100	45	45	10
17	100	45	44	100	34	27	26	34	100	45	44	10
18	100	45	43	100	34	27	26	34	100	45	45	10
19	100	41	39	100	32	25	24	32	100	44	43	10
20	100	38	35	100	30	24	23	30	100	42	41	10
21	100	35	32	100	29	23	22	28	100	42	41	10
22	100	33	30	100	28	22	21	27	100	41	40	10
23	100	32	28	100	27	21	20	26	100	40	39	10
...												
30	100	28	24	100	26	20	19	25	100	41	41	10
31	100	26	22	100	25	20	19	24	100	41	41	10
32	100	17	13	100	19	15	14	18	100	34	33	10
33	100	9	6	86	14	11	10	13	100	27	27	10
34	90	3	1	74	10	8	7	9	100	22	22	10
35	82	0	0	67	8	6	6	7	100	21	21	10
36	81	0	0	67	9	7	6	8	100	24	24	10
37	82	0	0	68	11	8	8	10	100	29	28	10
38	83	0	0	69	12	10	9	12	100	33	32	10
39	83	1	0	69	14	11	10	13	100	35	35	10
40	84	1	0	70	15	11	11	14	100	38	37	10
41	21	0	0	9	13	10	10	13	100	38	38	10
42	0	0	0	0	6	5	5	6	100	28	28	10
43	7	0	0	0	7	5	5	7	100	27	27	10
44	19	0	0	9	10	8	8	10	100	31	31	10
45	26	0	0	16	13	10	10	13	100	34	34	10
46	28	1	0	18	13	10	10	13	100	35	35	10
47	26	0	0	17	13	10	10	13	100	33	34	10
48	25	0	0	16	11	9	9	12	100	31	32	10
49	24	0	0	15	11	9	9	11	100	31	31	10
50	26	0	0	16	11	9	9	12	100	31	31	10
51	26	0	0	16	12	9	9	12	100	31	32	10
52	25	0	0	15	11	9	9	11	100	30	31	10
53	0	0	0	0	9	7	7	10	100	29	30	10
54	0	0	0	0	0	0	0	0	100	9	11	10
55	0	0	0	0	0	0	0	0	92	0	0	10
56	0	0	0	0	0	0	0	0	73	0	0	8
57	0	0	0	0	0	0	0	0	80	0	0	8
...												

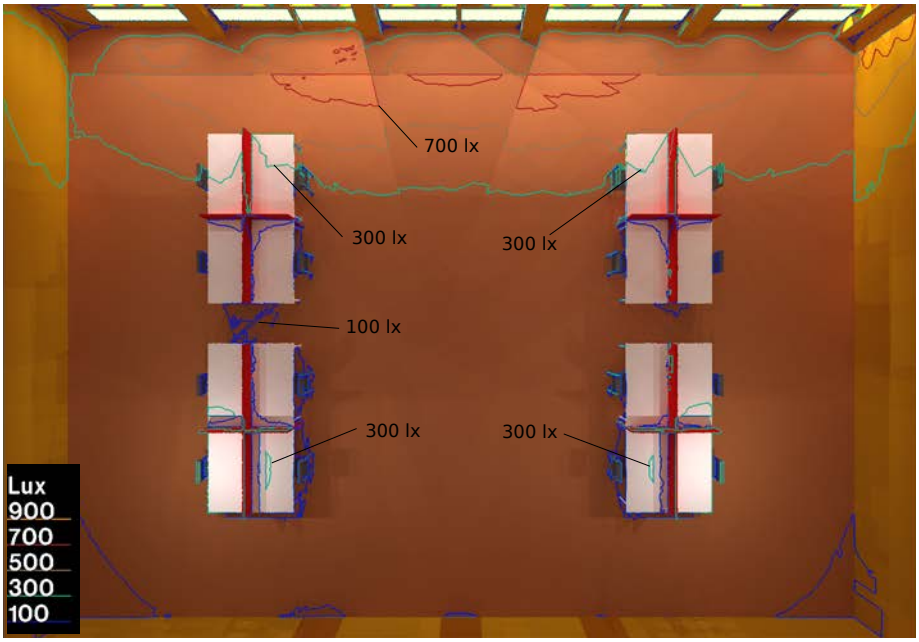

Figure 5.20: Plan view with isolux contour lines at 7:00 AM.

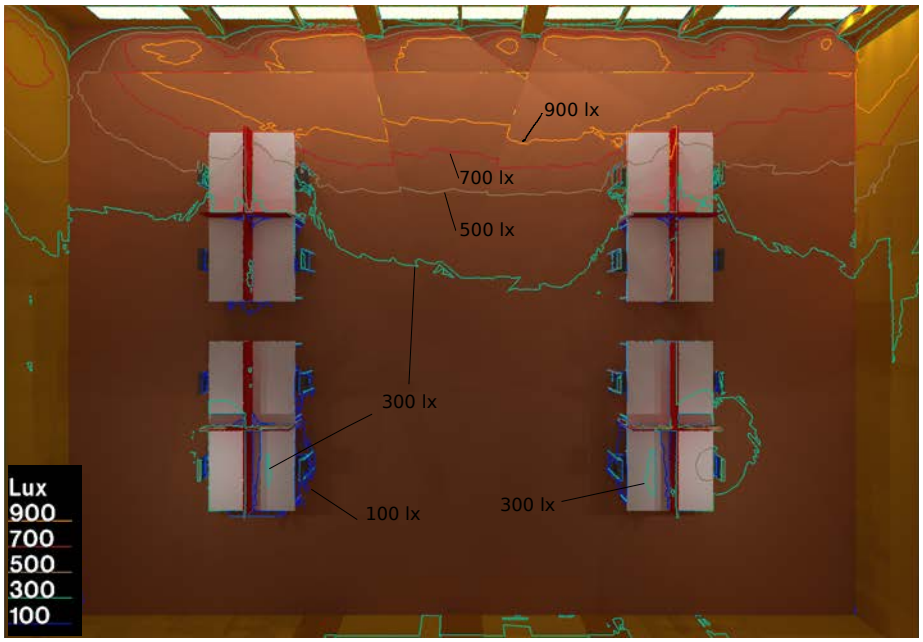

Figure 5.21: Plan view with isolux contour lines at 8:00 AM.

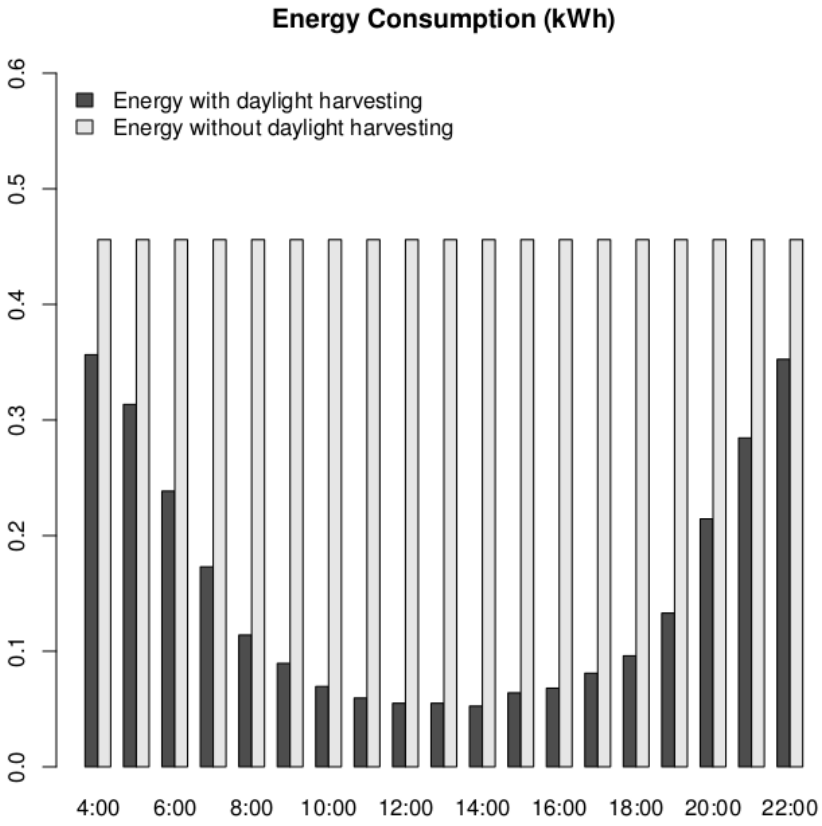

Figure 5.22: Hourly breakdown of the energy consumption.

Chapter 6

Validating the Control Scheme in a Real Scenario

While the previous chapters of this document have covered the definition of the control problem, a possible solution and the validation through a co-simulator, this chapter discusses the implementation of the control system in a real setting. The test results listed demonstrate the effectiveness of the control algorithm.

6.1 Testing Environment

The test bed used for validating the control algorithm is based on an existing test environment developed at the Mechatronic Systems Engineering (MSE) laboratory of Simon Fraser University. The core of the environment is a small room developed as a $1\,\mathrm{m} \times 1\,\mathrm{m} \times 1\,\mathrm{m}$ wooden box as depicted in Figure 6.1.

The room is equipped with two H042T LED luminaires, which are labelled as L_1 and L_2 in Figure 6.1, and two XCO100 illuminance sensors identified as S_1 and S_2. Figure 6.4 and 6.2 show the LED luminaire and the illuminance sensor respectively.

The controller, which has been implemented as a MATLAB/simulink process, sends control signals and receives illuminance sensor data by means of a communication system based on a MSP430F5438 microcontroller. The connection among the components of the test bed are represented in Figure 6.5. The details regarding both the simulink block diagrams and the electronic schematics are covered in the Laboratory Test Bed appendix C.

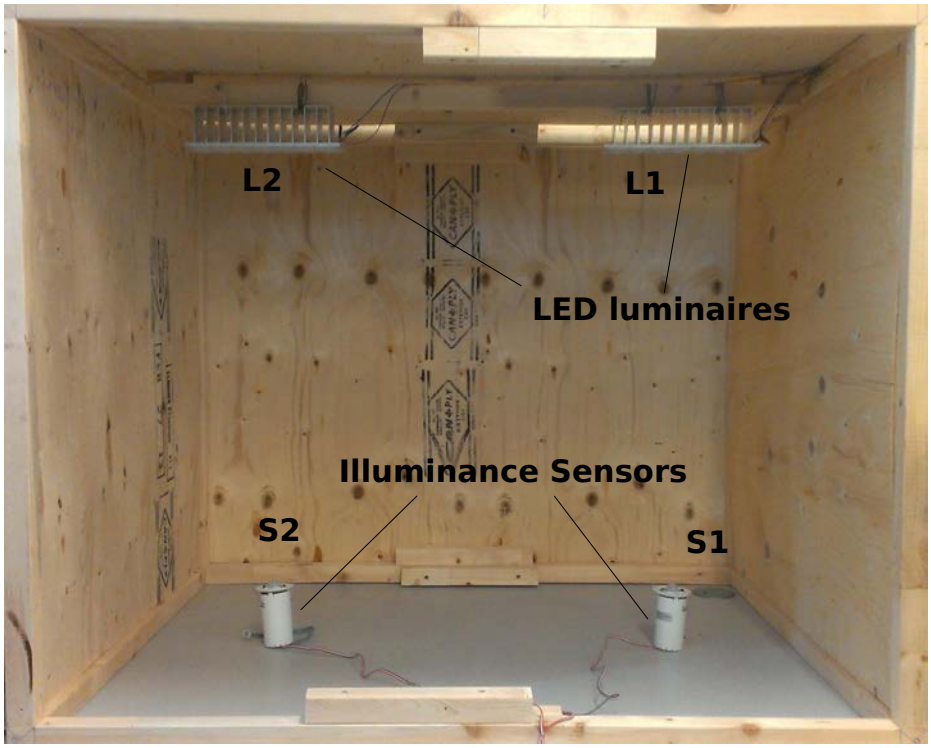

Figure 6.1: A small scale room used for testing.

6.2 System Identification

Considering that the number of the luminaries is equal to the number of the sensors, the system under control is described through a T matrix with two rows and two columns. The identification process, which is based on the procedure 1, has produced the matrices T and $T^{\#}$ as shown in 6.1 and 6.2 respectively.

$$T = \begin{bmatrix} 8.287 & 4.576 \\ 5.801 & 6.475 \end{bmatrix} \tag{6.1}$$

$$T^{\#} = \begin{bmatrix} 0.2388 & -0.1688 \\ -0.2140 & 0.3056 \end{bmatrix}. \tag{6.2}$$

Let us note that being T a square matrix, the pseudoinverse matrix $T^{\#}$ coincides with the inverse matrix T^{-1}.

Figure 6.2: The illuminance sensor.

6.3 Test Results

Let us validate the performances of the control scheme with respect to the small scale room by considering a procedure based on a time line characterized by a variable intake of daylight similar to what has been dome for the co-simulator . Albeit simple, this test procedure is fairly comprehensive since it shows how the controller responds to sudden changes of the disturbance. The intake of daylight were simulated through an external set of lamps since the facility did not allow to expose the small scale room to a substantial amount of natural light. The test results for the actual illuminance values, the error, and the control actions are shown in Figure 6.6, Figure 6.7, and Figure 6.8 respectively. Each diagrams clearly show three time intervals corresponding to the presence rather than the absence of daylight. It should be noted in particular how the controller reacts during the transitions between the presence of daylight and the absence of daylight. A sudden lack of daylight produces a drop in the total illuminance which is almost immediately brought to the desired level through an increase of the luminous flux generated by means of the LED luminaires. Considering that the reference $Y_R = \begin{bmatrix} 500 & 400 \end{bmatrix}$ is somewhat arbitrary, one can conclude that the behaviour of the control system is also satisfactory in a real scenario.

Figure 6.3: The communication unit based on a MSP430 evaluation board.

Figure 6.4: The LED Luminaire.

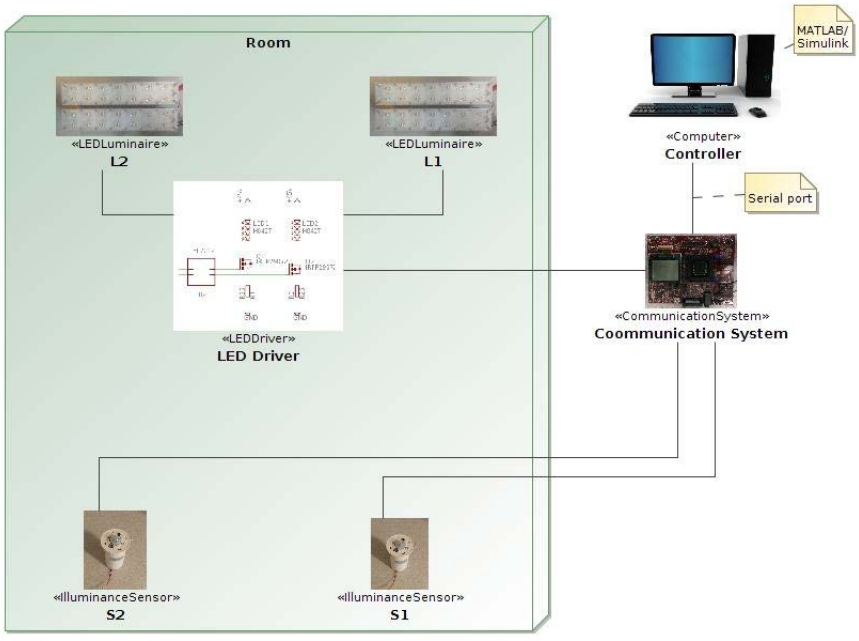

Figure 6.5: Test bed deployment diagram.

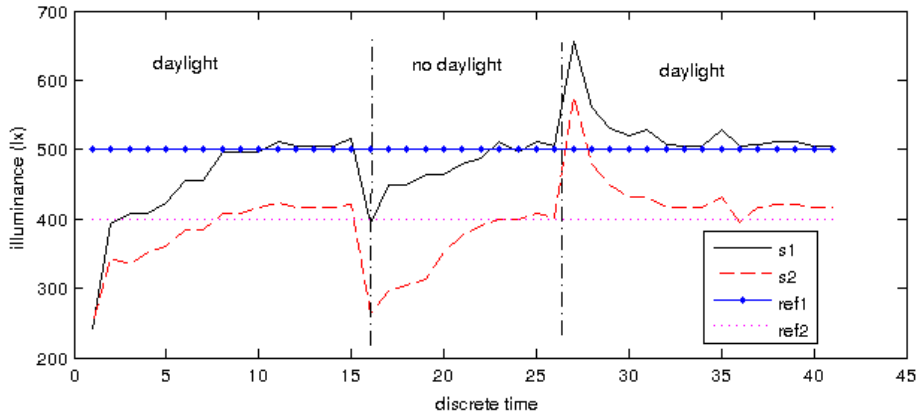

Figure 6.6: Test bed: actual illuminance values.

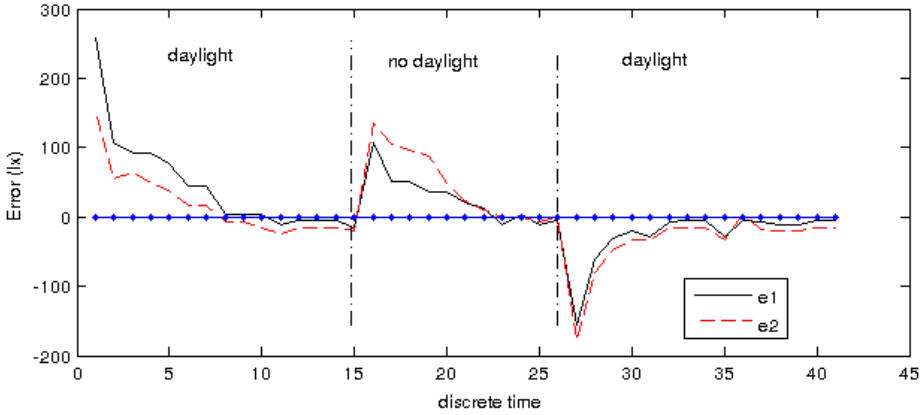

Figure 6.7: Test bed: error signals.

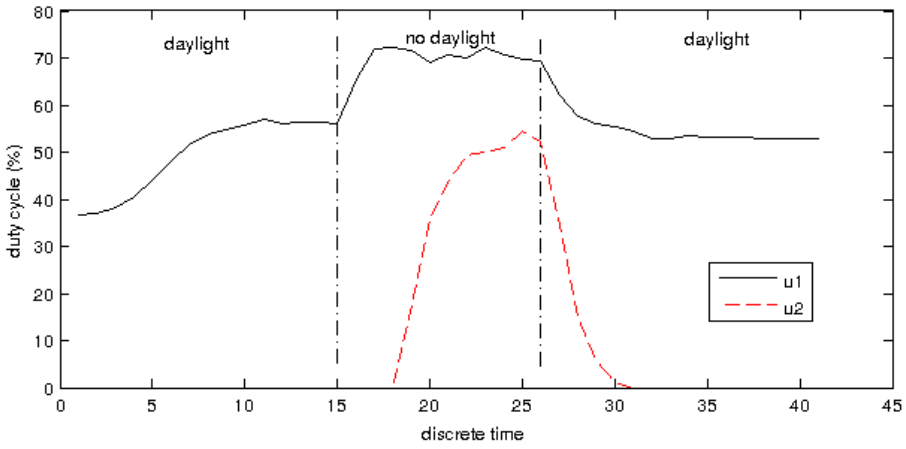

Figure 6.8: Test bed: input values.

Chapter 7

Conclusion and Future Research

The scope of this thesis was two-fold. The first part presented a self-tuning MIMO lighting control system for daylight harvesting. The case study was a typical open-plan office lit by both natural and artificial light. Experimental results were obtained through a co-simulator composed of a controller implemented in MATLAB and a scene simulator developed with the Radiance software. Further validations were also performed against a small scale room equipped with real LED light fixtures. Both test environments have demonstrated the effectiveness of the control scheme with respect to meeting the minimum levels of the illuminance values. Estimates of the energy that could be saved by adopting the so-called layered lighting design, that is the integration of natural and artificial light, demonstrate that daylight harvesting is a compelling business case.

The second part introduced a scene simulator developed with the Radiance software accessible through a REST API which allowed a quasi-real time validation of the control scheme. The proposed solution, which goes in the direction of the service-oriented lighting systems, offers several opportunities for integrating scene simulators in real scenarios.

One possible area of research is the use of the room model in parallel with the real system to estimate the illuminance in multiple points of interests of a given work plane. This research could lead to the adoption of virtual sensors whose data could be used by the real-time controller as if they were real sensors. Virtual sensors would be beneficial for many reasons including the ability to add sensors in a non-invasive manner. Data from virtual sensors could be integrated with real sensors through sensor fusion techniques.

Research in the automatic selection of the CIE sky type specific for a given location by using meteorological and satellite data as proposed in [17], could be particularly interesting

since weather data will be available through web services. A proper selection of the sky model could also enable further developments in the area of virtual sensors.

The proposed control scheme, being a daylight harvesting system, relies on estimates of the illuminance generated by the daylight in order to calculate the best control action. Therefore, a reliable daylight estimator is certainly a subject of further studies. Possible integrations of intelligent blinders within the proposed scheme are another important subject to investigate.

The core of the control system is the T matrix. This matrix could be identified not only during the commissioning phase but also during the life time of the system in order to improve the effectiveness of the control scheme. The need for the re-identification could be justified by occasional changes in the geometry of the room. A parallel off-line identification procedure could also be possible by using the scene simulator. The parallel model could then be used to offload the main system from heavy duty calculations. For example, what-if scenario could be tested against the parallel model without any impacts on the real system.

The benefits that intelligent lighting system will bring to the humankind are are already visible. Good will, the desire to learn and experiment, and most importantly the willingness to be open to different perspectives from various scientific and technical fields, will shape the landscape of the fascinating field of lighting.

This thesis has been an extraordinary opportunity to explore, once again, the wonders of engineering.

Bibliography

[1] A.M. Agogino and Y.J. Wen. Control of wireless-networked lighting in open-plan offices. *Lighting Research & Technology*, 43:235–248, 2010.

[2] M.A. Agogino, J. Granderson, and Y.J. Wen. Towards embedded wireless-networked intelligent daylighting systems for commercial buildings. In *Proceedings of IEEE International Conference on Sensor Networks, Ubiquitous, and Trustworthy Computing*, pages 326–331, 2006.

[3] P. Albertos and A. Sala. *Multivariable Control Systems*. Springer-Verlag, London, UK, 2004.

[4] M. Aldrich. *Dynamic Solid State Lighting*. PhD thesis, Massachusetts Institute of Technology, 2010.

[5] A. Bazaei and M. Moallem. Online neural identification of multi-input multi-output systems. *IET Control Theory Appl.*, 1:44–50, 2007.

[6] F. Cantin and M.C. Dubois. Daylighting metrics based on illuminance, distribution, glare and directivity. *Lighting Research & Technology*, 43:291–307, 2011.

[7] C.T. Chen. *Linear System Theory and Design 3rd edition*. Oxford University Press, USA, 1999.

[8] M. Chiogna, A. Mahdavi, R. Albatici, and A. Frattari. Energy efficiency of alternative lighting control systems. *Lighting Research & Technology*, 44:397–415, 2012.

[9] S.G. Colaco, C.P. Kurian, V.I. George, and A.M. Colaco. Integrated design and real-time implementation of an adaptive, predictive light controller. *Lighting Research & Technology*, 44:459–476, 2012.

[10] S. Darula and R. Kittler. Cie general sky standards defining luminance distributions. In *Proceedings of eSim 2002*, 2002.

[11] R.C. Dorf. *Modern Control Systems 6th edition*. Addison Wesley, USA, 1992.

[12] M.A. Duarte-Mermoud and R.A. Prieto. Performance index for quality response of dynamical systems. *ISA Transactions*, 43:133–151, 2004.

[13] M.G. Figueiro. Opinion: Why field measurements of circadian light expore are important. *Lighting Research & Technology*, 45:6–6, 2013.

[14] R. Fritz. Interactive modeling of luminaires for lighting simulation. Master's thesis, University of Washington, 2010.

[15] A.D. Galasiu, G.R. Newsham, G. Suvagau, and D.M. Sander. Energy saving lighting control systems for open-plan offices: a field study. *Leukos*, 4:7–29, 2007.

[16] J.Z. He. Opinion: The cie standard general sky and local climate. *Lighting Research & Technology*, 44:94–94, 2012.

[17] J.Z. He and E. Ng. Predicting sky types and zenith luminance from the cloud index derived from geostationary satellite data. *Lighting Research & Technology*, 44:139–148, 2012.

[18] S.Y. Ron Hui and Y.X. Qin. A general photo-electro-thermal theory for light emitting diode (led) systems. *IEEE Transactions on Industrial Electronics*, 24:1967–1976, 2009.

[19] E. Hull, K. Jackson, and J. Dick. *Requirements Engineering second Edition.* Springer, USA, 2005.

[20] F.P. Incropera and D.P. De Witt. *Fundamentals of Heat and Mass Transfer Third Edition.* Wiley, Singapore, 2005.

[21] R. De Keyser and C. Ionescu. Modelling and simulation of a lighting control system. *System Modelling Practice and Theory*, 18:165–176, 2010.

[22] C.P. Kurian, V. George, J. Bhat, and R.S. Aithal. Adaptive neuro fuzzy inference system model for the time series prediction of interior daylight illuminance. *AIML Journal*, 6:35–40, 2006.

[23] C.P. Kurian, V. George, J. Bhat, and R.S. Aithal. Robust control and optimisation of energy consumption in daylight-artificial light integrated schemes. *Lighting Research & Technology*, 40:7–24, 2008.

[24] W.L. Larson and R. Shakespeare. *Rendering with Radiance, The Art and Science of Lighting Visualization.* Randolph M. Fritz, Seattle, Washington, USA, 2011.

[25] H.C. Lee. *Introduction to Color Imaging Science.* Cambridge University Press, Cambridge, UK, 2005.

[26] R. Lenk and C. Lenk. *Practical Lighting Design with LEDs.* Wiley, IEEE Press on Power Engineering, USA, 2011.

[27] J.H. Lilly. *Fuzzy Control and Identification.* Wiley: Hoboken, New Jersey, USA, 2010.

[28] M.S. Mayhoub and D.J. Carter. Hybrid lighting systems: Performance and design. *Lighting Research & Technology*, 44:261–276, 2012.

[29] M. Moallem. Electron-beam position monitoring and feedback control in duke free-electron laser facility. *IEEE Transactions on Industrial Electronics*, 2:423–432, 2002.

[30] K.S. Narendra and A.M. Annaswamy. *Stable Adaptive Systems*. Dover, USA, 2005.

[31] M. Nørgaard, O. Ravn, N.K. Poulsen, and L.K. Hansen. *Neural Networks for Modelling and Control of Dynamic Systems*. Springer-Verlag, London, UK, 2003.

[32] J. Öhr. *Anti-Windup and Control of Systems with Multiple Input Saturations*. PhD thesis, Uppsala University, 2003.

[33] N. Ohta and A.R. Robertson. *Colorimetry Fundamentals and Applications*. John Wiley & Sons: Chichester, West Sussex, England, 2005.

[34] Y.X. Qin, D.Y. Lin, H.S. Chung, and S.Y.R. Hui. Dynamic control of a light-emitting diode system based on the general photo-electro-thermal theory. In *Proceedings of the Energy Conversion Congress and Exposition, San Jose, CA*, pages 2815–2820. IEEE, September 2009.

[35] Y. Quin, D. Lin, and S.Y. Ron Hui. A simple method for comparative study on the thermal performance of leds and fluorescent lamps. *IEEE Transactions on Industrial Electronics*, 24:1811–1818, 2009.

[36] O.F. Ransen. *Candelas, Lumens and Lux*. Ransens Software, 2013.

[37] M.S. Rea, M. G. Figueiro, and J.D. Bullough. Circadian photobiology: An emerging framework for lighting practice and research. *Lighting Research & Technology*, 34:177–190, 2002.

[38] M.S. Rea, M.G. Figueiro, A. Bierman, and R. Hamner. Modelling the spectral sensitivity of the human circadian system. *Lighting Research & Technology*, 44:386–396, 2012.

[39] L. Rutkowski. *Computational Intelligence Methods and Techniques*. Springer-Verlag, 2008.

[40] R.H. Simons and A.R. Bean. *Lighting Engineering Applied Calculations*. Architectural Press : Jordan Hill, Oxford, UK, 2001.

[41] X. Tao and S.Y. Ron Hui. Dynamic photoelectrothermal theory for light-emitting diode systems. *IEEE Transactions on Industrial Electronics*, 59:1751–1759, 2012.

[42] J.Y. Tsao and P. Waide. The world's appetite for light: Empirical data and trends spanning three centuries and six continents. *LEUKOS: The Journal of the Illuminating Engineering Society of North America*, 6:259–281, 2010.

[43] C. Villa and R. Labayrade. Multi-objective optimisation of lighting installations taking into account user preferences - a pilot study. *Lighting Research & Technology*, 45:176–196, 2013.

[44] C.W. Wampler. Manipulator inverse kinematic solutions based on vector formulations and damped least-squares methods. *IEEE Transactions on Systems, Man, and Cybernetics*, 16:93–101, 1986.

[45] Y.J. Wen. *Wireless Sensor and Actuator Networks for Lighting Energy Efficiency and User Satisfaction*. PhD thesis, University of California, Berkeley, 2008.

[46] M.S. Winchip. *Fundamentals of Lighting 2nd edition*. Fairchild Books, Canada, 2011.

[47] S. Winder. *Power Supplies for LED Driving*. Newnes: Burlinghton, MA, USA, 2008.

[48] Y. Zhong, H. Li, and M. Wu. Research of feedback control of lighting system based on dali. In *Proceedings of the 7th International Conference on Industrial Informatics (INDIN 2009)*, pages 396–401. IEEE, June 2009.

Appendix A

LSSI API Specification

A.1 Setting the Power Levels of the Luminaires

The following HTTP request sets the power levels of a given set of light fixtures. Each fixture is identified through a unique number and the power level goes from 0 to 100.

```
Request: http://<host>:<port>/lssi/power_level_events
Method: POST
Content Type: application/json
Body:
{"luminaire_array":
[{"id":<id>,"power_level_percent":<power_level>}
,{"id":<id>,"power_level_percent":<power_level>}
,...
,{"id":<id>,"power_level_percent":<power_level>}
]}

Response:
HTTP Response Code: 201 Created

{"id":0
,"request_status":"201000"
,"luminaire_array":[{"id":<id>,"power_level_percent":<power_level>}
```

```
                    ,{"id":<id>,"power_level_percent":<power_level>}
                    ,...
                    ,{"id":<id>,"power_level_percent":<power_level>}}
```

The following is an example of the HTTP requests:

```
Request: http://192.168.1.64:8080/lssi/power_level_events
Method: POST
Content Type: application/json
Body:
{"luminaire_array":
[{"id":1,"power_level_percent":90}
,{"id":2,"power_level_percent":90}
,{"id":3,"power_level_percent":90}
,{"id":4,"power_level_percent":20}
,{"id":5,"power_level_percent":20}
,{"id":6,"power_level_percent":20}
,{"id":7,"power_level_percent":90}
,{"id":8,"power_level_percent":90}
,{"id":9,"power_level_percent":90}
,{"id":10,"power_level_percent":20}
,{"id":11,"power_level_percent":20}
,{"id":12,"power_level_percent":20}
]}


Response:
HTTP Response Code: 201 Created

{"id":0,"request_status":"201000"
,"luminaire_array":[{"id":1,"power_level_percent":90}
,{"id":2,"power_level_percent":90}
,{"id":3,"power_level_percent":90}
,{"id":4,"power_level_percent":20}
```

```
,{"id":5,"power_level_percent":20}
,{"id":6,"power_level_percent":20}
,{"id":7,"power_level_percent":90}
,{"id":8,"power_level_percent":90}
,{"id":9,"power_level_percent":90}
,{"id":10,"power_level_percent":20}
,{"id":11,"power_level_percent":20}
,{"id":12,"power_level_percent":20}]}
```

A.2 Reading the Illuminance Levels

The following HTTP request returns the list of the illuminance values associated to the illuminance sensors.

```
Request: http://<host>:<port>/lssi/illumsensorlists/<id>
Method: GET
Content Type: application/json

Response:
{"id":1,"request_status":"200000"
,"number_of_sensors":<number of sensors>
,"sensor_array":[{"id":<id>
                  ,"position_x":<x position>
                  ,"position_y":<y position>
                  ,"position_z":<z position>
                  ,"illuminance_lux":<illuminance_lux>}
                 ,{"id":<id>
                  ,"position_x":<x position>
                  ,"position_y":<y position>
                  ,"position_z":<z position>
                  ,"illuminance_lux":<illuminance_lux>}
                 ,...
                 ,{"id":<id>
                  ,"position_x":<x position>
```

```
                ,"position_y":<y position>
                ,"position_z":<z position>
                ,"illuminance_lux":<illuminance_lux>}]}
```

The following is an example of the HTTP requests:

```
Request: http://192.168.1.64:8080/lssi/illumsensorlists/1
Method: GET
Content Type: application/json

Response:
{"id":1,"request_status":"200000"
,"number_of_sensors":4
,"sensor_array":[{"id":1
                 ,"position_x":5.5
                 ,"position_y":4.0
                 ,"position_z":0.85011
                 ,"illuminance_lux":94.8079093}
                ,{"id":2
                 ,"position_x":14.5
                 ,"position_y":4.0
                 ,"position_z":0.85011
                 ,"illuminance_lux":42.4013615}
                ,{"id":3
                 ,"position_x":5.5
                 ,"position_y":12.0
                 ,"position_z":0.85011
                 ,"illuminance_lux":98.4156041}
                ,{"id":4
                 ,"position_x":14.5
                 ,"position_y":12.0
                 ,"position_z":0.85011
                 ,"illuminance_lux":43.8541461}]}
```

Appendix B

Photometric Data

B.1 Luminaire: Cree24 50L

This appendix contains some information derived from the official data sheet of the CR24 troffer from Cree. The IES file is also provided.

IES file

```
IESNA:LM-63-2002
[TEST] 26013
[TESTLAB] Luminaire Testing Laboratory, Inc
[ISSUEDATE] 10/5/2011
[MANUFAC] Cree LED Lighting Solutions, Inc.
[LUMCAT] CR24-50L-35K-S
[LUMINAIRE] Formed white enamel steel housing, formed white enamel ste
[MORE] el outer reflector, extruded aluminum heatsink, frosted plastic enclos
[MORE] ures
[LAMP] One Cree light engine
[BALLAST] One unmarked LED power supply
[OTHER] 24.45 C, 120.04 V, 0.4223 A, 50.32 W, 0.993 PF, 60 Hz
[OTHER] This test was performed using the calibrated photodetector met
[MORE] hod of absolute photometry.
TILT=NONE
1 -1 1 361 5 1 1 1.792 3.813 0.000
1 1 50.32
0 0.5 1 1.5 2 2.5 3 3.5 4 4.5 5 5.5 6 6.5 7 7.5 8 8.5 9 9.5 10 10.5 11 11.5
 12 12.5 13 13.5 14 14.5 15 15.5 16 16.5 17 17.5 18 18.5 19 19.5 20 20.5
 21 21.5 22 22.5 23 23.5 24 24.5 25 25.5 26 26.5 27 27.5 28 28.5 29 29.5
 30 30.5 31 31.5 32 32.5 33 33.5 34 34.5 35 35.5 36 36.5 37 37.5 38 38.5
 39 39.5 40 40.5 41 41.5 42 42.5 43 43.5 44 44.5 45 45.5 46 46.5 47 47.5
 48 48.5 49 49.5 50 50.5 51 51.5 52 52.5 53 53.5 54 54.5 55 55.5 56 56.5
 57 57.5 58 58.5 59 59.5 60 60.5 61 61.5 62 62.5 63 63.5 64 64.5 65 65.5
 66 66.5 67 67.5 68 68.5 69 69.5 70 70.5 71 71.5 72 72.5 73 73.5 74 74.5
 75 75.5 76 76.5 77 77.5 78 78.5 79 79.5 80 80.5 81 81.5 82 82.5 83 83.5
 84 84.5 85 85.5 86 86.5 87 87.5 88 88.5 89 89.5 90 90.5 91 91.5 92 92.5
 93 93.5 94 94.5 95 95.5 96 96.5 97 97.5 98 98.5 99 99.5 100 100.5 101 101.5
 102 102.5 103 103.5 104 104.5 105 105.5 106 106.5 107 107.5 108 108.5 109
 109.5 110 110.5 111 111.5 112 112.5 113 113.5 114 114.5 115 115.5 116 116.5
 117 117.5 118 118.5 119 119.5 120 120.5 121 121.5 122 122.5 123 123.5 124
 124.5 125 125.5 126 126.5 127 127.5 128 128.5 129 129.5 130 130.5 131 131.5
 132 132.5 133 133.5 134 134.5 135 135.5 136 136.5 137 137.5 138 138.5 139
 139.5 140 140.5 141 141.5 142 142.5 143 143.5 144 144.5 145 145.5 146 146.5
 147 147.5 148 148.5 149 149.5 150 150.5 151 151.5 152 152.5 153 153.5 154
 154.5 155 155.5 156 156.5 157 157.5 158 158.5 159 159.5 160 160.5 161 161.5
 162 162.5 163 163.5 164 164.5 165 165.5 166 166.5 167 167.5 168 168.5 169
 169.5 170 170.5 171 171.5 172 172.5 173 173.5 174 174.5 175 175.5 176 176.5
 177 177.5 178 178.5 179 179.5 180
0 22.5 45 67.5 90
1765.0 1753.0 1753.0 1753.0 1753.0 1751.0 1751.0 1750.0 1748.0 1748.0 1746.0
 1745.0 1743.0 1742.0 1740.0 1738.0 1736.0 1734.0 1732.0 1730.0 1727.0 1725.0
 1722.0 1719.0 1716.0 1713.0 1710.0 1707.0 1703.0 1699.0 1696.0 1692.0 1688.0
 1684.0 1679.0 1674.0 1670.0 1664.0 1659.0 1653.0 1647.0 1641.0 1636.0 1630.0
 1624.0 1617.0 1611.0 1605.0 1598.0 1591.0 1585.0 1578.0 1570.0 1562.0 1555.0
 1547.0 1540.0 1531.0 1523.0 1515.0 1506.0 1499.0 1490.0 1480.0 1471.0 1462.0
 1451.0 1442.0 1432.0 1422.0 1413.0 1401.0 1391.0 1380.0 1369.0 1358.0 1346.0
 1335.0 1323.0 1312.0 1301.0 1289.0 1278.0 1265.0 1252.0 1240.0 1227.0 1214.0
 1202.0 1188.0 1175.0 1162.0 1148.0 1134.0 1120.0 1106.0 1091.0 1077.0 1063.0
 1049.0 1035.0 1020.0 1005.0 990.9 975.3 958.9 943.9 928.9 913.7 897.3 881.7
 866.1 849.7 834.0 818.6 802.3 786.3 769.0 753.2 737.5 722.0 705.8 689.0
 672.6 656.8 641.0 625.1 608.3 591.2 574.2 558.4 542.8 526.0 509.5 493.5
 478.0 461.4 445.2 428.7 413.2 398.6 382.5 368.4 352.1 336.4 321.0 305.4
 291.3 277.1 264.0 249.8 236.2 222.0 209.3 196.7 183.5 172.3 160.5 149.5
 137.9 127.1 116.4 105.6 95.4 84.7 76.0 66.3 58.5 49.0 42.0 34.6 27.5 20.5
 13.9 8.2 3.9 2.3 0.0 0.0 0.0 0.0 0.0 0.0 0.0 0.0 0.0 0.0 0.0 0.0 0.0 0.0
 0.0 0.0 0.0 0.0 0.0 0.0 0.0 0.0 0.0 0.0 0.0 0.0 0.0 0.0 0.0 0.0 0.0 0.0
 0.0 0.0 0.0 0.0 0.0 0.0 0.0 0.0 0.0 0.0 0.0 0.0 0.0 0.0 0.0 0.0 0.0 0.0
 0.0 0.0 0.0 0.0 0.0 0.0 0.0 0.0 0.0 0.0 0.0 0.0 0.0 0.0 0.0 0.0 0.0 0.0
 0.0 0.0 0.0 0.0 0.0 0.0 0.0 0.0 0.0 0.0 0.0 0.0 0.0 0.0 0.0 0.0 0.0 0.0
 0.0 0.0 0.0 0.0 0.0 0.0 0.0 0.0 0.0 0.0 0.0 0.0 0.0 0.0 0.0 0.0 0.0 0.0
```

```
 0.0 0.0 0.0 0.0 0.0 0.0 0.0 0.0 0.0 0.0 0.0 0.0 0.0 0.0 0.0 0.0 0.0 0.0
 0.0 0.0 0.0 0.0 0.0 0.0 0.0 0.0 0.0 0.0 0.0 0.0 0.0 0.0 0.0 0.0 0.0 0.0
 0.0 0.0 0.0 0.0 0.0 0.0 0.0 0.0 0.0 0.0 0.0 0.0 0.0 0.0 0.0 0.0 0.0 0.0
 0.0 0.0 0.0 0.0 0.0 0.0 0.0 0.0 0.0 0.0 0.0 0.0 0.0 0.0 0.0 0.0 0.0 0.0
 0.0 0.0 0.0 0.0 0.0 0.0 0.0 0.0
1765.0 1759.0 1759.0 1758.0 1758.0 1757.0 1757.0 1755.0 1755.0 1754.0 1752.0
 1751.0 1750.0 1748.0 1746.0 1745.0 1743.0 1741.0 1739.0 1737.0 1735.0 1732.0
 1730.0 1728.0 1725.0 1722.0 1719.0 1716.0 1712.0 1709.0 1706.0 1702.0 1698.0
 1694.0 1689.0 1685.0 1680.0 1675.0 1670.0 1665.0 1660.0 1655.0 1649.0 1643.0
 1638.0 1631.0 1625.0 1619.0 1613.0 1606.0 1600.0 1594.0 1586.0 1579.0 1572.0
 1565.0 1558.0 1550.0 1542.0 1535.0 1527.0 1519.0 1511.0 1502.0 1493.0 1484.0
 1475.0 1466.0 1457.0 1447.0 1438.0 1428.0 1418.0 1408.0 1398.0 1387.0 1377.0
 1366.0 1355.0 1344.0 1333.0 1322.0 1311.0 1300.0 1288.0 1276.0 1264.0 1251.0
 1239.0 1227.0 1215.0 1201.0 1190.0 1175.0 1162.0 1149.0 1135.0 1121.0 1107.0
 1094.0 1081.0 1067.0 1053.0 1038.0 1023.0 1008.0 993.1 978.4 963.4 947.5
 932.5 917.3 901.5 885.4 869.9 853.8 837.4 821.0 804.8 789.0 773.2 757.6
 740.9 724.8 708.2 692.4 676.4 658.5 642.3 625.3 607.8 590.8 574.0 556.5
 539.5 522.0 504.8 487.5 470.7 453.9 438.5 421.0 404.9 388.1 372.0 355.3
 339.7 324.0 309.3 295.0 280.1 265.2 251.7 238.3 224.5 212.3 199.6 186.2
 174.7 162.9 151.9 140.3 129.2 116.9 104.4 91.7 79.4 66.8 55.2 44.9 35.6
 25.8 17.2 10.1 6.0 2.4 0.6 0.0 0.0 0.0 0.0 0.0 0.0 0.0 0.0 0.0 0.0 0.0
 0.0 0.0 0.0 0.0 0.0 0.0 0.0 0.0 0.0 0.0 0.0 0.0 0.0 0.0 0.0 0.0 0.0 0.0
 0.0 0.0 0.0 0.0 0.0 0.0 0.0 0.0 0.0 0.0 0.0 0.0 0.0 0.0 0.0 0.0 0.0 0.0
 0.0 0.0 0.0 0.0 0.0 0.0 0.0 0.0 0.0 0.0 0.0 0.0 0.0 0.0 0.0 0.0 0.0 0.0
 0.0 0.0 0.0 0.0 0.0 0.0 0.0 0.0 0.0 0.0 0.0 0.0 0.0 0.0 0.0 0.0 0.0 0.0
 0.0 0.0 0.0 0.0 0.0 0.0 0.0 0.0 0.0 0.0 0.0 0.0 0.0 0.0 0.0 0.0 0.0 0.0
 0.0 0.0 0.0 0.0 0.0 0.0 0.0 0.0 0.0 0.0 0.0 0.0 0.0 0.0 0.0 0.0 0.0 0.0
 0.0 0.0 0.0 0.0 0.0 0.0 0.0 0.0 0.0 0.0 0.0 0.0 0.0 0.0 0.0 0.0 0.0 0.0
 0.0 0.0 0.0 0.0 0.0 0.0 0.0 0.0 0.0 0.0 0.0 0.0 0.0 0.0 0.0 0.0 0.0 0.0
 0.0 0.0 0.0 0.0 0.0 0.0 0.0 0.0 0.0 0.0 0.0 0.0 0.0 0.0 0.0 0.0 0.0 0.0
 0.0 0.0 0.0 0.0 0.0 0.0 0.0 0.0 0.0 0.0 0.0
1765.0 1770.0 1769.0 1769.0 1769.0 1768.0 1767.0 1766.0 1766.0 1764.0 1763.0
 1762.0 1761.0 1760.0 1758.0 1757.0 1755.0 1753.0 1751.0 1749.0 1747.0 1745.0
 1743.0 1741.0 1738.0 1736.0 1733.0 1730.0 1727.0 1724.0 1721.0 1718.0 1714.0
 1711.0 1707.0 1703.0 1699.0 1695.0 1691.0 1686.0 1682.0 1678.0 1673.0 1669.0
 1664.0 1659.0 1654.0 1648.0 1643.0 1637.0 1632.0 1626.0 1620.0 1614.0 1607.0
 1601.0 1594.0 1587.0 1580.0 1572.0 1565.0 1558.0 1551.0 1542.0 1534.0 1526.0
 1518.0 1510.0 1501.0 1492.0 1484.0 1475.0 1466.0 1456.0 1447.0 1438.0 1428.0
 1417.0 1407.0 1396.0 1386.0 1376.0 1365.0 1353.0 1342.0 1330.0 1318.0 1306.0
 1294.0 1282.0 1269.0 1257.0 1244.0 1231.0 1218.0 1204.0 1191.0 1177.0 1164.0
 1150.0 1137.0 1123.0 1108.0 1092.0 1077.0 1062.0 1046.0 1031.0 1015.0 998.9
 983.2 967.7 951.3 934.8 918.4 901.7 884.8 867.6 851.2 834.2 818.4 801.6
 784.9 767.9 750.5 733.3 716.6 699.8 682.4 666.8 648.5 631.9 615.3 598.0
 582.0 565.5 548.4 530.7 514.8 498.1 481.8 465.1 448.5 431.9 417.2 400.8
 384.5 368.7 350.5 330.9 311.0 290.9 270.5 249.9 230.1 212.0 192.9 173.5
 156.4 139.3 123.0 107.2 91.6 76.7 62.8 49.4 37.5 26.8 18.3 12.0 8.1 5.6
 4.4 3.6 2.7 1.2 0.0 0.0 0.0 0.0 0.0 0.0 0.0 0.0 0.0 0.0 0.0 0.0 0.0 0.0
 0.0 0.0 0.0 0.0 0.0 0.0 0.0 0.0 0.0 0.0 0.0 0.0 0.0 0.0 0.0 0.0 0.0 0.0
 0.0 0.0 0.0 0.0 0.0 0.0 0.0 0.0 0.0 0.0 0.0 0.0 0.0 0.0 0.0 0.0 0.0 0.0
 0.0 0.0 0.0 0.0 0.0 0.0 0.0 0.0 0.0 0.0 0.0 0.0 0.0 0.0 0.0 0.0 0.0 0.0
 0.0 0.0 0.0 0.0 0.0 0.0 0.0 0.0 0.0 0.0 0.0 0.0 0.0 0.0 0.0 0.0 0.0 0.0
 0.0 0.0 0.0 0.0 0.0 0.0 0.0 0.0 0.0 0.0 0.0 0.0 0.0 0.0 0.0 0.0 0.0 0.0
 0.0 0.0 0.0 0.0 0.0 0.0 0.0 0.0 0.0 0.0 0.0 0.0 0.0 0.0 0.0 0.0 0.0 0.0
 0.0 0.0 0.0 0.0 0.0 0.0 0.0 0.0 0.0 0.0 0.0 0.0 0.0 0.0 0.0 0.0 0.0 0.0
 0.0 0.0 0.0 0.0 0.0 0.0 0.0 0.0 0.0 0.0 0.0 0.0 0.0 0.0 0.0 0.0 0.0 0.0
 0.0 0.0 0.0 0.0 0.0 0.0 0.0 0.0 0.0 0.0 0.0 0.0 0.0 0.0 0.0 0.0 0.0 0.0
 0.0 0.0 0.0 0.0 0.0 0.0 0.0 0.0 0.0
1765.0 1771.0 1771.0 1771.0 1771.0 1771.0 1770.0 1770.0 1770.0 1769.0 1769.0
 1768.0 1767.0 1766.0 1764.0 1763.0 1762.0 1760.0 1758.0 1756.0 1754.0 1752.0
 1750.0 1747.0 1745.0 1743.0 1740.0 1738.0 1735.0 1732.0 1730.0 1727.0 1724.0
 1722.0 1719.0 1716.0 1713.0 1710.0 1706.0 1703.0 1699.0 1695.0 1692.0 1688.0
 1683.0 1679.0 1675.0 1670.0 1666.0 1660.0 1655.0 1650.0 1644.0 1638.0 1632.0
 1626.0 1620.0 1612.0 1605.0 1598.0 1592.0 1585.0 1578.0 1569.0 1561.0 1554.0
```

```
 1546.0 1538.0 1529.0 1521.0 1512.0 1504.0 1494.0 1485.0 1476.0 1466.0 1456.0
 1446.0 1435.0 1424.0 1413.0 1403.0 1392.0 1381.0 1368.0 1356.0 1343.0 1330.0
 1317.0 1304.0 1291.0 1277.0 1264.0 1250.0 1236.0 1222.0 1209.0 1195.0 1180.0
 1166.0 1152.0 1137.0 1123.0 1107.0 1092.0 1076.0 1061.0 1045.0 1029.0 1012.0
 995.5 979.1 961.9 944.6 928.0 911.1 893.8 876.8 858.6 841.7 824.8 807.7
 790.7 773.2 755.7 739.5 722.1 704.3 687.3 670.5 653.7 637.3 620.8 603.9
 587.5 571.5 554.1 536.6 517.7 496.7 476.2 451.8 428.3 405.3 381.3 357.7
 334.6 311.5 288.8 267.9 246.7 226.3 207.6 187.8 170.4 152.8 136.0 120.0
 104.9 90.2 76.0 62.7 50.4 38.0 28.4 20.1 14.3 10.4 8.2 6.7 6.2 5.3 4.8
 3.5 1.7 1.3 0.0 0.0 0.0 0.0 0.0 0.0 0.0 0.0 0.0 0.0 0.0 0.0 0.0 0.0 0.0
 0.0 0.0 0.0 0.0 0.0 0.0 0.0 0.0 0.0 0.0 0.0 0.0 0.0 0.0 0.0 0.0 0.0 0.0
 0.0 0.0 0.0 0.0 0.0 0.0 0.0 0.0 0.0 0.0 0.0 0.0 0.0 0.0 0.0 0.0 0.0 0.0
 0.0 0.0 0.0 0.0 0.0 0.0 0.0 0.0 0.0 0.0 0.0 0.0 0.0 0.0 0.0 0.0 0.0 0.0
 0.0 0.0 0.0 0.0 0.0 0.0 0.0 0.0 0.0 0.0 0.0 0.0 0.0 0.0 0.0 0.0 0.0 0.0
 0.0 0.0 0.0 0.0 0.0 0.0 0.0 0.0 0.0 0.0 0.0 0.0 0.0 0.0 0.0 0.0 0.0 0.0
 0.0 0.0 0.0 0.0 0.0 0.0 0.0 0.0 0.0 0.0 0.0 0.0 0.0 0.0 0.0 0.0 0.0 0.0
 0.0 0.0 0.0 0.0 0.0 0.0 0.0 0.0 0.0 0.0 0.0 0.0 0.0 0.0 0.0 0.0 0.0 0.0
 0.0 0.0 0.0 0.0 0.0 0.0 0.0 0.0 0.0 0.0 0.0 0.0 0.0 0.0 0.0 0.0 0.0 0.0
 0.0 0.0 0.0 0.0 0.0 0.0 0.0 0.0 0.0 0.0 0.0 0.0 0.0 0.0 0.0 0.0 0.0 0.0
 0.0 0.0 0.0 0.0 0.0 0.0 0.0 0.0
1765.0 1769.0 1769.0 1769.0 1770.0 1769.0 1769.0 1769.0 1770.0 1769.0 1769.0
 1768.0 1768.0 1767.0 1766.0 1764.0 1763.0 1761.0 1759.0 1757.0 1755.0 1753.0
 1751.0 1748.0 1746.0 1744.0 1741.0 1739.0 1737.0 1734.0 1731.0 1729.0 1727.0
 1724.0 1722.0 1719.0 1716.0 1714.0 1710.0 1708.0 1704.0 1701.0 1698.0 1694.0
 1689.0 1685.0 1681.0 1676.0 1671.0 1666.0 1661.0 1655.0 1650.0 1644.0 1638.0
 1631.0 1625.0 1619.0 1612.0 1606.0 1599.0 1592.0 1585.0 1578.0 1569.0 1561.0
 1553.0 1545.0 1536.0 1528.0 1518.0 1509.0 1500.0 1490.0 1481.0 1472.0 1461.0
 1451.0 1441.0 1430.0 1418.0 1407.0 1395.0 1382.0 1370.0 1357.0 1344.0 1332.0
 1318.0 1305.0 1292.0 1279.0 1265.0 1251.0 1237.0 1223.0 1209.0 1196.0 1180.0
 1166.0 1152.0 1137.0 1123.0 1107.0 1091.0 1075.0 1059.0 1043.0 1026.0 1009.0
 992.9 975.6 958.8 941.3 924.8 907.5 889.9 871.5 855.0 837.2 819.9 802.9
 786.3 769.2 751.5 733.8 716.3 699.8 682.0 665.2 648.9 633.4 616.2 598.8
 581.1 562.2 539.9 515.7 491.4 465.7 443.7 420.0 394.3 370.2 347.2 322.5
 299.9 275.1 257.0 239.1 218.1 199.5 181.2 163.1 145.8 130.8 114.8 100.2
 85.7 72.1 59.8 47.4 36.4 27.6 20.1 13.7 11.0 8.7 7.3 6.6 5.8 5.3 4.4 3.1
 1.6 1.3 0.0 0.0 0.0 0.0 0.0 0.0 0.0 0.0 0.0 0.0 0.0 0.0 0.0 0.0 0.0 0.0
 0.0 0.0 0.0 0.0 0.0 0.0 0.0 0.0 0.0 0.0 0.0 0.0 0.0 0.0 0.0 0.0 0.0 0.0
 0.0 0.0 0.0 0.0 0.0 0.0 0.0 0.0 0.0 0.0 0.0 0.0 0.0 0.0 0.0 0.0 0.0 0.0
 0.0 0.0 0.0 0.0 0.0 0.0 0.0 0.0 0.0 0.0 0.0 0.0 0.0 0.0 0.0 0.0 0.0 0.0
 0.0 0.0 0.0 0.0 0.0 0.0 0.0 0.0 0.0 0.0 0.0 0.0 0.0 0.0 0.0 0.0 0.0 0.0
 0.0 0.0 0.0 0.0 0.0 0.0 0.0 0.0 0.0 0.0 0.0 0.0 0.0 0.0 0.0 0.0 0.0 0.0
 0.0 0.0 0.0 0.0 0.0 0.0 0.0 0.0 0.0 0.0 0.0 0.0 0.0 0.0 0.0 0.0 0.0 0.0
 0.0 0.0 0.0 0.0 0.0 0.0 0.0 0.0 0.0 0.0 0.0 0.0 0.0 0.0 0.0 0.0 0.0 0.0
 0.0 0.0 0.0 0.0 0.0 0.0 0.0 0.0 0.0 0.0 0.0 0.0 0.0 0.0 0.0 0.0 0.0 0.0
 0.0 0.0 0.0 0.0 0.0 0.0 0.0 0.0 0.0 0.0 0.0 0.0 0.0 0.0 0.0 0.0 0.0 0.0
 0.0 0.0 0.0 0.0 0.0 0.0 0.0
```

CR24™

2'x4' Architectural LED Trofer

Product Description

The CR24 Architectural LED High Efficiency (HE) troffer delivers up to 130 lumens per watt of exceptional 90 CRI light at 4000 lumens. This breakthrough performance is achieved by combining the high efficacy and high-quality light of Cree TrueWhite® Technology with a unique thermal management design. The CR24 (HD) option delivers enhanced spectrum 80+CRI color quality. The CR24 product family is available in warm, neutral, cool, or daylight color temperatures and has step, 0-10V, or Lutron EcoSystem® Enabled dimming options. Its compact, lightweight design makes the CR24 perfect for use in commercial new construction or renovated spaces.

Performance Summary

- Utilizes Cree TrueWhite® Technology (90 CRI) or available in 80+CRI
- Active Color Management
- Room-Side Heat Sink
- Assembled in the US & Mexico
- Efficacy: 90-130 LPW
- Delivered Light Output: 2200, 3100, 4000, 5000 lumens
- Input Power: 22-50 watts
- CRI: 90 CRI (Cree TrueWhite® Technology), 80+CRI
- CCT: 3000K, 3500K, 4000K, 5000K
- Input Voltage: 120-277 VAC or 347 VAC*
- Warranty†: 10 years
- Lifetime: Designed to last from 50,000 hours (HD), 75,000 hours (Standard TW), and 100,000 hours (HE TW)
- Controls: Step Level to 50%, 0-10V Dimming or Lutron EcoSystem Enabled to 5%[1]
- Mounting: Recessed

*40L 100 LPW 10V types only - other types require addition of a 347 accessory kit

CR24™

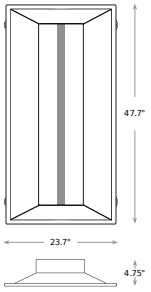

NOTE: Use of Expanded Junction Box will expand the depth to 6.67" and Emergency Backup will expand the depth to 6.30". Use of 347V will increase fixture height by 1/4".

Housings & Accessories

Accessories			
CPLCR Chicago Plenum Field Kit	CR-347V 347 Volt	PW-18/4-06-9T/SS-CR Power Whip	AC5-72-PD8-JB Adjustable Cable
CPLCR-EM Chicago Plenum Field Kit-Emergency	CR-347V-SD Step Dimming to 50%	AC5-18/4-72-PD8-JB Adjustable Cable	EJBCR-5PK Expanded size junction box for through wiring (5 pack)
	SMK-24 Surface Mount Kit		

Ordering Information

Example: CR24-40L-35K-S

QUICKSHIP™

For full list of Cree Quick Ship products visit **www.cree.com/lighting/quickship**

CR24					
Product	**Lumen Output**	**Color Temp**	**Voltage**	**Control**	**Options**
CR24	22L 22W 2200 lumens – 100 LPW 31L 34W 3100 lumens – 90 LPW 40L 40W 4000 lumens – 100 LPW 40L HE 40L HE 30.5W 4000 lumens – 130 LPW (30K) 32W 4000 lumens – 125 LPW (35K) 33W 4000 lumens – 120 LPW (40K) 34.5W 4000 lumens – 115 LPW (50K) 50L 50W 5000 lumens – 100 LPW	30K 3000 Kelvin 35K 3500 Kelvin 40K 4000 Kelvin 50K 5000 Kelvin	Blank 120-277 Volt (Standard) 34[6] 347 Volt (Optional)	S Step Dimming to 50% 10V 0-10V Dimming to 5% LES Lutron EcoSystem® Enabled to 5%	HD[7] CRI 80+ (44W 4000 lumens - 90 LPW) EB14[2,4] Emergency Backup - 1400 lumens EB14 SMK[2,3,5] Emergency Backup with surface mount kit - 1400 lumens

1. Reference www.cree.com/lighting for recommended dimming control options. 2. Not available in 50L. Not available in LES types except 40L LES type. 3. Not available with EB14 option. Use EB14 SMK. 4. EB14 not for use with SMK Kits. 5. Includes surface mount kit accessory (SMK-CR24). 6. 347V integrated option only available on 40L 100 LPW 10V fixtures. Wattage increases to 42W and fixture height increases by 1/4" over standard 120-277V fixtures. 7. HD only available in 40L.

†See www.cree.com/lighting/products/warranty for warranty terms.

Rev. Date: 02/06/2014

US: www.cree.com/lighting T (800) 236-6800 F (262) 504-5415
Canada: www.cree.com/canada T (800) 473-1234 F (800) 890-7507

CREE TRUE WHITE TECHNOLOGY · c UL us LISTED · EcoSystem Enabled · CREE

Figure B.1: CREE CR24 Product Specifications.

CR24™

Product Specif cations

CREE TRUEWHITE® TECHNOLOGY
A revolutionary way to generate high-quality white light, Cree TrueWhite® Technology mixes the light from the highest performing red and unsaturated yellow LEDs. This patented approach delivers an exclusive combination of 90+ CRI, beautiful light characteristics, and lifelong color consistency, all while maintaining high luminous eff cacy—a true no compromise solution.

ROOM-SIDE HEAT SINK
An innovative thermal management system designed to maximize cooling effectiveness by integrating a unique room-side heat sink into the diffusing lens. This breakthrough design creates a pleasing architectural aesthetic while conducting heat away from LEDs in a temperature-controlled environment. This enables the LEDs to consistently run cooler, providing signif cant boosts to lifetime, eff cacy, and color consistency.

LUMEN MAINTENANCE FACTORS
- Reference www.cree.com/lighting for detailed lumen maintenance factors.

CONSTRUCTION & MATERIALS
- Durable 20-gauge steel housing with standard troffer access plate for electrical installation.
- Field replaceable light engine integrates LEDs, driver, power supply, thermal management, and optical mixing components.
- One-piece lower ref ector f nished with a textured high ref ectance white polyester powder coating creates a comfortable visual transition from the lens to the ceiling plane.
- Provided t-bar clips and holes for mounting support wires enable recessed or suspended installation.
- Individual f xtures may be mounted end to end for a continuous row of illumination.

  NOTE: Reference www.cree.com/lighting for detailed instructions on f eld replacement of the light engine.

OPTICAL SYSTEM
- Unique combination of ref ective and refractive optical components achieves a uniform, comfortable appearance while eliminating pixelation and color fringing.
- Components work together to optimize distribution, balancing the delivery of high illuminance levels on horizontal surfaces with an ideal amount of light on walls and vertical surfaces. This increases the perception of spaciousness.
- Diffusing lens integrated with upward-facing LED strip eliminates direct view of LEDs while lower ref ector balances brightness of lens with the ceiling to create a low-glare high angle appearance.

ELECTRICAL SYSTEM
- Integral, high-eff ciency driver and power supply.
- Power Factor = 0.9 nominal
- Input Power: Stays constant over life.
- Input Voltage: 120-277V, 347V- 50/60Hz
- Battery Backup: Consult factory.
- Temperature Rating: Designed to operate in temperatures 0-35C and below room side and plenum side.
- Total Harmonic Distortion: <20%

CONTROLS
- Step dimming to 50% comes standard.*
- Optional continuous dimming to 5% with 0-10V DC control protocol.*
- Optional Lutron EcoSystem® Enabled option allows seamless integration with Lutron EcoSystem controls.*

REGULATORY & VOLUNTARY QUALIFICATIONS
- UL924 (EB14 option).
- cULus Listed.
- DLC qualif ed.**
- Suitable for damp locations.
- Designed for Indoor use.

*Reference www.cree.com/lighting for recommended dimming controls and wiring diagrams.
**Please refer to DLC QPL list for most current information.

US: www.cree.com/lighting T (800) 236-6800 F (262) 504-5415

Photometry

CR24-4000L BASED ON LTL REPORT TEST #: 22421
Fixture photometry has been conducted by a NVLAP accredited testing laboratory in accordance with IESNA LM-79-08. IESNA LM-79-08 specif es the entire luminaire as the source resulting in a f xture eff ciency of 100%

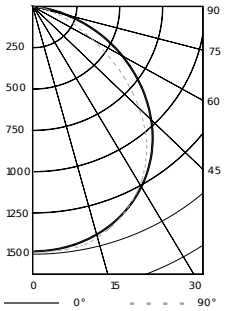

Coef cients Of Utilization

RCC %:	80			
RW %:	70	50	30	0
RCR: 0	119	119	119	119
1	109	105	101	97
2	100	92	85	79
3	91	80	72	66
4	83	71	63	56
5	76	64	55	48
6	71	57	48	42
7	65	52	43	37
8	61	47	39	33
9	57	43	35	30
10	53	40	32	27

Ef ective Floor Cavity Ref ectance: 20%

Average Luminance Table (cd/m2)

Vertical Angle \ Horizontal Angle	0°	45°	90°
0°	2174	2174	2174
45°	1976	2116	2152
55°	1807	2018	2074
65°	1553	1889	1879
75°	1149	1501	1119
85°	424	62	62

Zonal Lumen Summary

Zone	Lumens	% Lamp	Luminaire
0-30	1,115	27.9%	27.9%
0-40	1,835	45.9%	45.9%
0-60	3,245	81.1%	81.1%
0-90	4,000	100%	100%

Reference www.cree.com/lighting for detailed photometric data.

Application Reference

Open Space					
Spacing	**Lumens**	**Wattage**	**LPW**	**w/ft²**	**Average fc**
8 x 8	2200L	22W	100	0.35	30
	4000L	40W	100	0.69	54
	4000L	30.5W	130	0.56	54
	5000L	50W	100	0.78	68
8 x 10	2200L	22W	100	0.28	25
	4000L	40W	100	0.55	45
	4000L	30.5W	130	0.45	45
	5000L	50W	100	0.62	57
10 x 10	2200L	22W	100	0.22	21
	4000L	40W	100	0.44	38
	4000L	30.5W	130	0.36	38
	5000L	50W	100	0.50	48
10 x 12	2200L	22W	100	0.19	17
	4000L	40W	100	0.37	30
	4000L	30.5W	130	0.30	30
	5000L	50W	100	0.42	38

9' ceiling: 80/50/20 ref ectances; 2.5' workplane, open room. LLF: 1.0 Initial. Open Space: 50' x 40' x 10'

CREE

Canada: www.cree.com/canada T (800) 473-1234 F (800) 890-7507

Figure B.2: CREE CR24 Product Specifications (photometry).

Appendix C

Laboratory Test Bed

C.1 Simulink Block Diagram

The simulink block diagram of the control system developed for testing the control scheme at the SFU test lab is represented in Figure C.1.

C.2 Electronic Circuit Schematics

This appendix contains the simulink block diagram and the electronic circuit schematics of the components used in the test bed for driving the LED light fixtures and reading the motion detection sensor data generated by the XCO sensors.

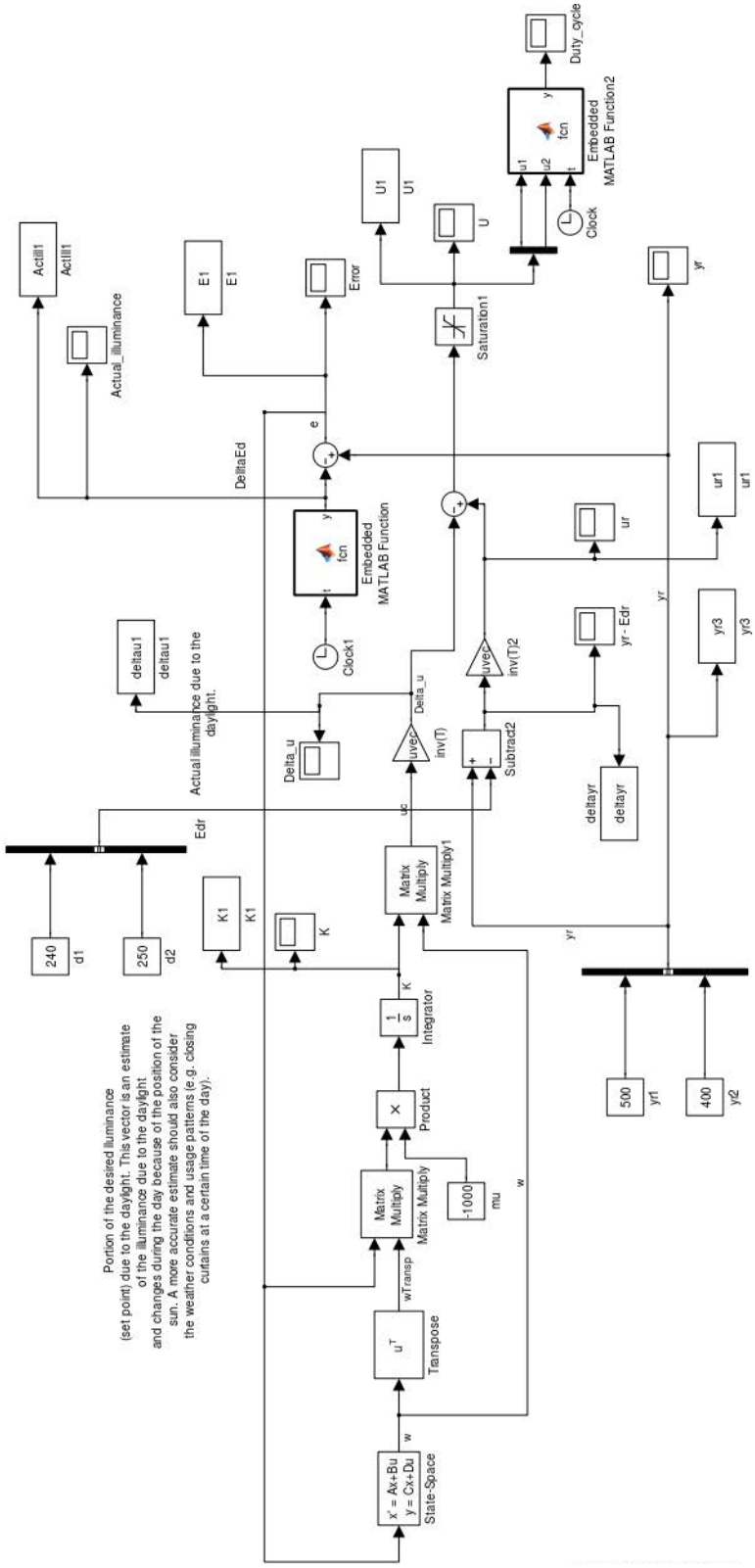

Figure C.1: Simulink block diagram.

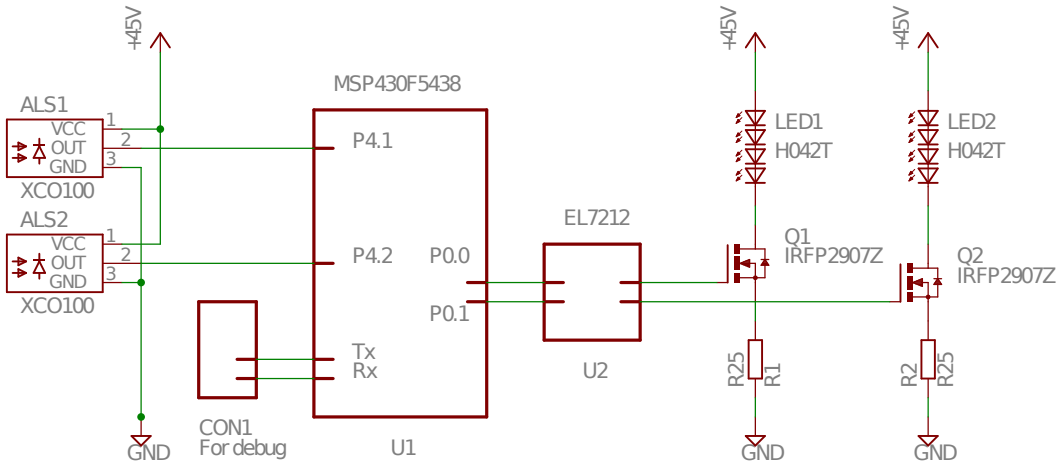

Figure C.2: LED driver electronic circuit schematics.

Index